T.C.
DOKUZ EYLÜL UNIVERSITY
GRADUATE SCHOOL OF NATURAL
AND APPLIED SCIENCES

THE INVESTIGATION OF CONTACT RESISTANCE IN RESISTANCE SPOT WELDING BY USING NUMERICAL AND EXPERIMENTAL METHODS

A Thesis Presented to the
Graduate School of Natural
and Applied Sciences
Dokuz Eylül University

In Partial Fulfillment of the
Requirements for the Doctorate
Degree in Mechanical Engineering

by
M.Şemseddin ÇİMEN

Advisor
Prof.Dr.Süleyman KARADENİZ

November, 1994
İZMİR

ABSTRACT

The method of electric resistance spot welding has an extensive application in the joining of sheet metal not only in mild steels but also in stainless steels, heat resisting alloys, aluminium and copper alloys and reactive metals. Particularly attractive features of this process are the high speed of operation, ease of mechanization, the self-jigging nature of the lap joint and the absence of edge preparation or filler metal.

The workpieces are joined to each other in resistance welding by using pressure and heat. The heat is generated by the resistance to the passage of the current according to the Joule's law. Temperature is the highest at the contact surface between the pieces. The contact resistance between sheets where nugget and, therefore, the heat is required is the most important resistance in early period of the welding.

In this investigation, finite element method and an experimental method have been used to find out the relationship between contact resistance and clamping force. Some experimental measurements have also been carried out to show the validity of the solution.

In the finite element process, isoparametric four-node quadrilateral element has been chosen and Lagrange polynomial has been used as interpolation function. Various special software computer programs have been developed to solve this problem. Mechanical properties of materials obtained from tensile test results have been used in this investigation. Elasto-plastic analysis has been done to find out relationship between micro contact force and the radius of contacted area of a micro contact point by using "initial stress method".

As a result of this study, the relationship between contact resistance and clamping force has been found and illustrated as graphics in figures. In addition, stress distribution in the workpiece and on the spherical surface of the micro contact point, forces applied to the micro contact points, the effects of the thickness of the workpiece, and the radius of electrode tip, and the material of the workpiece to the contact resistance have been investigated.

ÖZET

Elektrik direnç nokta kaynağı yalnızca karbon çeliklerinin değil aynı zamanda paslanmaz çeliklerin, ısıya dayanıklı alaşımların, aluminyum ve bakır alaşımların ve reaktif metallerin levha kaynağında geniş bir uygulama alanına sahiptir. Özellikle, yüksek operasyon hızı, mekanizasyondaki kolaylık, bindirme birleştirmeden dolayı kalınlık için elektrod sallama hareketine gerek olmaması, kaynak ağzına ve dolgu metaline gerek duyulmaması bu yöntemin cazip özellikleridir.

Direnç kaynağında, iş parçaları ısı ve basınç kullanılarak birbirlerine birleştirilir. Isı, Joule kanununa göre akım pasajına gösterilen direnç ile oluşturulur. En yüksek sıcaklık, parçalar arasındaki temas yüzeyindedir. Levhalar arasındaki yani kaynak pasosunun oluştuğu ve dolayısıyla ısıya gerek duyulan yerdeki kontak direnci, kaynak işleminin ilk anları için en önemli dirençtir.

Bu araştırmada, kontak direnci ve sıkıştırma kuvveti arasında bir bağıntı bulmak için sonlu elemanlar yöntemi ve deneysel bir yöntem kullanıldı. Aynı zamanda, sonucun geçerliliğini göstermek için bazı deneysel ölçümler yapıldı.

Sonlu elemanlar yönteminde, izoparametrik dört düğüm noktalı dörtgen eleman seçildi ve interpolasyon fonksiyonu olarak da Lagrange polinomu kullanıldı. Bu problemi çözmek için çeşitli bilgisayar programları geliştirildi. Bu araştırmada, çekme deneyi sonuçlarından bulunan mekanik malzeme özellikleri kullanıldı. Mikro kontak kuvveti ile bir mikro kontak noktasının temas eden alanının yarıçapı arasında bağıntı bulmak için, "Başlangıç gerilmesi metodu" kullanılarak elasto-plastik analiz yapıldı.

Bu çalışmada sonuç olarak, kontak direnci ile sıkıştırma kuvveti arasında bir bağıntı bulundu ve grafik olarak şekillerde gösterildi. Ayrıca, iş parçasındaki ve bir mikro kontağın küresel yüzeyindeki gerilme dağılımı, mikro kontak noktalarına uygulanan kuvvetler, iş parçası kalınlığının, elektrod ucu yarıçapının ve iş parçası malzemesinin kontak direncine etkisi incelendi.

ACKNOWLEDGMENTS

I am very grateful to Prof.Dr.Süleyman KARADENİZ for his patient supervision, valuable and continuous encouragement throughout this study.

I would like to extend very special thanks to Prof.Dr.Onur SAYMAN for his support and helpful suggestions.

I also thank to technician Süleyman GÜNEŞ, and technician Ahmet YİĞİT for their outstanding job in manufacturing the experimental device and preparing the specimens, and to all my friends helped me.

M.Şemseddin ÇİMEN

CONTENTS

LIST OF FIGURES

LIST OF TABLES

NOMENCLATURES

$\bar{\sigma}$	:Equivalent stress.
H'	:Slope of the plot at the particular value of σ.
$\{F\}_{\sigma_o}$	:Load vector corresponding to the initial stress.
σ_1'	:Deviatoric stress.
R_m'	:Material resistance of a cylindrical workpiece.
$\bar{r}_\mu$	:Average radius of contacted circular areas.
ν	:Poisson's ratio.
∇	:Laplace operator.
ϕ	:Stress function.
ρ	:Electrical resistivity.
Π	:Potential energy.
$\phi(x)$	:A polynomial function.
$\alpha_{\mu C}$	:Angle of micro contact point.
τ_I	:Element initial stresses.
δ_{ij}	:Kronecker delta.
$\sigma_{or}, \sigma_{oz},$ $\tau_{orz}, \sigma_{o\theta}$	:Components of the initial stress vector.
$\sigma_r, \sigma_\theta, \sigma_z,$ $\tau_{rz}, \tau_{r\theta}, \tau_{z\theta}$	:Stress components in polar coordinates.
$\varepsilon_r, \varepsilon_\theta, \varepsilon_z,$ $\gamma_{r\theta}, \gamma_{rz}, \gamma_{z\theta}$	:Strain components in polar coordinates.
ε_{up}	:Uniaxial plastic strain.
$\varepsilon_x, \varepsilon_y, \gamma_{xy}$	:Strain components in Cartesian coordinates.
$\sigma_x, \sigma_y, \sigma_z,$ $\tau_{xy}, \tau_{xz}, \tau_{yz}$	:Stress components in Cartesian coordinates.
σ_y	:Yielding stress.
$[\varepsilon]$	:Strain matrix of an element.
$[B]^e$	:Strain-displacement matrix of an element,e.
$[C]$	:Elasticity matrix.
$[C]_{ep}$	:Elasto-plastic matrix.
$[K]$	:2nX2n stiffness matrix of the system.
$[K]^e$	:Stiffness matrix of the element,e.
$\{\varepsilon\}$	:Strain vector.
$\{\varepsilon\}_e$	:Elastic strain vector.
$\{\sigma\}_e$	:Elastic stress vector.
$\{\sigma\}^e$	:Stress components of an element,e.
$\{\delta\}_n$	:Displacement vector.
$\{\sigma\}_n$	:Stress vector corresponding to the $\{\delta\}_n$ in the elasto-plastic region.

$\{\varepsilon\}_p$	:Plastic strain vector.
$\{\sigma_o\}$	:Initial stress vector.
$\{\sigma_{rs}\}$	:Residual stress vector.
$\{F\}$	:2nX1 column vector of resultant nodal forces.
$\{F\}^{(e)}$	:Column vector of the nodal forces of an element,e.
$\{u\}$	:2nX1 column vector of the nodal displacements.
$\{u\}^{(e)}$	:Nodal displacements vector of an element,e.
A_m	:Contact regions containing metallic contact points.
A_{qm}	:Contact regions containing quasi-metallic contact points.
A_t	:Contact regions containing a foreign or thick film.
A_T	:Total value of contacted circular area.
b_μ	:Radius of the contacted circular area.
d	:Rivet diameter.
D	:Diameter of a micro contact point.
detJ	:Determinant of Jacobian matrix.
E	:Modulus of elasticity.
F	:General yield function.
$F_{\mu C}$	:Force carried by one micro contact point.
f^B	:Element body forces.
f^C	:Element concentrated forces.
F_k	:Clamping force.
f^S	:Element surface forces.
G	:Shear modulus.
g	:A improvement factor.
H	:Heat induced.
H_t	:The hardness of micro contact points.
H_v	:Vickers hardness.
I	:Current in amperes.
J	:Jakobian operator.
J^{-1}	:Inverse of the J.
K	:Hardening parameter.
k	:A constant.
l	:Length of current path.
$L_k(x)$	:Lagrange polynomial.
n	:Number of micro contact points.
$n_{\mu C}$	:Number of micro contact points on a ring.
N_i	:Interpolation functions.
n_r	:Number of ring.
$P_n(x,y)$	:nth order polynomial.
R	:Resistance.
r,θ,z	:Polar coordinates.
r,s,t	:Natural coordinates.
R,Z	:Body force components in polar coordinates.

r_μ :Radius of one micro contact point.
$R_{\mu C}$:Electrical resistance for a micro contact point.
R_{1KS} :Resistance for one circular electrode.
R_{2KS} :Resistance for one elliptical electrode.
r_a :Radius of electrode.
R_B :Spreading resistance.
R_C :Contact resistance.
R_{CBS} :Contact resistance between sheets.
R_{e2KS} :Resistance for two spherical electrodes.
r_{et} :Radius of the electrode tip.
R_F :Contact resistance caused by oxide or other contaminants.
R_i :Parallel resistances.
r_i, s_j :Sampling points of Gauss numerical integration.
R_{ij} :Radius at any point.
R_{KT} :Total contact resistance.
R_{LC} :Contact resistance between lower electrode and sheet.
R_{LE} :Material resistance of lower electrode.
R_{LM} :Material resistance of lower sheet.
R_{LW} :Electrical resistance of lower wire.
R_m :Material resistance.
R_{M1} :Material resistance of a sheet.
R_T :Total electrical resistance.
$R_{T\mu C}$:Total electrical resistance between sheets for all micro contact points.
R_{T1} :Total resistance for two workpieces.
R_{T2} :Total resistance for one workpiece.
R_{UC} :Contact resistance between upper electrode and sheet.
R_{UE} :Material resistance of upper electrode.
R_{UM} :Material resistance of upper sheet.
R_{UW} :Electrical resistance of upper wire.
s :Cross-section area of a conductor
T :Time.
t :Sheet thickness.
t_e :Thickness of an element.
u, v, w :Displacement components at any point.
U_{AB} :Voltage applied between A and B.
u_i, v_i :Displacement of the element nodes.
V_n :(n+1)-dimensional vector space.
w_i :Weight factor of Gauss numerical integration.
X, Y :Body force components in Cartesian coordinates.
$x, y, z,$ x', y', z' :Cartesian coordinates.
x_i, y_i :Coordinates of the element nodes.

The other notations have been defined in the chapters.

CHAPTER 1

INTRODUCTION

It might be thought that the electric resistance spot welding process has a restricted field of application because of the limited variation in joint design which is permissible-that is, lap joints in sheets of the same order of thickness. The processes, however, have extensive application in the joining of sheet metal not only in mild steels but also in stainless steels, heat resisting alloys, aluminium and copper alloys and reactive metals. Spot welding has been used on steel as thick as 3/4in. Such applications are rare, however, requiring massive machines and long weld times, so that the normal upper limit is in the region of 1/4in. Particularly attractive features of the resistance spot-welding process are the high speed of operation, ease of mechanization, the self-jigging nature of the lap joint and the absence of edge preparation or filler metal.

The short interval of time of most resistance-welding processes, cycle makes possible the welding of thin sections to heavy ones, the welding together of dissimilar metals and the welding together of metals which have different thickness simultaneously. The metallurgical advantage of this process is that the metal is held at a temperature that is within the grain-growth range for only a short period of time.

All resistance-welding methods require physical contact between the current-carrying electrodes and the parts to be joined. Pressure is also required to place the parts in contact and consolidate the joints. The heat is generated by the resistance to the passage of the current according to the Joule's law. Fortunately, temperatures produced by the passage of current through the workpieces to be welded are the highest at the contact points between the pieces, thus heat does not extend throughout their entire thicknesses. This feature promotes the rapid production of high-quality welds. The contact resistance between sheets where nugget and, therefore, the heat is required is the most important resistance. Resistance here is important in early period of the welding. It has long been known that contact resistance between two metallic surfaces disappears at much less than 1 cycle after the start of welding[48].For this reason, some investigations have been done to find whether

contact resistance has a considerable effect on heat generation or not.

Karadeniz[24] developed the relationship between contact resistance and clamping force by using experimental results for copper.

According to Dix[14], contact resistance has no considerable effect on heat generation and weld nugget formation during welding.

According to Lheureux, and Blotte[32], in the very short time in which the contact resistance is very high and effective, heating is concentrated only in the contact region and causes the specific resistance to be the highest in this region.

According to Apps[6], although the contact resistances are effective at the start of heating,the efficiency of heat conduction away from the workpieces into the electrodes is more important than the contact resistance in determining the heat build-up and the time required to form a molten weld nugget of a given volume.

Satoh, and Katayama, and Abe[45], using two-dimensional models, showed that the sheet separation which occurs before the start of heating or immediately afterwards restricts the current path so that the heat generation occurs effectively in the region adjacent to the contact surface between specimens. In addition, they concluded that the heat which is generated by the current through contact resistance during a very short time in which contact resistance vanishes is not so significant compared with the heat generated by bulk resistance, but the contact surface condition between the specimens, even after contact resistance has disappeared, is an effective cause of heat generation.

Eryürek, and Anık[5],[16] concluded that the surface roughness has a great effect on the weld properties.

Lobasov[34] developed a method of calculating the instantaneous and effective welding current values in spot welding from the given thermal cycle of the reference point using the finite element method.

Schwab[46] developed a computing program for the numerical temperature field calculation in resistance welding. He

used an explicit difference method to solve the two-dimensional thermal conduction equation.

Rawicz[44] derived a correlation between electrical resistance and mechanical strength of welded joints, based on a model of the dislocation structure of the heat affected zone.

Abramov[1] developed a method of determining the plastic deformation of the micro projections of the bonded surface in solid-state pressure welding with heating.

Although some authors say that contact resistance has no considerable effect on heat generation and weld nugget formation during welding, it is known that the highest temperature occurs in the contact surface of the workpieces and the heat is generated by the resistance to the passage of the current. If contact resistance has no considerable effect on heat generation, temperatures in everywhere of the welding region have to be equal to each other for a condition that cooling does not exist. It is also known that material resistance increases with increasing the temperature and the temperature around the contact surface between sheets is greater than the temperature in the other regions of the workpieces in the early period of the welding, so material resistance around the contact surface must also be greater than the material resistance in the other regions of the workpieces. Material resistance around the contact surface becomes greater during welding because of the fact that the temperature here always becomes greater. So that, it can be said that the effect of contact resistance continues during welding although it disappears at much less than 1 cycle after the start of welding.

During recent years, considerable progresses have been made in solving the practically important problems. In cases where rigorous solution can not be readily obtained, approximate methods have been developed. For example, perturbation, power series, probability schemes, method of weighted residuals, finite difference method, Ritz method, and finite element method. In same cases, solutions have been obtained by using experimental methods. As an example of this, the photoelastic method of solving two-, or three-dimensional problems of elasticity may be mentioned.

In this investigation, finite element method and an experimental method have been used to find out the relationship between contact resistance and clamping force. Some

experimental measurements have also been carried out to show the validity of the solution. In addition, stress distribution in the workpiece, and on the spherical surface of the micro contact point, forces applied to the micro contact points, the effects of the thickness of the workpiece, and the electrode tip, and the material of the workpiece to the contact resistance have been investigated. When the problem has been solved by using finite element method, the effects of temperature have been neglected because of the fact that contact resistance disappears at much less than 1 cycle after the start of welding.

It is clear that high-speed computers affect the finite element methods, and now, finite element method known as one of the approximate-solution methods is a numeric method, and it finds results which are almost exact solution values, and it is accepted by authorities as a feasible solution technic. A lot of investigations have been done by using finite element methods so far, and some of them used in this study are as follows:

Zienkiewicz, and Valliappant, and King[56] proposed an "initial stress" computational process to yield more rapid convergence than alternative approaches and to permit large load increments without violating the yield criteria and thus simply to establish lower bound solutions.

Marcal, and King[35] suggested a method that describes increasing elasto-plastic analysis at two dimensional stress system. The relation between increasing stress and changing forms were obtained from Von-Mises yield criteria and Prandtl-Reuss equation. They also gave the solution for plane plate with a hole in the middle.

Karakuzu, and Sayman[26],[27] analyzed elasto-plastic stresses on rotating isotropic and anisotropic discs with hole, and calculated the residual stresses occurred by using finite element method.

Özel, and Belevi[42] observed that the strength of the silent chain links can be increased by residual stresses using finite element method.

Şen, and Önel[49] developed a computer program to find out stresses at any point within the deforming material at any state of deformation for different geometries and for the cases of different friction coefficients between the

die and material for upsetting and extrusion processes by using finite element method.

The other references used in this study have been given in References.

In the second chapter, two-dimensional elasticity is presented in the general form and plane-stress and axi-symmetric problems are introduced.

The general finite element method procedures are defined in the third chapter. These are generation of the finite element meshes, the isoparametric elements, interpolation functions, obtaining the element properties, assembly of the elements, solving the system equations, and making additional computations.

Definition of two-dimensional isoparametric finite element and the formulation and the calculation of their matrices and numerical integration are given in general form in the fourth chapter.

In the fifth chapter, general theory of plasticity is given. The following subjects are presented: Yield surface, total stress-strain relations, Prandtl-Reuss relations. In addition, "Initial Stress Method" is defined for calculation of elasto-plastic stress.

In the sixth chapter, definition of welding, and basic requirements of welding, and classification of welding processes are given.

In the seventh chapter, electric resistance welding, and its principles are presented.

In the eighth chapter, contact resistance, and methods to find relationship between contact resistance and load experimentally are presented.

In the ninth chapter, definition of the problem is given. It is also explained how the boundary conditions of problem and external forces are applied, and experimental studies and the method of experimental measurement used to find contact resistances for various forces are carried out.

Solutions, results and discussion take place in the tenth chapter. Conclusions are given in the eleventh chapter.

CHAPTER 2

BASIC EQUATIONS FOR TWO DIMENSIONAL ELASTIC PROBLEMS

2.1 Introduction

During recent years, the theory of elasticity has found considerable application in the solution of engineering problems. There are many cases in which the elementary methods of strength of materials are inadequate to furnish satisfactory information regarding stress distribution in engineering structures.

All structural materials possess to a certain extent of the property of elasticity, if external forces, producing deformation of a structure, do not exceed a certain limit. The deformation disappears with the removal of the forces in the elastic region.

In the theory of elasticity, It is assumed that the bodies undergoing the action of external forces are perfectly elastic. It is also assumed that the matter of an elastic body is homogeneous and continuously distributed over its volume so that the smallest element cut from the body possesses the same specific physical properties as the body. In addition, it is assumed that the body is isotropic to simplify the problem. Namely, the elastic properties of this body are the same in all direction.

Structural materials usually do not satisfy the above assumptions. Such an important material as steel, for instance, when studied with a microscope, is seen to consist of various kinds of crystals and various orientations. The material is very far from being homogeneous, but experience shows that elastic solutions based on the assumptions of homogeneity and isotropy can be applied to steel structures with very great accuracy.

There are 15 unknown quantities in three dimensional elasticity. These are six stress components, six strain components and three displacement components. Fig.2.1 shows the stress components for three-dimensional cases. So that 15 independent equations are necessary to solve a problem in three dimensional elasticity. The boundary conditions should be also added to these equations. Three equations of equilibrium, six stress-strain relations, and six strain-displacement relations can be written to solve this type of

problem. It should be noted that the equations of compatibility are derived from the strain-displacement relations so that, if 15 independent equations discussed above are satisfied, the equations of compatibility will also be satisfied.

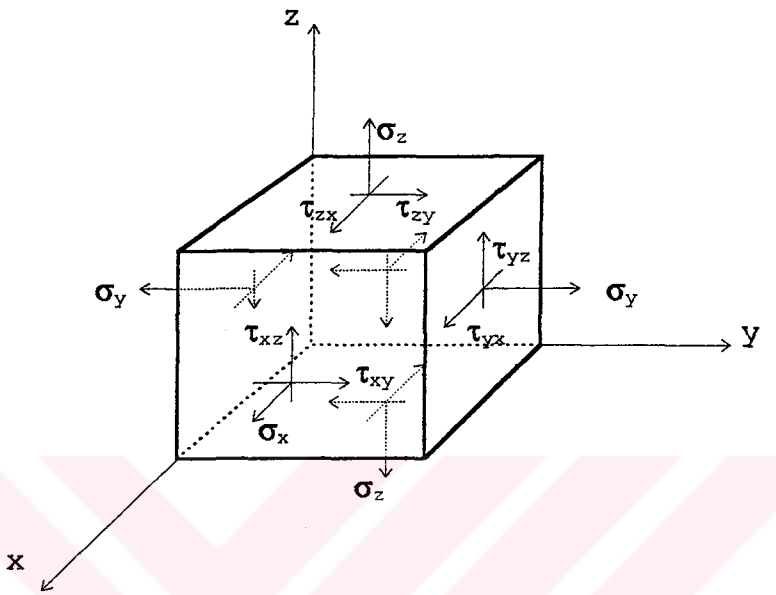

Figure 2.1 Stress components for three-dimensional cases.

2.2 Plane Stress Problems

Consider a thin plate is loaded by forces applied at the boundary where the load is parallel to the plane of the plate and distributed uniformly over the thickness as shown in Fig.2.2. In this case, the stress components σ_z, τ_{xz}, τ_{yz} are equal to zero on both faces of the plate, and it may be assumed that they are also equal to zero within the plate. Then, the state of the stress is specified by σ_x, σ_y, τ_{xy} only, and is called as plane stress. In the case of plane stress, it may also be assumed that these three components are independent of z, they do not vary through the thickness.

There are 8 unknown quantities in two dimensional elasticity. These are 3 stress components, 3 strain components and 2 displacement components. So that 8 independent equations are necessary to solve a problem in two dimensional elasticity. The boundary conditions should be also added to these equations. Two equations of equilibrium, three stress-strain relations, and three

strain-displacement relations can be written to solve this type of problem.

If X, Y denote the components of body force corresponding unit volume, the equations of equilibrium are,

$$\frac{\partial \sigma_x}{\partial x}+\frac{\partial \tau_{xy}}{\partial y}+X=0 \qquad (2.1)$$

$$\frac{\partial \sigma_y}{\partial y}+\frac{\partial \tau_{xy}}{\partial x}+Y=0 \qquad (2.2)$$

where, $\sigma_x, \sigma_y, \tau_{xy}$ denote stress components. In the case of a two dimensional problem, it is necessary to solve these differential equations of equilibrium and the solution must satisfy the boundary conditions. These equations are derived by application of the equation of static for absolutely rigid bodies. Elastic deformation of the body must also be considered to obtain the solution. In the case of two dimensional problem, strain-displacement relations are,

$$\varepsilon_x = \frac{\partial u}{\partial x}, \quad \varepsilon_y = \frac{\partial v}{\partial y}, \quad \gamma_{xy} = \frac{\partial u}{\partial y} + \frac{\partial v}{\partial x} \qquad (2.3)$$

where, ε_x, ε_y and γ_{xy} denote strain components, and u and v denote displacement components.

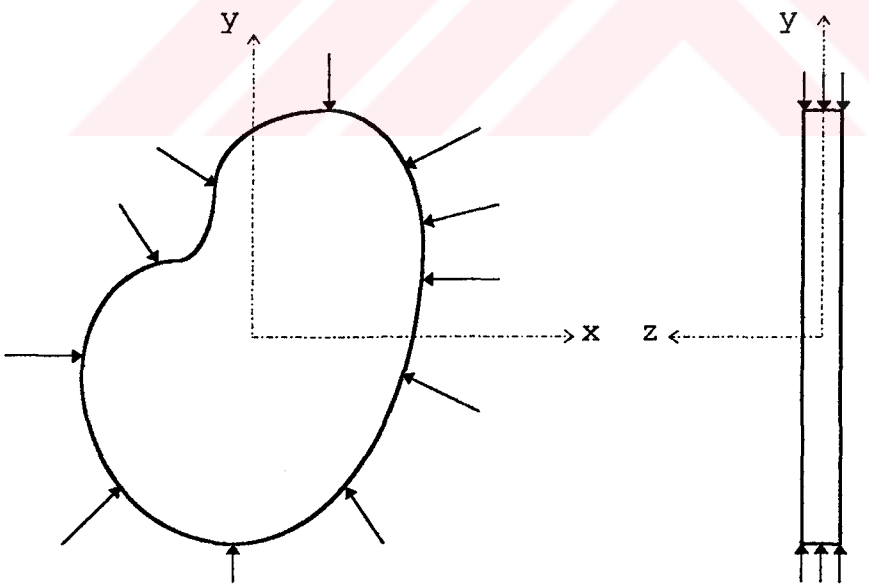

Figure 2.2 An example for state of plane stress.

In the case of plane stress, stress-strain relations are,

$$\varepsilon_x = \frac{1}{E}(\sigma_x - \nu\sigma_y), \qquad \varepsilon_y = \frac{1}{E}(\sigma_y - \nu\sigma_x) \qquad (2.4)$$

$$\gamma_{xy} = \frac{1}{G}\tau_{xy}, \qquad G = \frac{E}{2(1+\nu)} \tag{2.5}$$

$$\gamma_{xy} = \frac{2(1+\nu)}{E}\tau_{xy} \tag{2.6}$$

and

$$\gamma_{xz}=\gamma_{yz}=0, \qquad \varepsilon_z = -\frac{\nu}{E}(\sigma_x + \sigma_y) \tag{2.7}$$

where, E denotes modulus of elasticity and ν denotes Poisson's ratio and G denotes shear modulus. In the case of a two dimensional problem, the condition of compatibility is,

$$\frac{\partial^2 \varepsilon_x}{\partial y^2} + \frac{\partial^2 \varepsilon_y}{\partial x^2} = \frac{\partial^2 \gamma_{xy}}{\partial x \partial y} \tag{2.8}$$

This equation of the compatibility is derived from the strain-displacement relations. The condition can be transformed into a relation between the components of stress. This is,

$$\left(\frac{\partial^2}{\partial x^2} + \frac{\partial^2}{\partial y^2}\right)(\sigma_x + \sigma_y) = 0 \tag{2.9}$$

$$\nabla^2 (\sigma_x+\sigma_y)=0 \tag{2.10}$$

$$\nabla^2 = \frac{\partial^2}{\partial x^2} + \frac{\partial^2}{\partial y^2} \tag{2.11}$$

where, ∇ is called the Laplace or harmonic operator.

2.3 Stress Function

A solution of two dimensional problem can be reduced to a differential equation of equilibrium by introducing a new function, called the stress function or Airy stress function. This differential equation contains compatibility equation and the boundary conditions.

If it is assumed that the weight of the body is the only body force,

$$\sigma_x = \frac{\partial^2 \phi}{\partial y^2} - \rho g y, \qquad \sigma_y = \frac{\partial^2 \phi}{\partial x^2} - \rho g y, \qquad \tau_{xy} = -\frac{\partial^2 \phi}{\partial x \partial y} \tag{2.12}$$

In this manner, we can get a variety of solutions of the equation of equilibrium. The true solution of the problem

is that which satisfies also the compatibility equation. So that the stress function ϕ must satisfy the equation,

$$\frac{\partial^4\phi}{\partial x^4} + 2\frac{\partial^4\phi}{\partial x^2\partial y^2} + \frac{\partial^4\phi}{\partial y^4} = 0 \qquad (2.13)$$

This equation is found substituting expressions Eq.2.12 in to compatibility equation Eq.2.9 and it is called a biharmonic equation. Thus, the equation of a two-dimensional problem, when the weight of the body is the only body force, has been reduced a differential equation (Eq.2.13) which satisfies the boundary conditions of the problem. It is known that,

$$\frac{\partial^4}{\partial x^4} + 2\frac{\partial^4}{\partial x^2\partial y^2} + \frac{\partial^4}{\partial y^4} = \left(\frac{\partial^2}{\partial x^2} + \frac{\partial^2}{\partial y^2}\right)^2 = (\nabla^2)^2 = \nabla^4 \qquad (2.14)$$

So that, Eq.2.13 can be written as,

$$\nabla^4\phi = 0 \qquad (2.15)$$

2.4 Two Dimensional Problems In Polar Coordinates

In analysis of stresses in circular bodies, using polar coordinates is more convenient than using Cartesian coordinates. The basic equations of two dimensional elastic problem discussed above can be easily transformed from Cartesian to polar coordinates. The equations of equilibrium in polar coordinates are,

$$\frac{\partial\sigma_r}{\partial r} + \frac{1}{r}\frac{\partial\tau_{r\theta}}{\partial\theta} + \frac{\sigma_r - \sigma_\theta}{r} + R = 0 \qquad (2.16)$$

$$\frac{1}{r}\frac{\partial\sigma_\theta}{\partial\theta} + \frac{\partial\tau_{r\theta}}{\partial r} + \frac{2\tau_{r\theta}}{r} = 0 \qquad (2.17)$$

where, R is the body force corresponding unit volume in the radial direction and σ_r, σ_θ, $\tau_{r\theta}$ denote stress components.

Strain-displacement relations in polar coordinates are,

$$\varepsilon_r = \frac{\partial u}{\partial r}, \qquad \varepsilon_\theta = \frac{u}{r} + \frac{1}{r}\frac{\partial v}{\partial\theta} \qquad \gamma_{r\theta} = \frac{1}{r}\frac{\partial u}{\partial\theta} + \frac{\partial v}{\partial r} - \frac{v}{r} \qquad (2.18)$$

where, $\varepsilon_r, \varepsilon_\theta, \gamma_{r\theta}$ denote strain components.

Stress-Strain relations in polar coordinates are,

$$\varepsilon_r = \frac{1}{E}(\sigma_r - \nu\sigma_\theta), \qquad \varepsilon_\theta = \frac{1}{E}(\sigma_\theta - \nu\sigma_r), \qquad \gamma_{r\theta} = \frac{1}{G}\tau_{r\theta} \qquad (2.19)$$

If the stress distribution is symmetrical with respect to the origin, the stress components don't depend on θ and they are function of r only. From symmetry, it follows also that the shearing stress $\tau_{r\theta}$ must vanish. Then, only the first of the two equation of equilibrium remains, and we have,

$$\frac{\partial \sigma_r}{\partial r} + \frac{\sigma_r - \sigma_\theta}{r} + R = 0 \qquad (2.20)$$

In this case, strain-displacement are,

$$\varepsilon_r = \frac{\partial u}{\partial r}, \qquad \varepsilon_\theta = \frac{u}{r}, \qquad \gamma_{r\theta} = 0 \qquad (2.21)$$

Stress-strain relations are,

$$\varepsilon_r = \frac{1}{E}(\sigma_r - \nu\sigma_\theta), \qquad \varepsilon_\theta = \frac{1}{E}(\sigma_\theta - \nu\sigma_r), \qquad \gamma_{r\theta} = 0 \qquad (2.22)$$

There are 5 unknown quantities in the case discussing above. These unknown quantities are $\sigma_r, \sigma_\theta, \varepsilon_r, \varepsilon_\theta$ and u. They can be found by using equations shown above.

2.5 Axi-Symmetric Problems

Many problems in stress analysis which have practical importance are deformed symmetrically with respect to the axis of revolution (Fig.2.3). The simplest examples are the circular cylinder strained by uniform internal or external pressure, and the rotating circular disk. It is often convenient to use polar coordinates for these type of problems.

The deformation being symmetrical with respect to the z axis, it follows that the stress components are independent of the angle θ, and all derivatives with respect to θ vanish. The components of shearing stress $\tau_{r\theta}$ and $\tau_{\theta z}$ also vanish on account of the symmetry. Thus, equations of equilibrium are,

$$\frac{\partial \sigma_r}{\partial_r} + \frac{\partial \tau_{rz}}{\partial_z} + \frac{\sigma_r - \sigma_\theta}{r} = 0 \qquad (2.23)$$

$$\frac{\partial \tau_{rz}}{\partial r} + \frac{\partial \sigma_z}{\partial z} + \frac{\tau_{rz}}{r} = 0 \qquad (2.24)$$

where, $\sigma_r, \sigma_\theta, \sigma_z$ and τ_{rz} denote stress components.

Strains and stresses involved in the analysis of axi-symmetric solids are indicated in Fig.2.4.

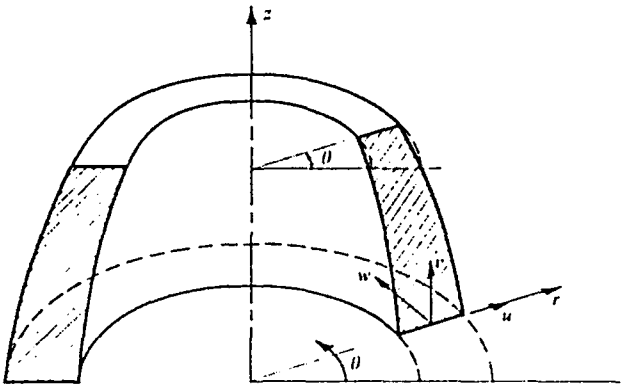

Figure 2.3 An axi-symmetric solid. Co-ordinates and displacements components in an axi-symmetric body.

The strain-displacement relation for axi-symmetric problems are,

$$\varepsilon_r = \frac{\partial u}{\partial r}, \quad \varepsilon_\theta = \frac{u}{r}, \quad \varepsilon_z = \frac{\partial w}{\partial z}, \quad \gamma_{rz} = \frac{\partial u}{\partial z} + \frac{\partial w}{\partial r} \tag{2.25}$$

where, $\varepsilon_r, \varepsilon_\theta, \varepsilon_z$ and γ_{rz} denote strain components.

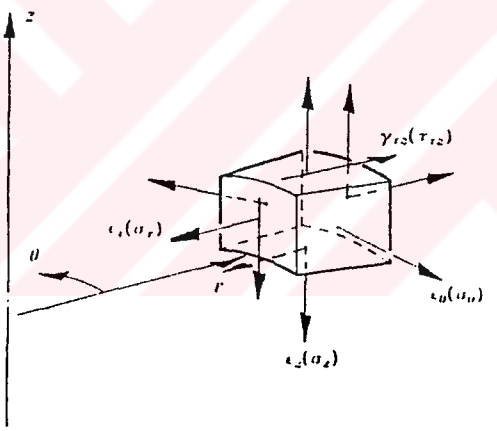

Figure 2.4 Strains and stresses involved in the analysis of axi-symmetric solids.

The stress-strain relations for axi-symmetric problems are,

$$\varepsilon_r = \frac{1}{E}[\sigma_r - \nu(\sigma_\theta + \sigma_z)] \tag{2.26}$$

$$\varepsilon_\theta = \frac{1}{E}[\sigma_\theta - \nu(\sigma_r + \sigma_z)] \tag{2.27}$$

$$\varepsilon_z = \frac{1}{E}[\sigma_z - \nu(\sigma_r + \sigma_\theta)] \tag{2.28}$$

$$\gamma_{rz} = \frac{2(1+\nu)}{E}\tau_{rz} \tag{2.29}$$

CHAPTER 3

FINITE ELEMENT METHOD

3.1 Introduction

Scientists and engineers are often faced with practical physical problems whose solutions by conventional analytical methods are either too difficult or even impossible. In recent years, the finite element method of analysis has rapidly become a very popular technique for the computer solution of complex problems in engineering.

The finite element method can be understood as an extension of earlier established analysis techniques. At present, the finite element method is the most general analysis tool and is used in practically all fields of engineering analysis. For example, finite element methods are used in analysis of heat transfer, fluid flow, lubrication, electric and magnetic field, electric motors, heat engines, ships, airframes, buildings, spacecraft, and so on.

The development of the finite element method as an analysis tool essentially began with the advent of the electronic digital computer. For the numerical solution of a structural or continuum problem it is basically necessary to establish and solve algebraic equations that govern the response of the system. Using the finite element method on a digital computer, it becomes possible to establish and solve the governing equations for complex problems in a very effective way. The finite element method was initially developed on a physical basis for the analysis of problems in structural mechanics; however, it was soon recognized that the method can be applied equally well to the solution of many other classes of problem.

In this method, a continuum complex region is discretized into simple geometric shapes called finite elements. The material properties and the governing relationships are considered over these elements and expressed in terms of unknown values at element corners.

Fig.3.1.a shows a plane structure loaded by pressure, "p". Fig.3.1.b consists of some triangular and quadrilateral elements (If done properly, there is no difficulty in combining the different element types). Block dots, called nodes or node points, indicate where elements are connected

to one another. The distributed pressure, p, has been converted to concentrated forces at nodes.

From Fig.3.1, it may appear that discretization is accomplished simply by saving the "continuum" into pieces and then pinning the pieces together again at node points. But such a model does not deform like continuum. Strain concentrations appear at the nodes under load. The elements must be restricted in their deformation modes as edges will be kept straight (Fig.3.1.c), then adjacent elements will neither overlap nor separate. In this way, we satisfy the basic requirement that deformation of a continuum medium must be compatible.

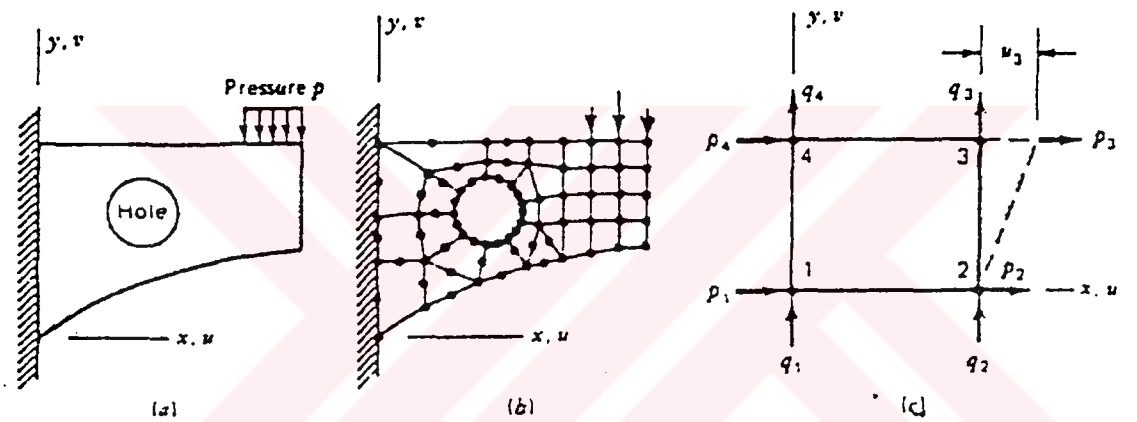

Figure 3.1 (a)A plane structure of arbitrary shape. (b)A possible finite element model of the structure. (c) A plane rectangular element showing nodal forces P_i and Q_i. The dashed line shows the deformation displacements of node 3.

A finite element analysis typically involves the following steps:

1. Discretization of continuum problems
2. Selection of interpolation functions
3. Finding the element properties
4. Assembly of the element properties
5. Solving the system equation
6. Making additional computations if desired.

The power of the finite element is its versatility. The method can be applied to various physical problems. The body analyzed can have arbitrary shape, loads, and support condition. The mesh can mix different types, shapes, and physical properties of elements. The great

versatility is contained within a single computer program. Preparing input data, selection of problem type, geometry, boundary conditions, element selection, and so on are prepared by user.

The finite element method also has disadvantages. A specific numerical result is found for a specific problem. A finite element analysis provides no closed-form solution that permits analytical study of the effects of changing various parameters. A computer, a reliable program, and intelligent use are essential. Experience and good engineering judgment are needed in order to define a good model. Many input data required and voluminous output must be sorted and understood.

3.2 Generation of Finite Element Meshes

The two-dimensional region is divided into straight-sided triangles. The points where the corners of the triangles meet are called nodes, and each triangle formed by three nodes and three sides is called an element. The elements fill the entire region except a small region at the boundary. This unfilled region exists for curved boundaries and it can be reduced by choosing smaller elements or elements with curved boundaries. The idea of the finite element method is to solve the continuous problem approximately, and this unfilled region contributes to some part of this approximation.

It is an easy matter to obtain a coarse subdivision of the analysis domain with a small number of isoparametric elements. The originally circular boundaries in Fig.3.2.a are approximated by simple parabola and a geometric error can be developed there. Another form of mapping, originally developed for representation of complex car motor body shapes, can be adapted to overcome this difficulty. If the coordinates x and y are used by interpolation or shape function in local coordinates, then any complex region can be mapped by any single element. The region of Fig.3.2 is in fact so mapped and a mesh subdivision obtained directly without any geometric error on the boundary.

3.3 The Isoparametric Elements

The principal idea of the isoparametric finite element formulation is to achieve the relationship between the element

displacements at any point and the element nodal point displacements directly through the use of interpolation functions (also called shape functions). This means that the transformation matrix is not evaluated; instead, the element matrices corresponding to the required degrees of freedom are obtained directly.

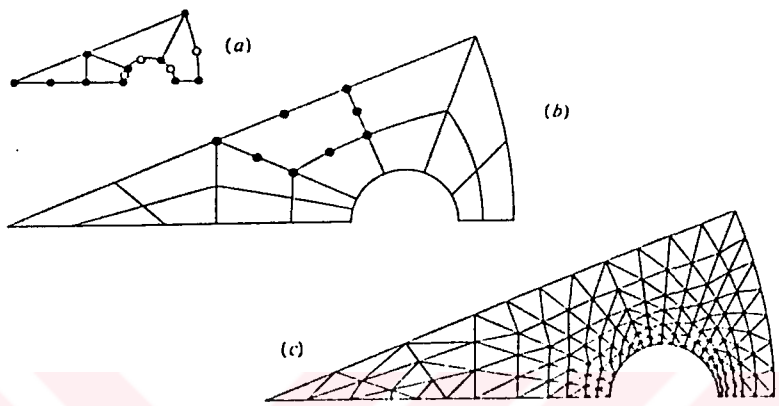

Figure 3.2 Automatic mesh generation by parabolic isoparametric elements. (a) Specified mesh points. (b) Automatic subdivision into small number of isoparametric elements. (c) Automatic subdivision into linear triangles.

The isoparametric formulation makes it possible to generate elements which are non-rectangular and have curved sides. These shapes are used in grading a mesh from coarse to fine, in modeling arbitrary shapes, and in modeling curved boundaries (Fig.3.3). The isoparametric family includes elements for plane, solid, plate, and shell problems. There are also special elements for fracture mechanics and elements for non-structural problems.

Natural coordinate systems (r,s,t) must be used in the isoparametric elements shown in Fig.3.4. Displacements are expressed in terms of natural coordinates, but must be differentiated with respect to global coordinates x, y, and z. Accordingly, a transformation matrix must be obtained. In addition, integration's must be done numerically rather than analytically if elements are non-rectangular.

The term isoparametric means the same parametric. The nodal values may or may not be associated with the same nodes as used to specify the element geometry. For example in Fig.3.5 the points marked with a circle are used to define the element geometry. We could use the values defined at

nodes marked with a square to define the variation of the unknown. In Fig.3.5.(a), the same points define the geometry and the finite element analysis points. If the shape function defining geometry and finite element analysis points are the same, the elements will be called isoparametric.

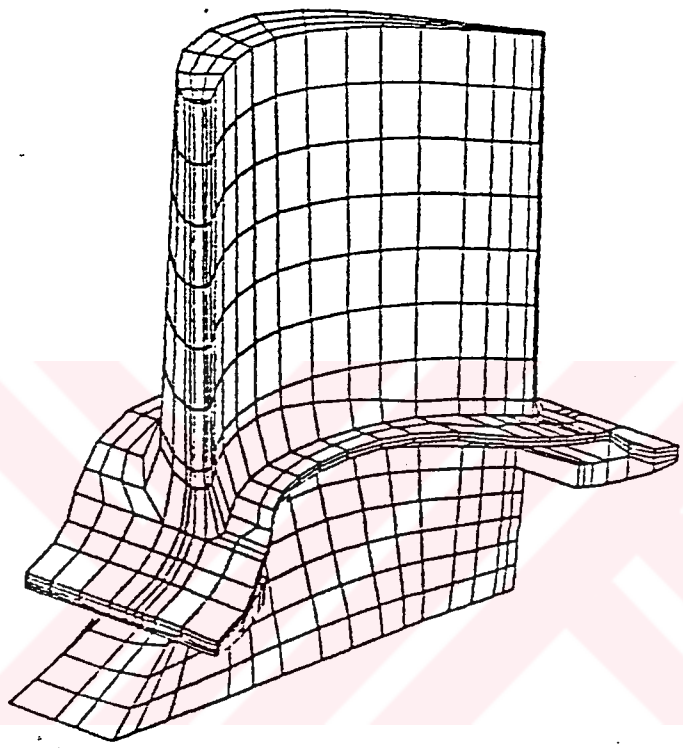

Figure 3.3 Tribune blade, modeled by solid element.

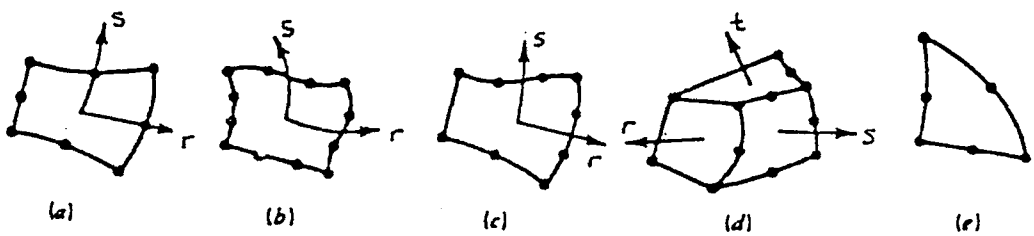

Figure 3.4 Example isoparametric elements. (a)Quadratic plane element. (b)Cubic plane element. (c)A "degraded" cubic element. The left and lower sides can be joined to linear and quadratic elements.(d)Quadratic solid element with some linear edges. (e)A quadratic plane triangle.

We could, however, use only the four corner points to define the variation of unknown, Fig.3.5.(b). Such an element is called as super-parametric. The variation of geometry is more general than variation of actual unknown. Similarly, if for instance we introduce more nodes to define actual unknown that are used to define geometry, the elements will be called sub-parametric, Fig.3.5.(c). Such elements are more often used in practice.

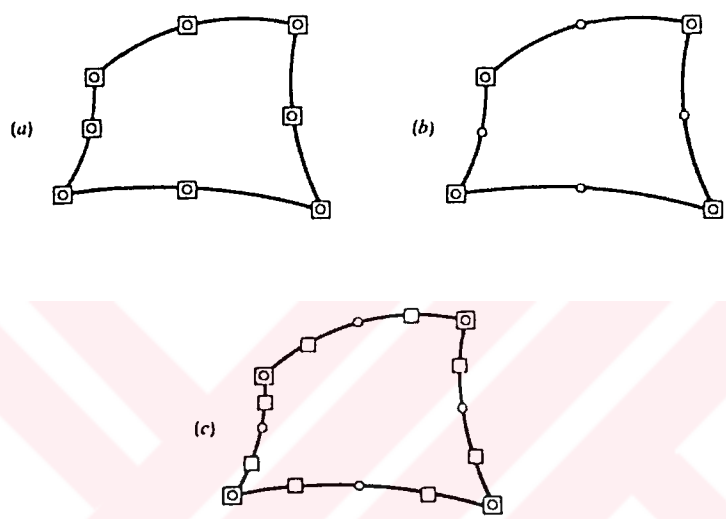

Figure 3.5 Various elements specifications. O point at which coordinate specified, □ points at which nodal unknown parameters specified.(a) Isoparametric, (b) Superparametric, (c) Subparametric.

An important consideration in the construction of curved elements is preservation of the continuity conditions in the global coordinate system. In this regard, three useful guidelines have been advanced:

1. If two adjacent curved elements are generated from parent elements whose interpolation functions satisfy inter element continuity, these curved isoparametric elements will be continuous.
2. If the interpolation functions are given in the local coordinate system and they are continuous in the parent element, they will also be continuous in the curved isoparametric elements.
3. The isoparametric element formulation offers the attractive feature that, if the completeness criterion is satisfied in the parent element, it is automatically satisfied in the curved isoparametric element.

3.4 Interpolation Functions

The interpolations of the element coordinates and element displacements using the same interpolation functions, which are defined in a natural coordinate system, are the basis of the isoparametric finite element formulation.

In the finite element literature, the functions used to represent the behavior of a field variable within an element are called interpolation functions, shape functions, or approximating functions. Although it is conceivable that many types of functions could serve as interpolation functions, only polynomials have received widespread use. The reason is that polynomials are relatively easy to manipulate mathematically, in order words, they can be integrated or differentiated without difficulty. Trigonometric functions also posses this property, but they are seldom used.

Ignoring for the moment any inter element continuity considerations, we can say that the order of the polynomial used to represent the field variable within an element depends on the number of degrees of freedom. In other words, the number of coefficients in the polynomial should be equal to the number of nodal variables to evaluate these coefficients.

We could not expect a good approximations to the reality if our field variable representation change with changing origin or orientation of the coordinate system. Hence, our polynomial interpolation functions must ensure geometric isotropy.

Fortunately, we have two simple guidelines that allow us construct polynomial series with the desired property:

1. Polynomials of order n that are complete (contain all the terms) have geometric isotropy.
2. Polynomials of order n that are incomplete, yet contain the appropriate terms to preserve symmetry, have geometric isotropy.

There are three types of polynomials as,

1. One independent variable
2. Two independent variable
3. Three independent variable

Here, only two independent variable will be given.

3.4.1 Two Independent Variable

In two dimensions, a complete nth-order polynomial may be written as,

$$P_n(x,y)=\sum_{k=1}^{T_n}\alpha_k x^i y^i, \qquad i+j\le n \tag{3.1}$$

where, the number of terms in the polynomial is

$$T_n=\frac{(n+1)(n+2)}{2} \tag{3.2}$$

second-order polynomials with two independent variable are given as,

$$P_2(x,y)=\alpha_1+\alpha_2 x+\alpha_3 y+\alpha_4 xy+\alpha_5 x^2+\alpha_6 y^2 \tag{3.3}$$

3.4.2 Interpolation Functions Of Rectangular Elements

Interpolation functions have been developed for one, two, and three dimensional elements. Here, only two dimensional interpolation function will be shown for rectangular element.

The basic ideas can be illustrated by a simple example in two dimensions. Suppose that we wish to construct a rectangular element with nodes positioned at the corners of the element shown Fig.3.6.(a). If we assign one value of interpolation function to each node, the element then has four degrees of freedom, and we may select as an interpolation model a four-term polynomial such as,

$$P(x,y)=\alpha_1+\alpha_2 x+\alpha_3 y+\alpha_4 xy \tag{3.4}$$

and for rectangular element with eight nodes (Fig.3.6.(b)), an eight-term polynomial is chosen as,

$$P(x,y)=\alpha_1+\alpha_2 x+\alpha_3 y+\alpha_4 xy+\alpha_5 x^2+\alpha_6 y^2+\alpha_7 x^2 y+\alpha_8 xy^2 \tag{3.5}$$

3.4.3 Natural Coordinates

The interpolation functions are defined in the natural coordinate system of the element, which has variables r,s, and t that each vary from -1 to +1. The fundamental property of the interpolation function is that its value in the natural coordinate system is unity at node i and is zero at all other nodes. We may construct natural coordinate system

for two-node line elements, three-node triangular elements, four-node rectangular elements, and so on into n-dimensional hyperspace. Natural coordinates in n dimensions are called barycentric coordinates.

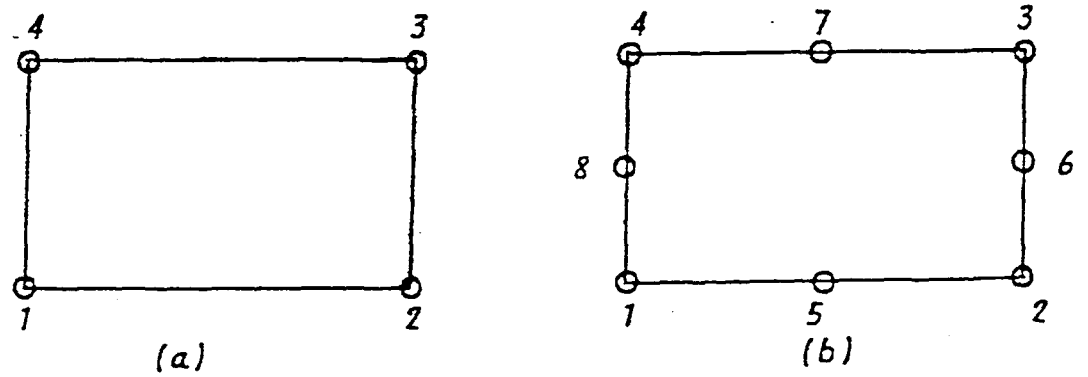

Figure 3.6 Rectangular elements. (a) Four-node element, (b) Eight-node element

The basic purpose of the natural coordinate system is to describe the location of a point inside an element in terms of coordinates associated with the nodes of the element. It will become evident that the natural coordinates are functions of the global Cartesian coordinate system in which the element is defined.

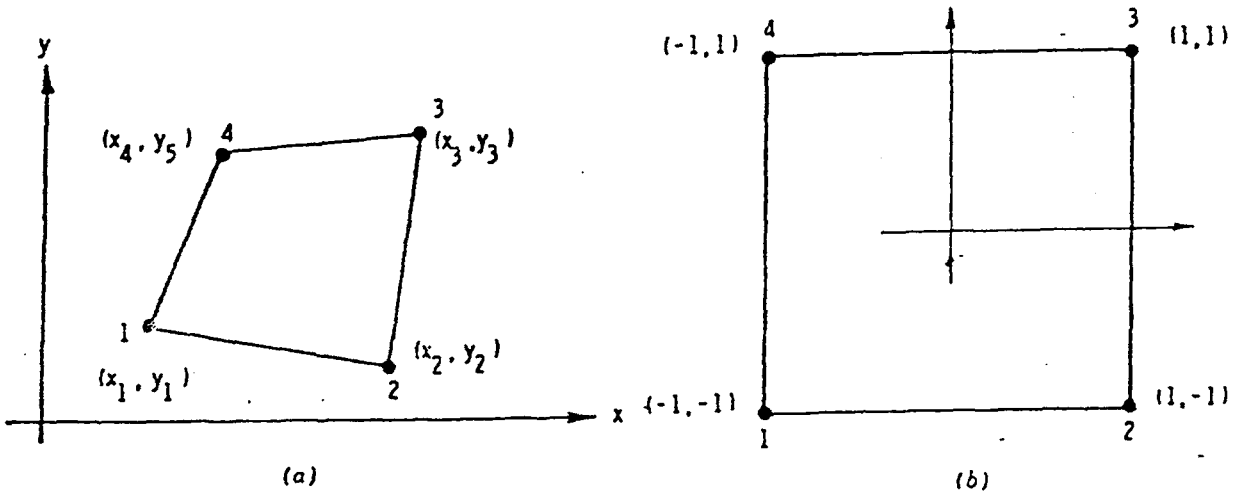

Figure 3.7 Natural coordinates for a general quadrilateral. (a) Cartesian coordinates, (b) Natural coordinates.

Here only natural coordinate will be shown for a four-node quadrilateral element in two dimensions. Fig.3.7 shows a

general quadrilateral elements in the global Cartesian coordinate system and local natural coordinate system. The quadrilateral element whose origin is at the center in the natural coordinate system is a square with sides extending $r=\pm1$, $s=\pm1$ (Fig.3.7.(b)). The local and global coordinates are related by the following equations:

$$x=\frac{1}{4}[(1-r)(1-s)x_1+(1+r)(1-s)x_2+(1-r)(1+s)x_3+(1+r)(1+s)x_4] \qquad (3.6)$$

$$y=\frac{1}{4}[(1-r)(1-s)y_1+(1+r)(1-s)y_2+(1-r)(1+s)y_3+(1+r)(1+s)y_4] \qquad (3.7)$$

3.4.4 Lagrange Polynomials

Assume that $F(x)$ has been evaluated at the $n+1$ distinct points $x_0, x_1, \ldots\ldots, x_n$ to obtain $F_0, F_1, \ldots\ldots, F_n$, respectively, and that a polynomial $\Phi(x)$ is to be passed through these data. Then there is a unique polynomial $\Phi(x)$ given as,

$$\Phi(x)=a_0+a_1x+a_2x^2+\cdots\cdots+a_nx^n \qquad (3.8)$$

$\Phi(x)$ is equal to $F(x)$ at the $n+1$ interpolating points approximately. The number of evaluations of $F(x)$ and the positions of the sampling points in the interval from a to b determines how well $\Phi(x)$ approximates to $F(x)$.

A more convenient way to obtain $\Phi(x)$ is to use Lagrangian interpolation. First, it can be said that the $n+1$ functions $1, x, x^2, \ldots\ldots, x^n$ form an $(n+1)$-dimensional vector space, called V_n, in which $\Phi(x)$ is an element. Since the coordinates $a_0, a_1, a_2, \ldots\ldots, a_n$ of $\Phi(x)$ are relatively difficult to evaluate, we seek to use a different basis for the space V_n, in which the coordinates of $\Phi(x)$ are more easily evaluated. This basis is provided by the fundamental polynomials of Lagrangian interpolation, given as,

$$L_j(x)=\sum_{i=0;i\neq j}^{n}\frac{x-x_i}{x_j-x_i}=\frac{(x-x_0)(x-x_1)\cdots(x-x_{j-1})(x-x_{j+1})\cdots(x-x_n)}{(x_j-x_0)(x_j-x_1)\cdots(x_j-x_{j-1})(x_j-x_{j+1})\cdots(x_j-x_n)} \qquad (3.9)$$

and $$L_j(x_i)=\delta_{ij} \qquad (3.10)$$

where δ_{ij} is the Kronecker delta; i.e., $\delta_{ij}=1$ for $i=j$, and $\delta_{ij}=0$ for $i\neq j$. Using the property in (Eq.3.10), the coordinates of the base vectors are simply the values of $F(x)$, and the polynomial $\Phi(x)$ is,

$$\Phi(x) = F_0 L_0(x) + F_1 L_1(x) + \cdots + F_n L_n(x) \qquad (3.11)$$

For example, suppose that an arbitrary function $\Phi(x)$ over an interval on the x axis is given by discrete values at four points in the closed interval $[x_0, x_3]$ Fig.3.8.(a). A polynomial at degree 3 passing through the four discrete values $\Phi_i = \Phi(x_i)$ $(i=0,1,2,3)$ and approximating the function $\Phi(x)$ in the interval may be written at once as,

$$\Phi(x) = \overline{\Phi}(x) = \sum_{i=0}^{3} \Phi_i L_i(x_i) = [L]\{\Phi\} \qquad (3.12)$$

and we recognize that $L_i(x)$ plays role as $N_i(x)$.

The Lagrange polynomials L_i in the expression for $\Phi(x)$ are sometimes called Lagrangian interpolation coefficients. Fig.3.8.(b) shows how these coefficients take the value zero or unity as required. The coefficient for Φ_2, for instance, would become,

$$L_1(x) = \frac{(x-x_0)(x-x_2)(x-x_3)}{(x_1-x_0)(x_1-x_2)(x_1-x_3)} \qquad (3.13)$$

Since the Lagrangian coefficients posses the desired properties of the nodal interpolation functions, we may write immediately for any line element within only Φ_I, specified at the nodes (not derivatives),

$$N_i(x) = L_i(x) \qquad (3.14)$$

We assign to the element with the order of the interpolation polynomials depending on the number of nodes.

3.5 Analysis of Continuous Systems

In the analysis of continuum systems, two different approaches can be followed to generate the system governing differential equations: The direct method and the Variational method. Variational procedure can be regarded as the basis of the finite element method. Variational approach provides a particularly powerful mechanism for the analysis of continuum systems. The main reason for this effectiveness lies in the way by which some boundary conditions can be generated and taken into account when using the Variational approach. Another important observation is that once a function has been established for a certain class of problems, the function can be employed to generate the governing equations for all problems in that class and therefore provides a general analysis tool. For example, the

principle of minimum potential energy is generally applicable to all problems in linear elasticity theory.

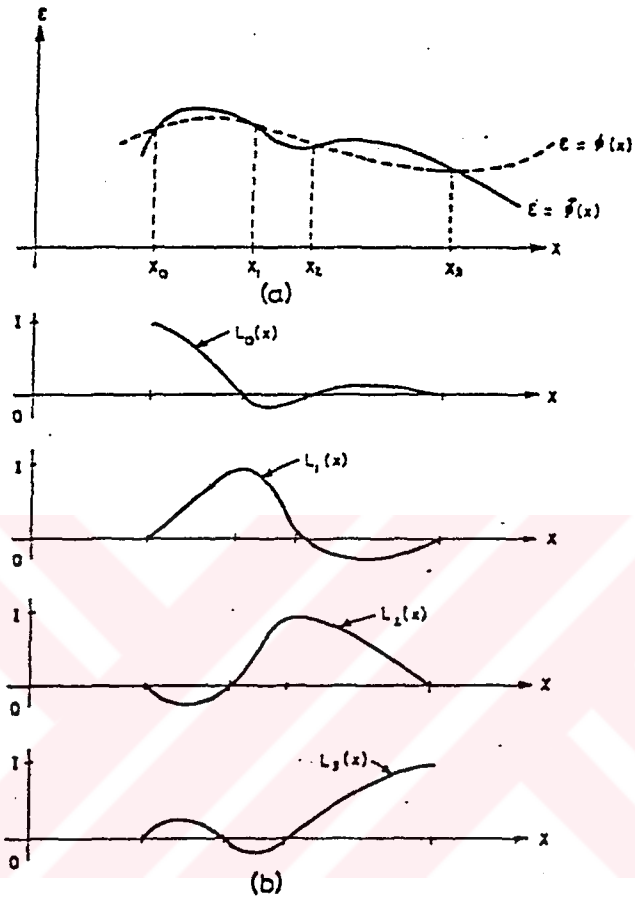

Figure 3.8 Interpolation using Lagrange polynomials. (a) The given function and its approximate representation. (b) Lagrange interpolation coefficients.

3.6 Obtaining the Element Properties

In the analysis of continuous system, the most important steps of the complete analysis are the proper idealization of the actual problem. The complete structure is idealized as an assemblage of individual structural elements that are interconnected at the structural joints. The element stiffness matrices corresponding to the global degrees of freedom of the structural idealization are calculated. As a result of the Variational principle, the force-displacements equation for an element can be written as follows,

$$[K]^{(e)}\{u\}^{(e)} = \{F\}^{(e)} \qquad (3.15)$$

where, $\{F\}^{(e)}$ is a column vector of the nodal forces for an element (e), $\{u\}^{(e)}$ is the nodal displacement vector for an element, and $[K]^{(e)}$ is the stiffness matrix for an element.

3.7 Assembly of The Element Properties

The total stiffness matrix is formed by the addition of the element stiffness matrices where the summation includes all elements and all nodes. The system equations have the same form as the element equations (Eq.3.15).When the discretized system has n nodes, the system equations become,

$$[K]\{u\} = \{F\} \tag{3.16}$$

where, [K] is the 2nx2n stiffness matrix, {u} and {F} are 2nx1 column vector of the nodal displacements for the entire system, and resultant nodal forces, respectively.

3.8 Solving the System Equations

Before solving the system equations of the structure, we need to impose the boundary conditions. If body forces and initial strains are absent, the vector {F} only includes components corresponding to nodes where concentrated external forces or displacement are specified. After the boundary conditions have been imposed, the system equation can be solved using any of the standard algebraic methods. The solution of the system equations gives the structure displacements and therefore the element nodal point displacements.

3.9 Making Additional Computations

After the system equations are solved for the nodal displacements, the basic relations between stress, strain, and displacements can be used to find the stress at any point in any of the element. The stresses within an element can be evaluated using the following relation,

$$\{\sigma\}^e = [C]^e[B]^e\{u\}^e \tag{3.17}$$

CHAPTER 4

FORMULATION AND CALCULATION OF ISOPARAMETRIC FINITE ELEMENT MATRICES

4.1 Introduction

A very important phase of a finite element analysis is the calculation of the finite element matrices. Our objective in this chapter is to present the formulation of isoparametric finite elements and describe an effective implementations. The principle idea of the isoparametric finite element formulation is to achieve the relationship between the element displacements at any point and element nodal point displacements directly through the use of interpolation functions (also called shape function). This means that the element matrices corresponding to the required degrees of freedom are obtained directly.

4.2 Formulation of Continuum Elements

Considering the calculation of a continuum element, it is in most cases effective to directly calculate the element matrices corresponding to the global degrees of freedom. However, we shall first present the formulation of the matrices that correspond to the element local degrees of freedom, because additional consideration may be necessary when the element matrices that correspond to the global degrees of freedom are calculated directly. In the following we consider the derivation of the element matrices of two dimensional plane stress, plane strain, and axisymmetric elements.

4.2.1 The Four-Node Quadrilateral

The basic procedure in the isoparametric finite element formulation is to express the element coordinates and element displacements in the form of interpolations using the natural coordinate system of the element. This coordinate system is one-, two-, or three-dimensional depending on the dimension of the element. The formulation of the element matrices is the same whether we deal with a one-, two-, or three-dimensional element. For this reason we will investigate the equations of a two-dimensional element.

Consider the general quadrilateral element shown in Fig.4.1. The local nodes are numbered as 1,2,3, and 4 in a counterclockwise fashion as shown, and (x_i, y_i) are the coordinates of node i. The vector $\{u\}=[u_1, v_1, u_2, v_2, \ldots, u_4, v_4]^T$ denotes the element displacements vector. The displacement of an interior point P located at (x,y) is represented as $u=[u(x,y), v(x,y)]^T$.

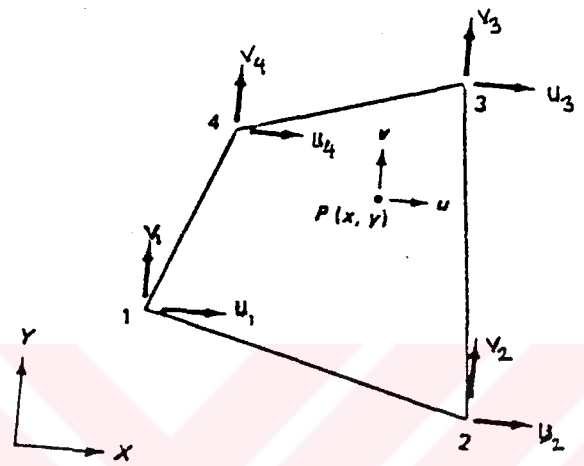

Figure 4.1 Four-node quadrilateral element.

4.2.2 Shape Function

We first develop the shape functions on a master element, shown in Fig.4.2. The shape functions are defined in the natural coordinate system of the element, which has variables r, and s that each vary from -1 to +1. The fundamental property of the shape function N_i is that its value in the natural coordinate system is an unity at node i and is zero at all other nodes. Using these conditions the functions N_i corresponding to a specific nodal point layout can be solved for in a systematic manner. In particular, consider the definition of N_i:

$N_i=1$ at node 1

$N_i=0$ at nodes 2,3,4 (4.1)

Now, the required that $N_1=0$ at nodes 2,3, and 4 is equivalent to requiring that $N_1=0$ along edges r=+1 and s=+1 (Fig.4.2). Thus, N_1 has to be of the form,

$$N_1 = c(1-r)(1-s) \tag{4.2}$$

where, c is a constant.

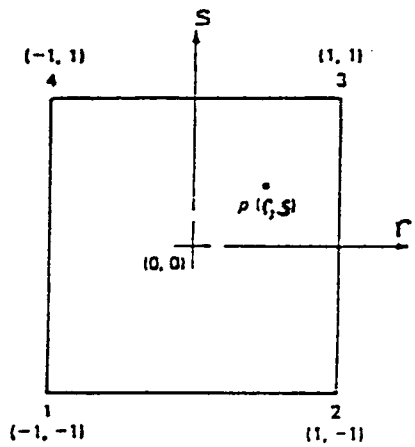

Figure 4.2 The quadrilateral element in r,s space (the master element).

The constant is determined from the condition $N_1=1$ at node 1. Since r=-1, s=-1 at node 1, we have,

$$1=c(2)(2) \tag{4.3}$$

Which yields $c=\frac{1}{4}$, Thus,

$$N_1=\frac{1}{4}(1-r)(1-s) \tag{4.4}$$

All the four shape functions can be written as,

$$\begin{aligned} N_1&=\frac{1}{4}(1-r)(1-s)\\ N_2&=\frac{1}{4}(1+r)(1-s)\\ N_3&=\frac{1}{4}(1+r)(1+s)\\ N_4&=\frac{1}{4}(1-r)(1+s) \end{aligned} \tag{4.5}$$

We now express the element displacements in terms of the nodal values, These are,

$$\begin{aligned} u&=N_1u_1+N_2u_2+N_3u_3+N_4u_4\\ v&=N_1v_1+N_2v_2+N_3v_3+N_4v_4 \end{aligned} \tag{4.6}$$

where, u, and v are the local element displacements at any point of the element and u_i, v_i, and i=1,2,3,4, are the corresponding element displacements and its nodes. Eq.4.6 can be written in matrix form as,

$$u=N\{u\} \tag{4.7}$$

where,

$$N=\begin{bmatrix} N_1 & 0 & N_2 & 0 & N_3 & 0 & N_4 & 0 \\ 0 & N_1 & 0 & N_2 & 0 & N_3 & 0 & N_4 \end{bmatrix} \tag{4.8}$$

In the isoparametric formulation, we use the same shape functions N_i to also express the coordinates of a point within the element in terms of nodal coordinates. Thus,

$$\begin{aligned} x &= N_1x_1+N_2x_2+N_3x_3+N_4x_4 \\ y &= N_1y_1+N_2y_2+N_3y_3+N_4y_4 \end{aligned} \tag{4.9}$$

To be able to evaluate the stiffness matrix of an element, we need to calculate the strain-displacement transformation matrix. The element strains are obtained in terms of derivatives of element displacements with respect to the local coordinates. Because the element displacements are defined in the natural coordinate system (Eq.4.6). We need to relate the x, and y derivatives to the r, and s derivatives where we realize that Eq.4.9 is of the form,

$$x=f_1(r,s); \qquad y=f_2(r,s) \tag{4.10}$$

where, f_i denotes "function of". The inverse relationship is,

$$r=f_4(x,y); \qquad s=f_5(x,y) \tag{4.11}$$

We require the derivatives $\partial/\partial x$, and $\partial/\partial y$ and it seems natural to use the chain rule in the following form:

$$\begin{aligned} \frac{\partial}{\partial x} &= \frac{\partial}{\partial r}\frac{\partial r}{\partial x}+\frac{\partial}{\partial s}\frac{\partial s}{\partial x} \\ \frac{\partial}{\partial y} &= \frac{\partial}{\partial r}\frac{\partial r}{\partial y}+\frac{\partial}{\partial s}\frac{\partial s}{\partial y} \end{aligned} \tag{4.12}$$

To evaluate $\partial/\partial x$ in Eq.4.12, we need to calculate $\partial r/\partial x$ which means that the explicit inverse relationship in Eq.4.11 would need to be evaluated. These inverse relationships are in general difficult to establish explicitly, and it is necessary to evaluate the required derivatives in the following way. Using the chain rule, we have,

$$\begin{bmatrix} \frac{\partial}{\partial r} \\ \frac{\partial}{\partial s} \end{bmatrix} = \begin{bmatrix} \frac{\partial x}{\partial r} & \frac{\partial y}{\partial r} \\ \frac{\partial x}{\partial s} & \frac{\partial y}{\partial s} \end{bmatrix} \begin{bmatrix} \frac{\partial}{\partial x} \\ \frac{\partial}{\partial y} \end{bmatrix} \tag{4.13}$$

or

$$\begin{bmatrix} \frac{\partial}{\partial r} \\ \frac{\partial}{\partial s} \end{bmatrix} = J \begin{bmatrix} \frac{\partial}{\partial x} \\ \frac{\partial}{\partial y} \end{bmatrix} \tag{4.14}$$

or in matrix notation,

$$\frac{\partial}{\partial r} = J \frac{\partial}{\partial x} \tag{4.15}$$

where, J is the Jakobian matrix, and it can be written as,

$$J = \begin{bmatrix} \frac{\partial x}{\partial r} & \frac{\partial y}{\partial r} \\ \frac{\partial x}{\partial s} & \frac{\partial y}{\partial s} \end{bmatrix} \tag{4.16}$$

In view of Eq.4.5 and 4.9, we have,

$$J = \frac{1}{4} \begin{bmatrix} -(1-s)x_1 + (1-s)x_2 + (1+s)x_3 - (1+s)x_4 \\ -(1-r)x_1 - (1+r)x_2 + (1+r)x_3 + (1-r)x_4 \end{bmatrix}$$
$$\begin{bmatrix} -(1-s)y_1 + (1-s)y_2 + (1+s)y_3 - (1+s)y_4 \\ -(1-r)y_1 - (1+r)y_2 + (1+r)y_3 + (1-r)y_4 \end{bmatrix} \tag{4.17}$$

or

$$J = \begin{bmatrix} J_{11} & J_{12} \\ J_{21} & J_{22} \end{bmatrix} \tag{4.18}$$

Equation 4.14 can be inverted as,

$$\begin{bmatrix} \frac{\partial}{\partial x} \\ \frac{\partial}{\partial y} \end{bmatrix} = J^{-1} \begin{bmatrix} \frac{\partial}{\partial r} \\ \frac{\partial}{\partial s} \end{bmatrix} \tag{4.19}$$

where,

$$J^{-1} = \frac{1}{\det J} \begin{bmatrix} \frac{\partial y}{\partial s} & -\frac{\partial x}{\partial s} \\ -\frac{\partial y}{\partial r} & \frac{\partial x}{\partial r} \end{bmatrix} \tag{4.20}$$

$$\det J = \frac{\partial x}{\partial r}\frac{\partial y}{\partial s} - \frac{\partial x}{\partial s}\frac{\partial y}{\partial r} \tag{4.21}$$

These expression will be used in the derivation of the element stiffness matrix. For additional result, it will be needed the relation as,

$$dxdy = \det J dr ds \tag{4.22}$$

4.2.3 Element Stiffness Matrix

The stiffness matrix for the quadrilateral element can be derived from the strain energy in the body, given by,

$$U = \int_v \frac{1}{2}\sigma^T \varepsilon dv \tag{4.23}$$

or

$$u = \sum_e t_e \int_e \frac{1}{2}\sigma^T \varepsilon dA \tag{4.24}$$

where, t_e is the thickness of element e. The strain-displacement relations are,

$$\varepsilon = Bu = \begin{Bmatrix} \varepsilon_x \\ \varepsilon_y \\ \gamma_{xy} \end{Bmatrix} = \begin{bmatrix} \frac{\partial u}{\partial x} \\ \frac{\partial v}{\partial y} \\ \frac{\partial u}{\partial y} + \frac{\partial v}{\partial x} \end{bmatrix} \tag{4.25}$$

Using Eq.4.19, we have,

$$\begin{bmatrix} \frac{\partial u}{\partial x} \\ \frac{\partial u}{\partial y} \end{bmatrix} = J^{-1} \begin{bmatrix} \frac{\partial u}{\partial r} \\ \frac{\partial u}{\partial s} \end{bmatrix} \tag{4.26}$$

Similarly,

$$\begin{bmatrix} \frac{\partial v}{\partial x} \\ \frac{\partial v}{\partial y} \end{bmatrix} = J^{-1} \begin{bmatrix} \frac{\partial v}{\partial r} \\ \frac{\partial v}{\partial s} \end{bmatrix} \tag{4.27}$$

We require the first derivatives of displacements. We can find them using Eq.4.5 and 4.6 as follows,

$$\begin{aligned}
\frac{\partial u}{\partial r} &= -\frac{1}{4}(1-s)u_1 + \frac{1}{4}(1-s)u_2 - \frac{1}{4}(1+s)u_3 + \frac{1}{4}(1+s)u_4 \\
\frac{\partial u}{\partial s} &= -\frac{1}{4}(1-r)u_1 - \frac{1}{4}(1+r)u_2 + \frac{1}{4}(1-r)u_3 + \frac{1}{4}(1+r)u_4 \\
\frac{\partial v}{\partial r} &= -\frac{1}{4}(1-s)v_1 + \frac{1}{4}(1-s)v_2 - \frac{1}{4}(1+s)v_3 + \frac{1}{4}(1+s)v_4 \\
\frac{\partial v}{\partial s} &= -\frac{1}{4}(1-r)v_1 - \frac{1}{4}(1+r)v_2 + \frac{1}{4}(1-r)v_3 + \frac{1}{4}(1+r)v_4
\end{aligned} \tag{4.28}$$

Using Eqs.4.26, 4.27, and 4.28, the strain-displacement relation can be written as,

$$\{\varepsilon\}=\frac{1}{4}J^{-1}\begin{bmatrix}-(1-s) & 0 & (1-s) & 0 & -(1+s) & 0 & (1+s) & 0\\ 0 & -(1-r) & 0 & -(1+r) & 0 & (1-r) & 0 & (1+r)\\ -(1-r) & -(1-s) & -(1+r) & (1-s) & (1-r) & -(1+s) & (1+r) & (1+s)\end{bmatrix}\{u\} \tag{4.29}$$

where, {u} is a vector listing the element nodal point displacements. Using Eqs.4.25, and 4.29, the strain-displacements transformation matrix B can be written as follows,

$$[B]=\frac{1}{4}J^{-1}\begin{bmatrix}-(1-s) & 0 & (1-s) & 0 & -(1+s) & 0 & (1+s) & 0\\ 0 & -(1-r) & 0 & -(1+r) & 0 & (1-r) & 0 & (1+r)\\ -(1-r) & -(1-s) & -(1+r) & (1-s) & (1-r) & -(1+s) & (1+r) & (1+s)\end{bmatrix} \tag{4.30}$$

The strain in the element is expressed in terms of its nodal displacement. The stress is now given by,

$$\sigma = CBu \tag{4.31}$$

where, C is a (3X3) material matrix. The strain energy in Eq.4.24 becomes,

$$u=\sum_e \frac{1}{2}u^T[t_e\int_{-1}^{1}\int_{-1}^{1}B^TCB\det J\,dr\,ds]u \tag{4.32}$$

$$u=\sum_e \frac{1}{2}u^TK^eu \tag{4.33}$$

where,

$$K^e=t_e\int_{-1}^{1}\int_{-1}^{1}B^TCB\det J\,dr\,ds \tag{4.34}$$

K^e is the element stiffness matrix. The dimension of the element stiffness matrix is (8X8). We should note here that quantities B and detJ in the above integral are involved functions of r, and s, and so the integration has to be performed numerically.

4.2.4 Element Stiffness Matrix For Axi-symmetric Problems

The strain-displacements transformation matrix B has been found for plane stress and plane strain element. In the case of axi-symmetric element, two modifications are necessary. Firstly, we consider one radian of the structure. Hence, the thickness to be employed in all integrals is that corresponding to one radian, which means that at an integration point the thickness is equal to the radius at that point. So the thickness or the radius at that point can be written as follows,

$$R_{ij} = \sum_{k=1}^{4} N_k \Big|_{r_i s_j} r_k \tag{4.35}$$

Secondly, it is recognized that also circumferential strains and stresses are developed. Hence, the strain-displacement matrix must be augmented by one row for the hoop strain u/r, we have,

$$B = \begin{bmatrix} \cdots & \cdots & \cdots & \cdots & \cdots & \cdots & \cdots & \cdots \\ \frac{N_1}{R} & 0 & \frac{N_2}{R} & 0 & \frac{N_3}{R} & 0 & \frac{N_4}{R} & 0 \end{bmatrix} \tag{4.36}$$

where, the first three rows have already been defined in Eq.4.30 and t is equal to the radius. To obtain the strain-displacement matrix at integration point (i,j), we use Eq.4.35 to evaluate R and substitute into Eq.4.36. In the case of axi-symmetric formulation, considering the elemental volume shown in Figure 4.3, the potential energy can be written in the form

$$\Pi = \frac{1}{2}\int_0^{2\pi}\int_A \sigma^T \varepsilon R dA d\theta - \int_0^{2\pi}\int_A u^T f^B R dA d\theta - \int_0^{2\pi}\int_L u^T f^S R dl d\theta - \sum_i u_i{}^T P_i \tag{4.37}$$

where, $rdld\theta$ is the elemental surface area, and the point load P_i represents a line load distributed around a circle, R is the radius of the sampling point.

All variables in the integrals are independent of θ. Thus, Eq.4.37 can be written as,

$$\Pi = 2\pi\left(\frac{1}{2}\int_A \sigma^T \varepsilon R dA - \int_A u^T f^B R dA - \int_L u^T f^S R dl\right) - \sum_i u_i{}^T P_i \tag{4.38}$$

where,

$$u = [u, w]^T \tag{4.39}$$

$$f^B = [f_r^B, f_z^B]^T \tag{4.40}$$

$$f^S = [f_r^S, f_z^S]^T \tag{4.41}$$

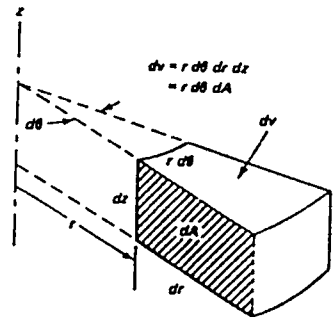

Figure 4.3 Elemental volume

The strain-displacement relationship for axi-symmetric problems can be written as,

$$\varepsilon = [\varepsilon_r, \varepsilon_z, \gamma_{rz}, \varepsilon_\theta]^T = \left[\frac{\partial u}{\partial r}, \frac{\partial w}{\partial z}, \frac{\partial u}{\partial z} + \frac{\partial w}{\partial r}, \frac{u}{r}\right]^T \tag{4.42}$$

The stress vector is correspondingly defined as

$$\sigma = [\sigma_r, \sigma_z, \tau_{rz}, \sigma_\theta]^T \tag{4.43}$$

The stress-strain relations are given in the usual form as,

$$\sigma = C\varepsilon \tag{4.44}$$

where, (4X4) material matrix C can be written as,

$$C = \frac{E(1-\nu)}{(1+\nu)(1-2\nu)} \begin{bmatrix} 1 & \frac{\nu}{1-\nu} & 0 & \frac{\nu}{1-\nu} \\ \frac{\nu}{1-\nu} & 1 & 0 & \frac{\nu}{1-\nu} \\ 0 & 0 & \frac{1-2\nu}{2(1-\nu)} & 0 \\ \frac{\nu}{1-\nu} & \frac{\nu}{1-\nu} & 0 & 1 \end{bmatrix} \tag{4.45}$$

The element strain energy U_e can be written as,

$$U_e = \frac{1}{2} u^T (2\pi \int_e B^T C B R dA) u \tag{4.46}$$

The quantity inside the parentheses is the element stiffness matrix,

$$K^e = 2\pi \int_e B^T C B R dA \tag{4.47}$$

4.2.5 Element Force Vectors

The external forces acting onto the body are surface forces f^S, body forces f^B, and concentrated forces f^C. Those forces include all externally applied forces and reactions. In addition there is a nodal forces f_i due to initial stresses. These forces corresponding to the local element degrees of freedom are defined as follows,

$$F_B = \int_V N^T f^B dV \tag{4.48}$$

$$F_S = \int_S (N^S)^T f^S dS \tag{4.49}$$

$$F_I = \int_V B^T \tau_I dV \tag{4.50}$$

where, N is a matrix of the interpolation functions. These equations have been defined for three dimensional element.

In the case of axi-symmetric problem, assume that an uniformly distributed load with components f_r^S and f_z^S is applied on edge 2-3 of the quadrilateral element. Along this edge, we have r=1. In this case, the surface forces can be written in the following form,

$$F_S = 2\pi \int_{-1}^{1} (N^S)^T \{f^S\} \left[\left(\frac{dx}{ds}\right)^2 + \left(\frac{dy}{ds}\right)^2 \right]^{\frac{1}{2}} R ds \tag{4.51}$$

where, R is the radius of the sampling point. In this case, it should be noted that only one-dimensional numerical integration is required, because R is not a variable.

4.3 Convergence Considerations For Continuum Elements

To investigate the compatibility of an element assemblage, we need to consider each edge, or rather face, between adjacent elements. For compatibility it is necessary that the coordinates and the displacements of the elements at the common face be same. This is the case if the elements have same nodes on the common face, and the coordinates and displacements along the common face are in each element defined by the same interpolation functions.

Examples of adjacent elements that preserve compatibility, and that do not, are shown in Figure 4.4.

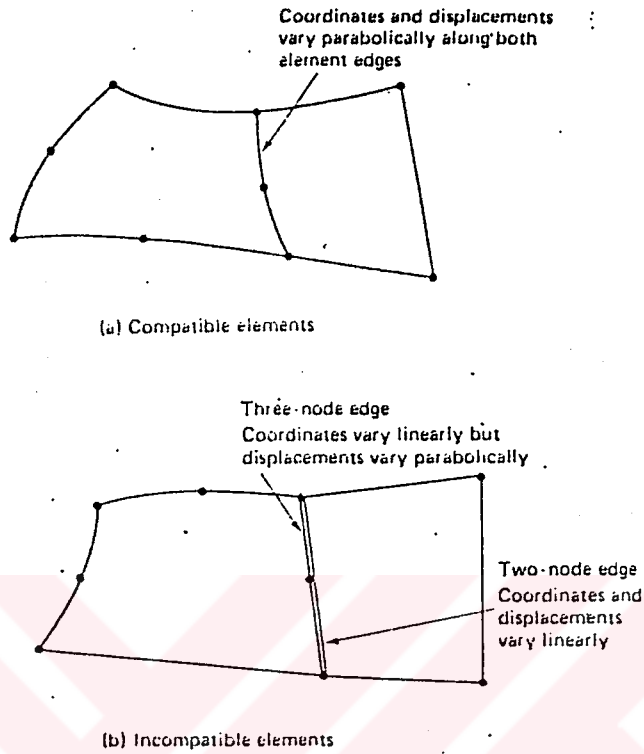

Figure 4.4 Compatible and incompatible two dimensional elements.

Completeness requires that the rigid body displacements and constant strain states be possible. For the rigid body and constant strain states to be possible, the following displacements defined in the local element coordinate system must be contained in the isoparametric formulation.

$$u = a_1 + b_1 x + c_1 y$$
$$v = a_2 + b_2 x + c_2 y \qquad (4.52)$$

where, the a_j, b_j, and c_j, $j=1,2$ are constants. The nodal point displacements corresponding to this displacement field are,

$$u_i = a_1 + b_1 x_i + c_1 y_i$$
$$v_i = a_2 + b_2 x_i + c_2 y_i \qquad (4.53)$$

where, $i=1,.....,q$ and q=number of nodes. To show that the displacements in Eq.4.52 are possible when the isoparametric formulation is employed, assume that the nodal point displacements of the element are given by Eq.4.53, we should find that, with these nodal point displacements, the displacements in the isoparametric formula-

tion are actually those given in Eq.4.52. In the isoparametric formulation, displacements can be written as,

$$u = a_1 \sum_{i=1}^{q} N_i + b_1 x + c_1$$
$$v = a_2 \sum_{i=1}^{q} N_i + b_2 x + c_2 y \qquad (4.54)$$

The displacements defined in Eq.4.54, however, are the same as those given in Eq.4.53, provided that for any point in the element,

$$\sum_{i=1}^{q} N_i = 1 \qquad (4.55)$$

The relation in Eq.4.55 is the condition on the interpolation functions for the completeness requirements to be satisfied. We may note that Eq.4.55 is certainly satisfied at the nodes of an element, because the interpolation functions N_i has been constructed to be unity at node i with all other interpolation functions h_j, $j \neq i$, being zero at that node; but in order that an isoparametric element be properly constructed, the condition must be satisfied for all points in the element.

4.4 Numerical Integration

An important aspect of isoparametric and related finite element analysis is the required numerical integration. The required matrix integrals in the finite element calculations are written as,

$$I = \int_{-1}^{1} F(r)dr, \qquad I = \int_{-1}^{1}\int_{-1}^{1} F(r,s)drds \qquad (4.56)$$

in the one-, and two-dimensional cases, respectively.

The Gaussian quadrature approach for evaluating I is given below. This method has proved most useful in finite element work. Extension to integrals in two and three dimensions follows readily. Consider the n-point approximation,

$$I = \int_{-1}^{1} f(r)dr \approx w_1 f(r_1) + w_2 f(r_2) + \cdots + w_n f(r_n) \qquad (4.57)$$

where, $w_1, w_2, \ldots\ldots, w_n$ are the weights and $r_1, r_2, \ldots\ldots r_n$ are the sampling points or Gauss points. The idea behind Gaus-

sian quadrature is to select the n Gauss points and n weights such that Eq.4.57 provides an exact answer for polynomials f(r) of as large a degree as possible. In other words, the idea is that if the n-point integration formula is exact for all polynomials up to as high a degree as possible, then the formula will work well even if f is not a polynomial. To get some intuition for the method, the one-point and two-point approximations are discussed below.

4.4.1 One-point Formula

Consider the formula with n=1 as,

$$\int_{-1}^{1} f(r)dr = w_1 f(r_1) \qquad (4.58)$$

Since there are two parameters, w_1 r_1, we consider requiring the formula in Eq.4.58 to be exact when f(r) is a polynomial of order 1. Thus, if $f(r)=a_0+a_1r$, then we require,

$$\text{Error}=\int_{-1}^{1}(a_0+a_1r)dr - w_1 f(r_1) = 0 \qquad (4.59)$$

or

$$\text{Error}=2a_0-w_1(a_0+a_1r_1)=0 \qquad (4.60)$$

or

$$\text{Error}=a_0(2-w_1)-w_1a_1r_1=0 \qquad (4.61)$$

From Eq.4.61, we see that the error is zeroed if $w_1=2$, and $r_1=0$. For any general f, we have,

$$I=\int_{-1}^{1} f(r)dr \cong 2f(0) \qquad (4.62)$$

Which is seen to be the familiar midpoint rule (Fig.4.5).

4.4.2 Two-point Formula

Consider the formula with n=2 as,

$$\int_{-1}^{1} f(r)dr = w_1 f(r_1) + w_2 f(r_2) \qquad (4.63)$$

We have four parameters to choose: w_1, w_2, r_1, and r_2. We can therefore expect the formula in Eq.4.63 to be exact for

a cubic polynomial. Thus, choosing $f(r)=a_0+a_1r+a_2r^2+a_3r^3$ yields,

$$\text{Error}=\left[\int_{-1}^{1}(a_0+a_1r+a_2r^2+a_3r^3)dr\right]-[w_1f(r_1)+w_2f(r_2)] \qquad (4.64)$$

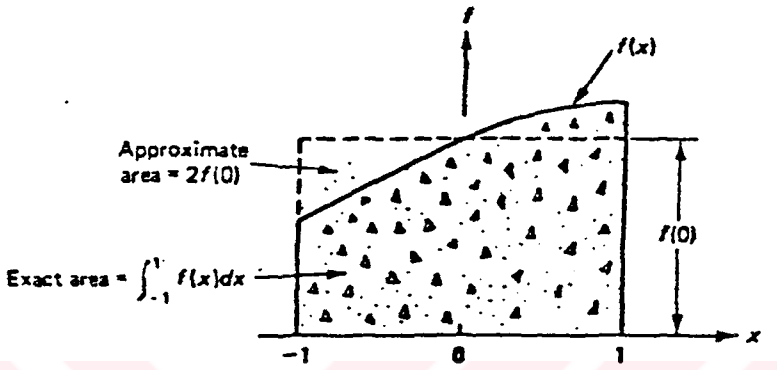

Figure 4.5 One-point Gauss quadrature.

Requiring zero error yields,

$$\begin{aligned} w_1+w_2&=2\\ w_1r_1+w_2r_2&=0\\ w_1r_1^2+w_2r_2^2&=\frac{2}{3}\\ w_1r_1^3+w_2r_2^3&=0 \end{aligned} \qquad (4.65)$$

These nonlinear equations have the unique solution which is written as,

$$w_1=w_2=1; \qquad -r_1=r_2=\frac{1}{\sqrt{3}}=0.5773502691 \qquad (4.66)$$

From above, we can conclude that n-point Gaussian quadrature will provide an exact answer if f is a polynomial of order (2n-1) or less. Table 4.1 gives the values of w_i and r_i for Gauss quadrature formulas of orders n=1 through n=6. Note that the Gauss points are located symmetrically with respect to the origin, and that symmetrically placed points have the same weights. Moreover, the large number of digits given in Table 4.1 should be used in the calculations for accuracy; i.e.,use double precision on the computer.

Number of points, n	Location, r_i	Weights, w_i
1	0.0	2.0
2	$\pm 1/\sqrt{3} = \pm 0.5773502692$	1.0
3	± 0.7745966692 0.0	0.5555555556 0.8888888889
4	± 0.8611363116 ± 0.3399810436	0.3478548451 0.6521451549
5	± 0.9061798459 ± 0.5384693101 0.0	0.2369268851 0.4786286705 0.4786286705
6	± 0.9324695142 ± 0.6612093865 ± 0.2386191861	0.1713244924 0.3607615730 0.4679139346

$$\int_{-1}^{1} f(r)dr \approx \sum_{i=1}^{n} w_i f(r_i)$$

Table 4.1 Gauss points and weights for Gaussian quadrature.

4.4.3 Two Dimensional Integral

The most obvious way of obtaining the integral,

$$I = \int_{-1}^{1}\int_{-1}^{1} f(r,s)drds \tag{4.67}$$

is to first evaluate the inner integral keeping r constant, i.e.,

$$\int_{-1}^{1} f(r,s)ds = \sum_{j=1}^{n} w_j f(r,s_j) = \Psi(r) \tag{4.68}$$

Evaluating the outer integral in a similar manner, we have,

$$I = \int_{-1}^{1} \Psi(r)dr = \sum_{i=1}^{n} w_i \Psi(r_i)$$

$$= \sum_{i=1}^{n} w_i \sum_{j=1}^{n} w_j f(r_i,s_j)$$

$$= \sum_{i=1}^{n}\sum_{j=1}^{n} w_i w_j f(r_i,s_j) \tag{4.69}$$

4.4.4 Stiffness Integration

To illustrate the use of Eq.4.69, consider the element stiffness matrix of a quadrilateral element for axi-symmetric analysis,

$$K^e = 2\pi \int_{-1}^{1}\int_{-1}^{1} RB^T CB \det J \, dr\,ds \tag{4.70}$$

where, B and detJ are functions of r and s. Note that the integral above actually consists of the integral of each element in an (8X8) matrix. However, using the fact that K^e is symmetric, we do not need to integrate elements below the main diagonal. Let ϕ represent the ij'th element in the integral. That is let,

$$\phi(r,s) = 2\pi(RB^T CB \det J)_{ij} \tag{4.71}$$

Then, if we use a 2X2 rule, we get,

$$K_{ij} \approx w_1^2\phi(r_1,s_1) + w_1w_2\phi(r_1,s_2) + w_2w_1\phi(r_2,s_1) + w_2^2\phi(r_2,s_2) \tag{4.72}$$

where, $w_1=w_2=1.0$, $r_1=s_1=-0.57735...$, and $r_2=s_2=+0.57735....$ Alternatively, if we label the Gauss points as 1,2,3, and 4, then K_{ij} in Eq.4.72 can also be written as,

$$K_{ij} = \sum_{IP=1}^{4} w_{IP}\phi_{IP} \tag{4.73}$$

where, ϕ_{IP} is the value of ϕ and w_{IP} is the weight factor at integration point IP. We note that $w_{IP}=(1)(1)=1$. Computer implementation is sometimes easier using Eq.4.73. The evaluation of three-dimensional integrals is similar.

4.5 The Boundary Condition

The equations of the system (Eq.3.16) can be solved after the prescribed support displacements have been substituted.

The process of specifying the boundary conditions and the procedure for modification of specified displacements is tied to the method adopted to store the global arrays, e.g., stiffness and mass matrices. In our computer program only those coefficient within a non-zero profile in the global arrays are stored.

Clearly, without substitutions of a minimum number of pre-scribed displacements to present rigid body movements of the structure, it is impossible to solve this system,

because the displacements can not be uniquely determined by the forces. The non-zero nodal forces or displacements associated with each degree of freedom must be specified. In our program, these are both stored in the array {F} and the destination between load and displacements is made by comparing the corresponding value of the restrained boundary condition for each degree of freedom. After the prescription of appropriate displacements, specified displacements are modified by deleting appropriate rows and columns of the stiffness, and load matrices.

4.6 Obtaining The Displacements

After the stiffness matrix [K] and the force vector {F} are obtained and all the boundary conditions are inserted, the equations of system can be solved to find unknown displacements.

The Gauss elimination method has been used to solve the equation of the system. A very important aspect in the computer implementation of the Gauss solution procedure is that a minimum solution time should be used. In addition, the high speed storage requirements should be as small as possible to avoid the use of back-up storage. However, for large systems, it will nevertheless be necessary to use back-up storage, and for this reason, it should also be possible to modify the solution algorithm for effective out-of-core solution. An advantage of the finite element analysis is that the stiffness matrix of the element assemblage is not only symmetric and positive definite but also banded; i.e., $K_{ij}=0$ for $j>i+m_k$ where, m_k is the half-bandwidth of the system, i and j are numbers of row and column of the stiffness matrix respectively, and K_{ij} is the value of the stiffness matrix corresponding to the row i and column j. The fact that in finite element analysis, all none-zero elements are clustered around the diagonal of the system matrices greatly reduces to total number of operations and the high speed storage required in the solution of equation. However, this property depends on the nodal point numbering of the element mesh, and the analyst must obtain an effective number of nodal point. Such a computer program is developed to solve the equations of the system.

4.7 Calculation of Stresses

After the nodal point displacements have been calculated, the stresses within an element can be calculated using the relation,

$$\{\sigma\} = [C][B]\{u\} \tag{4.74}$$

This relation gives the stresses at any point of the element, in practice, the element stresses are only calculated and printed for some specific points. These may be the center of the element, the nodal point locations or numerical integration points used in the evaluation of the element stiffness matrix.

Assuming that an element idealization satisfied all convergence criteria is employed. This does not mean that the predicted stresses are in general continuous across the element boundaries. Hence, considering a compatible element mesh, the displacements are continuous from element to element, but the stress components are not continuous unless a stress field which is contained in the element formulation is analyzed.

We should note here that the stress discontinuities between elements and the violation of the local stress boundary conditions will decrease as the element mesh is refined. Therefore, the magnitude of the stress discontinuities between elements can be employed in practice as a measure to indicate whether the finite element idealization has to be refined.

Another observation in the stress calculations is that the stresses at some points in an element can be significantly more accurate when compared with the exact solution that at other points. In particular, it has been observed that the stresses may be considerably more accurate at the Gauss integration points than at the nodal points of an element.

The objective in practice is usually to obtain the best stress predictions which is possible after the nodal point displacements have been evaluated. For this purpose, if the difference between the element boundary stress is not too large, it may be appropriate to simply average them. In an alternative approach, the stresses are only calculated within the elements and then a least squares fit or other interpolation procedure is employed to predict the stresses at the element boundaries or other desired points.

CHAPTER 5

ELASTO-PLASTIC FINITE ELEMENT ANALYSIS OF ISOTROPIC MATERIALS

5.1 Introduction

In the finite element formulation, given in section 4.2, we assume that the displacement of the finite element assemblage are infinitesimally small and that the material is linearly elastic. In addition, we also assumed that the nature of the boundary conditions remains unchanged during the application of the loads on the finite element assemblage.

The fact that the displacement must be small has entered into the evaluation of the matrix [K] and load vector {F}, because all integrals have been performed over the original volume of the finite elements, and the strain-displacement matrix B of each element was assumed to be constant and independent of the element displacement. The assumption of a linear elastic material is implied in the use of a constant stress-strain matrix C. With these assumptions, the finite element equilibrium equations derived were for static analysis.

$$[K]\{u\}=\{F\} \tag{5.1}$$

These equations correspond to a linear analysis of a structural problem because the displacement response u is a linear function of the applied load vector F. If the loads are αR instead of R, where α is a constant, the corresponding displacements are αu, we perform a nonlinear analysis.

In the nonlinear problems, a displacement boundary condition can change, and a degree of freedom which was free becomes restrained at a certain load level, the response is only linear prior to change in boundary condition.

The above discussion of the basic assumptions used in a linear analysis defines what we mean by a nonlinear analysis and also suggests how to categorize different nonlinear analysis. This classification is used very conveniently in practical nonlinear analysis because this classification considers separately material nonlinear effects and kinematic nonlinear effects. These categories can be written as,

1.Materially-nonlinear-only
2.Large displacements, large rotations, but small strains
3.Large displacements, large rotations, and large strains

In an actual problem is to be analyzed, for formulative and computational reasons, the problem is effectively described and analyzed as a problem in one of the categories given above. But, we note that other formulations may be applicable to the solution of a problem as well.

We should note that in a materially-nonlinear-only analysis, the nonlinear effect lies in the nonlinear stress-strain relation. The displacements and strains are infinitesimally small, therefore, the usual engineering stress and strain measures can be employed in the response description.

In actual analysis, it is necessary to decide whether a problem falls into one or the other category of analysis. Surely, the use of the most general large strain formulation "will always be correct"; however, the use of a more restrictive formulation may be computationally more effective and may also provide more insight into the response prediction.

5.2 General Theory of Plasticity

Plastic behavior of solids is characterized by a non-unique stress-strain relationship. Indeed, one definition of plasticity may be the presence of irrecoverable strain and load removal.

If uniaxial behavior of a material is considered as shown in Figure 5.1.(a), a non-linear relationship on loading alone does not determine whether non-linear elastic or plastic behavior is exhibited. Unloading will immediately discover the difference with elastic material following the same path and the plastic material showing a history dependent, different, path.

Many materials show an ideal plastic behavior in which a limiting yield stress, σ_y exists at which the strains are in determinate. For all stresses such yield, a linear (or

non-linear) elasticity is assumed. Figure 5.1.(b) illustrates this.

A further refinement of this model is one of hardening/softening plastic material in which the yield stress depends on some parameter k (such as plastic strain ε_p), Figure 5.1.(c).

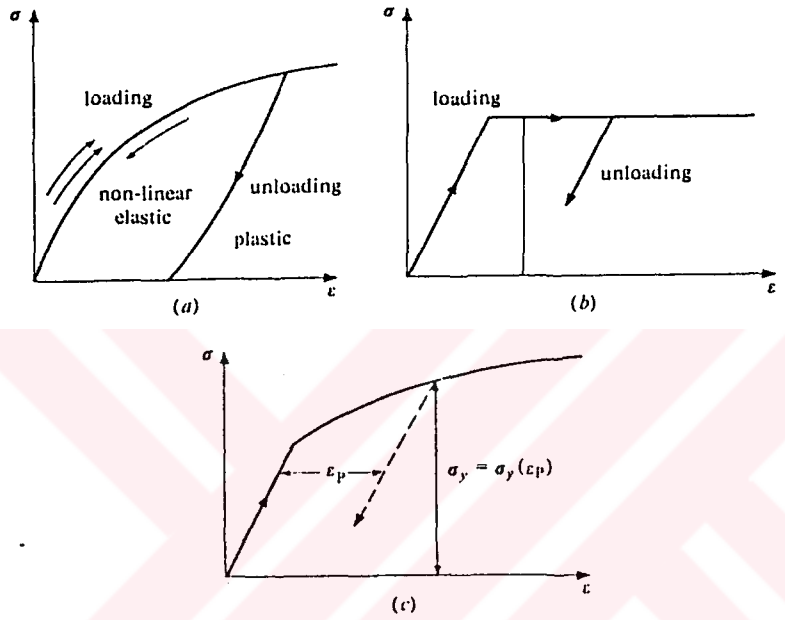

Figure 5.1 Uniaxial behavior; (a)Non-linear elastic and plastic, (b)Ideal plasticity, (c)Strain hardening plasticity.

It is with the latter two kinds of plasticity that this section is concerned and for which many theories have been developed [54].

In a general state of stress σ, the theory needs some expansion and the concepts of yield stresses need to be generalized.

5.2.1 Yield Surface

It is quite generally postulated, as an experimental fact, that yielding can occur only if the stresses $\{\sigma\}$ satisfy the general yield criterion.

$$F(\{\sigma\},k) = 0 \qquad (5.2)$$

where, k is a 'hardening' parameter. This yield condition can be visualized as a surface in n-dimensional space of stress with the position of the surface dependent on the instantaneous value of the parameter k.

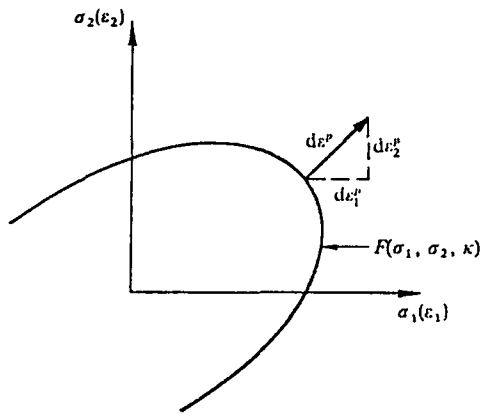

Figure 5.2 Yield surface and normality criterion in two-dimensional stress space.

5.2.2 Flow Rule (Normality Principle)

Von Mises first suggested the basic constitutive relation defining the plastic increments in relation to the yield surface. Heuristic arguments for the validity of the relationship proposed have been given by various workers in this field and at the present time, the following hypothesis appears to be generally accepted:

If $d\varepsilon_p$ denotes the increment of plastic strain then,

$$d\{\varepsilon\}_p = \lambda \frac{\partial F}{\partial \{\sigma\}} \tag{5.3}$$

or for any component n,

$$d\varepsilon_{n,p} = \lambda \frac{\partial F}{\partial \sigma_n} \tag{5.4}$$

where, λ is a proportionally constant, as yet undetermined. The rule is known as the normality principle because relation in Eq.5.3 can be interpreted as requiring the normality of the plastic strain increment 'vector' to the yield surface in the space of n stress dimensions.

5.2.3 Total-Stress-Strain Relations

During an infinitesimal increment of stress, changes of strain are assumed to be divisible into elastic and plastic parts. Thus,

$$d\{\varepsilon\} = d\{\varepsilon\}_e + d\{\varepsilon\}_p \tag{5.5}$$

The elastic strain increments are related to stress increments by a symmetric matrix of constants [C] as usual where, [C] is the elasticity matrix. The elastic strain increments can be written as,

$$d\{\varepsilon\}_e = [C]^{-1} d\{\sigma\} \tag{5.6}$$

We can thus write Eq.5.5 as,

$$d\{\varepsilon\} = [C]^{-1} d\{\sigma\} + \frac{\partial F}{\partial \{\sigma\}} \lambda \tag{5.7}$$

When plastic yield occurs, the stresses given by Eq.5.2 are on the yield surface. Differentiating this, we can write therefore,

$$dF = \frac{\partial F}{\partial \sigma_1} d\sigma_1 + \frac{\partial F}{\partial \sigma_2} d\sigma_2 + \cdots + \frac{\partial F}{\partial k} dk = 0$$

or (5.8)

$$\left\{ \frac{\partial F}{\partial \{\sigma\}} \right\}^T d\{\sigma\} - A\lambda = 0$$

In which we make the substitution

$$A = -\frac{\partial F}{\partial k} dk \frac{1}{\lambda} \tag{5.9}$$

Equations (5.7) and (5.8) can be written in a single symmetric matrix form as,

$$\begin{Bmatrix} d\{\varepsilon\} \\ 0 \end{Bmatrix} = \begin{bmatrix} [C]^{-1} & \frac{\partial F}{\partial \{\sigma\}} \\ \left(\frac{\partial F}{\partial \{\sigma\}} \right)^T & -A \end{bmatrix} \begin{Bmatrix} d\{\sigma\} \\ \lambda \end{Bmatrix} \tag{5.10}$$

This form is convenient to use directly provided that 'A' is not zero as shown in a particular form by Marcal and King [35]. Alternatively, indeterminate constant λ can be eliminated (taking care not to multiply or divide by A which may be zero in general). This result in an explicit expansion which determines the stress changes in terms of imposed strain changes with,

$$d\{\sigma\} = [C]^*_{ep} d\{\varepsilon\} \tag{5.11}$$

where,

$$[C]^*_{ep} = [C] - [C]\left\{\frac{\partial F}{\partial \{\sigma\}}\right\}\left\{\frac{\partial F}{\partial \{\sigma\}}\right\}^T [C]\left[A + \left\{\frac{\partial F}{\partial \{\sigma\}}\right\}^T [C]\left\{\frac{\partial F}{\partial \{\sigma\}}\right\}\right]^{-1} \tag{5.12}$$

The elasto-plastic matrix $[C]^*_{ep}$ takes place of the elasticity matrix [C] in incremental analysis. It is symmetric, positive definite, and the expression in Eq.5.11 is valid whether or not A is equal to zero.

5.2.4 Axi-Symmetric Form of the Elasto-Plastic Relationship

Consider the general relationship Eq.5.10. This relationship can be written in terms of the four axi-symmetric stress components. Axi-symmetric stress components in polar coordinates as discussed in section 2.4,

$$\{\sigma\} = \{\sigma_r,\ \sigma_z,\ \tau_{rz},\ \sigma_\theta\} \tag{5.13}$$

For axi-symmetric problem in polar coordinates, we can thus write Eq.5.10 as,

$$\begin{Bmatrix} d\varepsilon_r \\ d\varepsilon_z \\ d\gamma_{rz} \\ d\varepsilon_\theta \end{Bmatrix} = \begin{bmatrix} & & & & \frac{\partial F}{\partial \sigma_r} \\ & [C]^{-1} & & & \frac{\partial F}{\partial \sigma_z} \\ & & & & \frac{\partial F}{\partial \tau_{rz}} \\ \cdots & \cdots & \cdots & \vdots & \frac{\partial F}{\partial \sigma_\theta} \\ \frac{\partial F}{\partial \sigma_r} & \frac{\partial F}{\partial \sigma_z} & \frac{\partial F}{\partial \tau_{rz}} & \frac{\partial F}{\partial \sigma_\theta} & -A \end{bmatrix} \begin{bmatrix} d\sigma_r \\ d\sigma_z \\ d\tau_{rz} \\ d\sigma_\theta \\ \lambda \end{bmatrix} \tag{5.14}$$

where, C is the simple axi-symmetric elasticity matrix and F is the cross-section of the yield surface.

5.2.5 Significance of Parameter A

Clearly, for ideal plasticity with no hardening, A is simply zero. If hardening is considered, attention must be given to the nature of the parameter (or parameters) k on which the shifts of the yield surface depend.

With a 'work hardening' material k is taken to be represented by the amount of plastic work done during plastic deformation. Thus,

$$dk = \sigma_1 d\varepsilon_1^{\,p} + \sigma_2 d\varepsilon_2^{\,p} + \cdots = \{\sigma\}^T d\{\varepsilon\}_p \qquad (5.15)$$

Substituting the flow rule (Eq.5.3), we have, simply

$$dk = \lambda \sigma^T \frac{\partial F}{\partial \{\sigma\}} \qquad (5.16)$$

By Eq.5.9, we now see that λ disappears and we can write,

$$A = -\frac{\partial F}{\partial k} \{\sigma\}^T \frac{\partial F}{\partial \{\sigma\}} \qquad (5.17)$$

This is a strictly determinate form if explicit relationship between F and k is known.

5.2.6 Prandtl-Reuss Relation

To illustrate some of the concepts, consider the particular case of the well-known Huber-Von Mises yield surface with an associated flow rule. This is given by,

$$F = \left[\frac{1}{2}(\sigma_1 - \sigma_2)^2 + \frac{1}{2}(\sigma_2 - \sigma_3)^2 + \frac{1}{2}(\sigma_3 - \sigma_1)^2 + 3\sigma_4^{\,2} + 3\sigma_5^{\,2} + 3\sigma_6^{\,2}\right]^{\frac{1}{2}} - \sigma_y$$

$$\equiv \bar{\sigma} - \sigma_y \qquad (5.18)$$

In which suffixes 1,2,3 refer to the normal stress components and 4,5,6 to shear stress components in a general three-dimensional stress state.

On differentiation it will be found that

$$\frac{\partial F}{\partial \sigma_1} = \frac{3\sigma_1'}{2\bar{\sigma}}, \qquad \frac{\partial F}{\partial \sigma_2} = \frac{3\sigma_2'}{2\bar{\sigma}}, \qquad \frac{\partial F}{\partial \sigma_3} = \frac{3\sigma_3'}{2\bar{\sigma}}$$

$$\frac{\partial F}{\partial \tau_{yz}} = \frac{3\tau_{yz}}{\bar{\sigma}}, \qquad \frac{\partial F}{\partial \tau_{xz}} = \frac{3\tau_{xz}}{\bar{\sigma}}, \qquad \frac{\partial F}{\partial \tau_{xy}} = \frac{3\tau_{xy}}{\bar{\sigma}} \qquad (5.19)$$

In which the dashes stand for so called deviatoric stresses, i.e.,

$$\sigma_1' = \sigma_1 - \frac{(\sigma_1 + \sigma_2 + \sigma_3)}{3} \quad \text{etc.} \qquad (5.20)$$

The quantity $\sigma_y = \sigma_y(k)$ is the uniaxial stress at yield if a plot of the uniaxial test giving $\bar{\sigma}$ versus, the plastic

uniaxial strain ε_{up} is available and if simple work hardening is assumed, then,

$dk=\sigma_y d\varepsilon_{up}$

and

$$-\frac{\partial F}{\partial k}=\frac{\partial \sigma_y}{\partial k}=\frac{\partial \sigma_y}{\partial \varepsilon_{up}}\frac{1}{\sigma_y}=\frac{H'}{\sigma_y} \qquad (5.21)$$

in which H' is the slope of the plot at the particular value of $\bar{\sigma}$.

On substituting into Eq.5.17, we obtain after some transformation, simply,

$$A=H' \qquad (5.22)$$

This re-establishes the well-known Prandtl-Reuss stress-strain relations.

5.2.7 Corners of a Yield Surface

It happens, not in frequently, that the yield surface is defined not by a single continuous (and convex) functions but by a series of functions:

$$F_1,\ F_2,\ .....,Fn \qquad (5.23)$$

The state of strain below the yield limit being defined by negative values of all the functions F.

For the most of the bounding surface, only a single condition such as $F_m=0$ defines the yield surface and flow rules discussed in section 5.2.2 are applied at a corner of the yield surface, we may have however the condition that,

$$F_h=.....F_m=0 \qquad (5.24)$$

Here, the Koiter[29] generalization replaces Eq.5.3. This is given as,

$$d\{\varepsilon_p\}=\lambda_h\left\{\frac{\partial F_h}{\partial\{\sigma_h\}}\right\}+\cdots+\lambda_m\left\{\frac{\partial F_m}{\partial\{\sigma_m\}}\right\} \qquad (5.25)$$

where, quantities of λ_i are positive constants (Fig.5.1) Matrices like Eq.5.14 can once again be written now with several undetermined parameters. Procedures which are similar to those above will yield forms for the elasto-plastic matrix which is applicable at such corners.

It is avoided for the best from the computation of singular points on yield surfaces by a suitable choice of continuous surface which represents a good degree of accuracy to the true conditions.

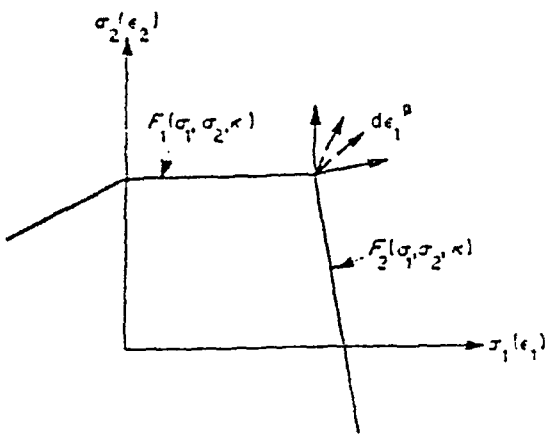

Figure 5.3 Corners in a yield surface

5.3 Calculation of Elasto-Plastic Stresses

Various computational procedures have been used successfully for a limit range of elasto-plastic problems utilizing the finite element approach. There are two main formulations. In the first formulation, during an increment of loading, the increase of plastic strain is computed and treated as an initial strain for which the elastic stress distribution is adjusted. This approach manifestly fails if ideal plasticity is postulated or if the hardening is small. The second approach is that in which the stress-strain relationship for every load increment is adjusted to take into account plastic deformation with properly specified elasto-plastic matrix, this incremental elasticity approach can successfully treat ideal as well as hardening plasticity.

From the computational point of view, the incremental elasticity process has one serious disadvantage. At each step of computation the stiffness of the structure is changed and it is necessary to avoid from excessive computer times for iterative solution processes. The initial stress method is developed by Zienkiewicz [56] as alternative approach to the incremental elasticity processes. By using the fact that even in ideal plasticity, increments of strain prescribe uniquely the stress system (while the reverse is not

true for ideal plasticity), an adjustment process is derived in which initial stresses are distributed elastically through the structure. This approach permits the advantage of initial processes (in which the basic elasticity matrix remains unchanged) to be retained. The process appears to be the most rapidly convergent. To start elasto-plastic stress analysis, this method uses one dimensional tensile specimen in elasto-plastic region, then moves onto the two and three dimensional stress case. For a tensile specimen loaded just over the elastic region ($\varepsilon_{total}=\varepsilon_1$), stress σ_x is calculated linear elastically, thus the initial stress σ_{o1} as shown Fig.6.4 is given by the following form,

$$\sigma_{o1}=\sigma_x-\sigma_{f1}=\sigma_1-\sigma_{f1} \tag{5.26}$$

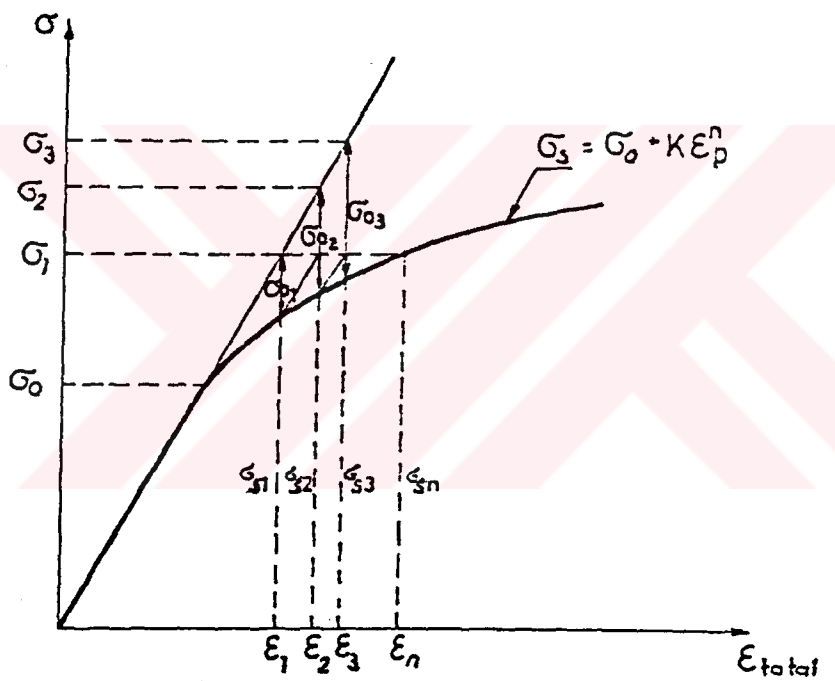

Figure 5.4 Representation of initial stress method (Modified Newton-Raphson method)

By using σ_{o1}, increasing stress value can be written as,

$$\sigma_2=\sigma_x+\sigma_{o1} \tag{5.27}$$

Which correspond to ε_z. The stress difference between σ_2 and real stress at ε_2 gives σ_{o2}. σ_3 is obtained by replacing σ_{o2} with σ_{o1} in Eq.5.27. The following analog iteration steps lead to the point corresponding to the elasto-plastic strain ε_n and stress σ_x where σ_{oi} is the initial stress.

For calculation of stresses in two-dimensional cases equivalent stress is usually obtained according to the Von Mises Criterion (Distortion Energy Theory). The equivalent stress in the case of axi-symmetric problem is,

$$\bar{\sigma} = \left\{ \frac{1}{2}[(\sigma_r - \sigma_z)^2 + (\sigma_r - \sigma_\theta)^2 + (\sigma_\theta - \sigma_z)^2] + 3\tau_{rz}^2 \right\}^{\frac{1}{2}} \qquad (5.28)$$

where, σ_r, σ_z, σ_θ, and τ_{rz} are the stress components. Therefore initial stress can be obtained for one-dimensional case in plastic region as,

$$\sigma_o = \bar{\sigma} - \sigma_f \qquad (5.29)$$

where, σ_f is obtained from σ, ε_{total} diagram for a uniaxially loaded tensile specimen. But the initial stress can not be exactly described as in Fig.5.4 for axi-symmetric case. It can be mathematically described as follows,

$$\{\sigma_o\} = \{\sigma_{or} \ \sigma_{oz} \ \tau_{orz} \ \sigma_{o\theta}\} \qquad (5.30)$$

where, σ_{or}, σ_{oz}, $\sigma_{o\theta}$, and τ_{orz} are components of the initial stress in axi-symmetric case. By using the following formal way, it is obtained as,

$$\{\sigma_o\} = \{\sigma\}\frac{\sigma_o}{\bar{\sigma}} \qquad (5.31)$$

where, the component of $\{\sigma_o\}$ are proportional to elastically calculated stress. The related equivalent stress value is equal to $\{\sigma_o\}$ obtained in one-dimensional case, According to Eq.5.28,

$$\bar{\sigma}_o = \left\{ \frac{1}{2}[(\sigma_{or} - \sigma_{oz})^2 + (\sigma_{or} - \sigma_{o\theta})^2 + (\sigma_{o\theta} - \sigma_{oz})^2] + 3\tau_{orz}^2 \right\}^{\frac{1}{2}} \qquad (5.32)$$

The loading corresponding to the initial stress as follows,

$$\{F\}_{\sigma_o} = \int_V [B]^T \{\sigma_o\} dV \qquad (5.33)$$

First the solution displacement vector is calculated for $\{F\}_{\sigma_{o1}}$, as follows,

$$\{\delta\}_1 = [K]^{-1}\{F\}_m \qquad (5.34)$$

where $\{F\}_m = \{F\}_s + \{F\}_{\sigma_o}$ then the following iteration steps $\{\delta\}_I$, i=1,2,....,n are calculated until there is no difference between $\{\delta\}_i$ and $\{\delta\}_{i+1}$. Then the displacement vector is ,

$$\{\delta\}_n = [K]^{-1} \{F\}_m \quad (5.35)$$

Finally, the stress σ_n corresponding to $\{\delta\}_n$ in elasto-plastic region is calculated as,

$$\{\sigma\}_n = [C][B]\{\delta\}_n - \{\sigma_{oi}\} \quad (5.36)$$

Residual stresses can be found at the end of the iteration as follows,

$$\{\sigma_{rs}\} = \{\sigma\}_n - \{\sigma\}_e \quad (5.37)$$

where, $\{\sigma\}_e$ is the linear elastic stress.

CHAPTER 6

PROPERTIES AND CLASSIFICATION OF WELDING PROCESSES

6.1 Definition Of Welding

A weld is defined by the American Welding Society as a "Localized coalescence of metals where in coalescence is produced by heating to suitable temperatures, with or without the application of pressure and with or without the use of filler metal. The filler metal either has a melting point approximately the same as the base metals or has a melting point below that of the base metals but above 426^{0}C (800^{0}F) [3].

The simplest welding process would be one in which the two parts to be joined have their surfaces prepared to contours matching with atomic precision. Such surfaces brought together in vacuum, so as to enable electrons to be shared between atoms across the interface could result in an ideal weld. The preparation of surfaces with this degree of precision and cleanliness is not feasible at present, although it is approached in space technology when metals may be in contact in the ultra-high vacuum of outer space. Slight rubbing of surfaces under these conditions can induce welding by satisfying the first two conditions above at limited points of contact, the third being supplied already by the vacuum while such conditions of cleanliness and vacuum might be visualized for special micro-welding applications, alternative solutions must be found for practical welding.

The problem of achieving atomic contact between the parts to be joined is solved in one of two ways. Pressure may be applied so that abutting surfaces are plastically deformed giving the required intimacy of contact at least at asperity as indicated in Fig.6.1.(a). The deformation also helps to satisfy the cleaning requirement by rupturing films. With ductile metals, the plastic deformation can be accomplished cold but less malleable metals may be first softened by heat. Alternatively, the surfaces to be joined may be bridged with liquid metal. The required adjustments in contour and structure are then affected as the melted metal solidifies (Fig.6.1.(b)).

The two types of welding process described are fundamentally different and the division between them forms the first breakdown in the classification of welding processes.

Those welding methods employing pressure to deform the contact surfaces plastically are frequently called 'solid-phase' methods. There is no accepted term for the methods in which union is made through liquid metal but they may be called 'liquid-phase' methods.

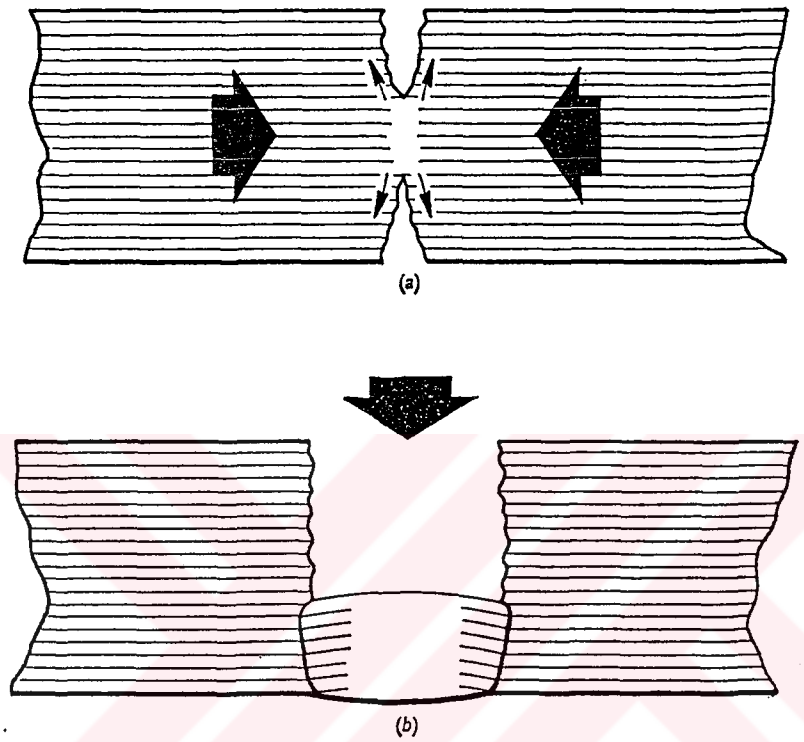

Figure 6.1 Basic mechanisms of welding. (a)Union by flow. (b)Union by molten metal bridging.

For some years, it has been customary to divide welding processes into 'pressure' and 'fusion' welding methods. The pressure-welding processes were those in which pressure is used at some stage in welding, and while this classification included all the methods which could be truly classed as solid-phase methods it also included several methods in which fusion takes place. So, word 'fusion' must be used with care in the welding context.

6.2 Basic Requirements Of Welding

The ideal weld is one in which there is complete continuity between the parts joined and every part of the joint is indistinguishable from the metal in which the joint is made. Although this ideal is never achieved in practice, welds which give satisfactory service can be made in many ways.

Not every welding process is equally suitable for each metal, type of joint or application. Much of the skills of the welding engineer consists the choice of the appropriate welding processes in the recognition of the essential requirements which can be a particular weld.

For a permanent joint to be made, it is not enough just to bring one member with its surface thoroughly cleaned into contact with another member with a similarly prepared surface.

Each welding processes must fulfill a number of conditions. Most important, energy in some form, usually heat, must be supplied to the joints so that the parts can be united by being fused together. The heat may be generated by a flame, an arc, the resistance to an electric current, radiant energy or by mechanical means. In a limited number of processes such as pressure welding, the union of the parts is accomplished without melting, but energy is expended in forcing together the parts to be joined and heat may be used to bring the weld region to a plastic condition. Fusion is generally considered as synonymous with melting, but in the context of welding, it is desirable to distinguish at once between these words. By common usage the word fusion implies melting with subsequent union, and it is possible for the parts of a joint to be melted but not fused together.

Two surfaces can only be united satisfactorily if they are free from oxide or other contaminants. Cleaning the surfaces before welding, though helpful, is not usually adequate and it is a feature of every welding process that the contaminated surface film is dissolved or dispersed. This may be done by the chemical action of a flux or the sputtering of an electric arc or even by mechanical means such as rupturing and rubbing. The contaminants which must be removed from the surface are of three types-organic films, absorbed gases and chemical compounds of the base metal, generally oxides. Heat effectively removes thin organic films and absorbed gases so that with the majority of welding processes where heat is employed it is the remaining oxide film which is of greatest importance.

Once removed, surface films and particularly nitrides, must be prevented from forming during the process of welding. In almost every welding process, therefore, there must be some way of excluding the atmosphere while the process is carried out. If a flux is used for cleaning the fusion faces

of the joints, this also performs the function of shielding. If a flux is not used, shielding can be provided by a blanked of an inert gas, or a gas which does not form refractory compounds with the base metal. The atmosphere may also be excluded mechanically by welding with the faces to be joint in close contact and the ultimate in protection from the atmosphere is obtained by removing it entirely by welding in a vacuum where welding operation is carried out at high speed and with such limited heating that there is no time for appreciable oxidation, shielding may be unnecessary. It is possible with a few processes, however, for any contaminated molten metal to be expelled before the joint is completed or for the properties of the weld metal to be corrected by making alloying additions to the weld pool.

One further important requirement is that the joint produced by the welding process should have satisfactory metallurgical properties. In methods which involve melting of some part of the joint, it is often necessary to add deoxidants or alloying additions, just as is done in the foundry. Frequently the material to be welded must have a controlled composition. Some alloys-happily few-are unweldable by almost any process, but a great many are only suitable for welding if their composition is controlled within close limits. These considerations are the basis of welding metallurgy.

To summarize: every welding process must fulfill four requirements:

1. A supply of energy to create union by fusion or pressure.
2. A mechanism for removing superficial contamination from the joint faces.
3. Avoidance of atmospheric contamination or its ef fects.
4. Control of weld metallurgy.

6.3 Classification Of Welding Processes

Welding processes may be classified according to the way in which the four basic requirements -particularly the first three-are satisfied. The energy for welding is almost always supplied as heat so that divisions can be made according to the methods by which the heat is generated locally. These methods may be defined and grouped as follows,

a. Mechanical. Heat generated by impact or friction or liberated by the elastic or plastic deformation of the metal.
b. Thermo-chemical. Exothermic reactions, flames and arc plasmas. It is necessary to explain why plasmas should be put in the same class as oxyfuel gas flames. Although chemical reactions may not take place in a plasma, the method of heat transfer to the work is the same as for processes employing an envelope of burning gas. This holds for all processes in which the work does not form part of the arc circuit. The so called nontransferred arc procedures a plasma flame, whereas the transferred arc is a constricted arc and falls in the arc process category.
c. Electric resistance. Heat generated by either the passage of a current introduced directly to the metal to be joint or by a current induced within the parent metal.
d. Electric arc. Both a.c. and d.c. arcs with electrodes which melts and those which do not.
e. Radiation. This category is suggested to cover the new processes such as laser and electron-beam welding and others which may yet be developed. The essential feature of a radiation process is that energy is focused on the workpiece and heat is generated only where the focused beam is intercepted.

It is not possible to define all welding processes completely by the source of thermal energy. This applies particularly to the many variations of arc welding and it is customary to complete the definition by reference to the way the processes satisfies the condition of atmosphere control. All welding processes can be examined in the same way by placing the names of the processes within a grid formed by listing the sources of heat along one axis and methods of avoiding atmospheric contamination along the other axis as is done Fig.6.2. The diagram can now be divided up into areas enclosing processes with a basic similarity. Seven such areas are readily identified corresponding to processes as follows: (1)Solid-phase, (2)Thermo-chemical, (3)Electric-resistance, (4)Unshielded arc, (5)Flux-shielded arc, (6)Gas-shielding arc, (7)Radiation.

Certain areas in the diagram can be marked out as regions where welding processes could not exist-for example flames can not be used in vacuum. This way of classifying welding processes is less rigid than the family tree method and makes it possible to account for certain anomalies. The resistance butt welding process, for example, while truly a

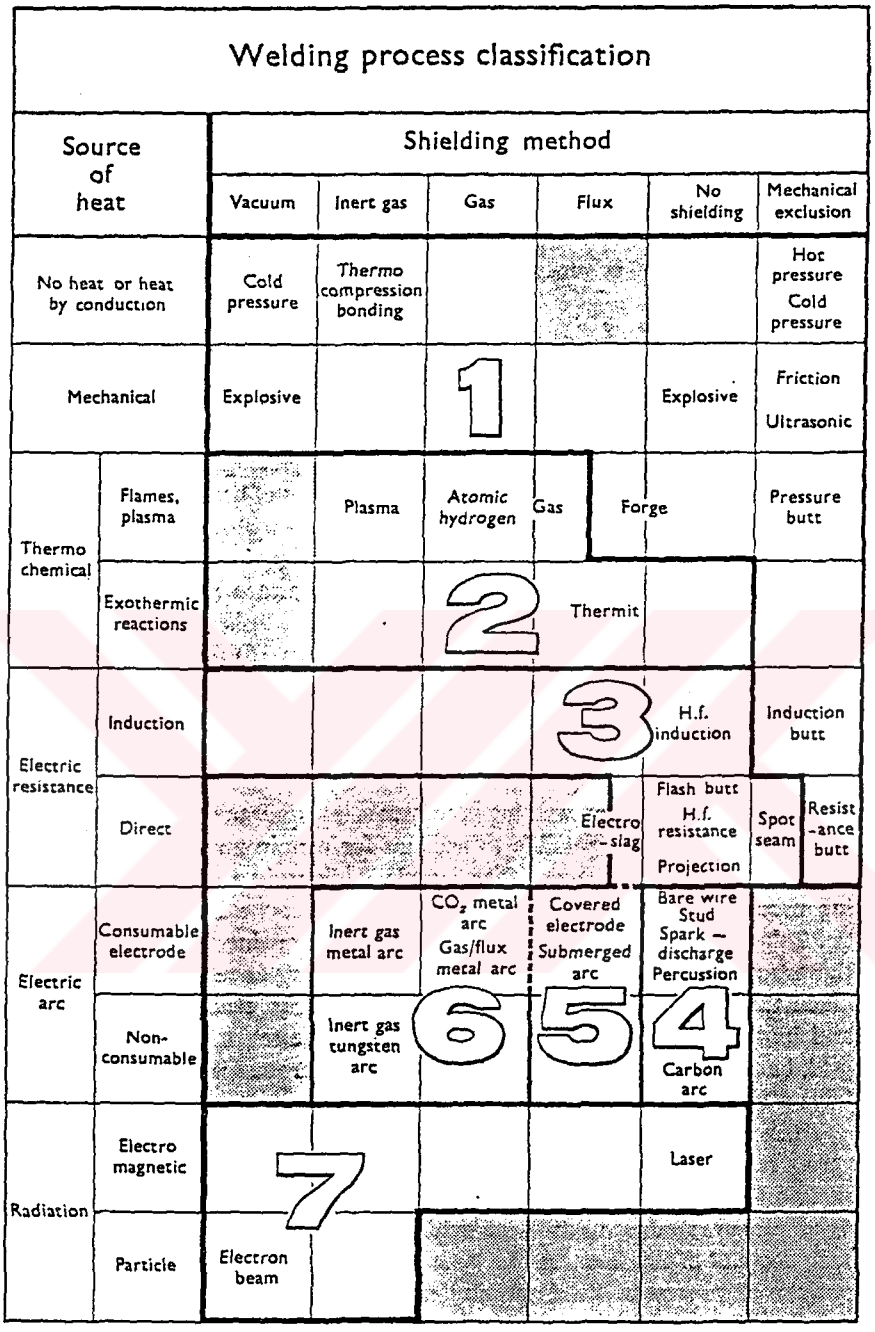

Figure 6.2 Grouping of welding processes according to heat source and shielding method.

solid-phase welding process, is normally included in the resistance welding category. In Fig.6.2, the position of this process is clarified by drawing the boundary of the group as: (1)Solid-phase processes to include resistance butt and to exclude the remaining resistance processes. Similarly, electro-slag welding and its derivatives can be

placed correctly in the resistance heat source grid, but may be linked with the flux-shielded arc processes with which they have a great deal in common.

There is no uniform method of naming welding processes. Many processes are named according to the heat source or shielding method, but certain specialized processes are named after the type of joint produced. Examples are stud, spot and butt welding. An overall classification can not take account of this because the same type of joint may be produced by a variety of processes. Stud welding may be done by arc or projection welding and spot welding by electric resistance, arc, or electron beam processes. Butt welding may be done by resistance, flash or any of a number of other methods. Although in common usage, many processes have abbreviated names, the full names often follow the pattern: First, a statement of the type of shielding (where mentioned); secondly, the type of heat or energy sources; thirdly, the type of joint (where this is of specific and not general importance) The full names discussed above can be shown as Table 6.1.

Type of shielding	Type of heat or energy source	Type of joint
Inert gas	Tungsten-arc	Spot
(unshielded)	Arc	Stud
---	Resistance	Butt
---	(Resistance)	Projection
(vacuum)	Electron beam	---
(Flux-covered electrode)	Metal-arc	---
---	Friction	(Butt)

Table 6.1 The full names of welding processes (Brackets enclose terms implied but not mentioned.).

It is often necessary when referring to processes to mention the way they are used, particularly whether the operation is manual or automatic. The practical operation of welding can be divided into three main parts as follows,

a. The control of welding condition, particularly arc length and electrode or filler wire feed rate and time.
b. The movement and guiding of the electrode, torch or welding head along the weld line.
c. The transfer or presentation of parts for welding.

Processes are described as manual, semi-automatic, or automatic, depending on the extend to which the parts mentioned above are performed manually. Manual welding is understood to be that in which the welding variables are continuously controlled by the operator and the means for welding are held in the operator's hand. Semi-automatic welding is that in which there is automatic control of welding conditions such as arc length, rate of filler wire addition and weld time, but the movement and guiding of the electrode torch or welding head is done by hand. With automatic welding at least parts (a) and (b) of the operation must be done by the machine. As feed-back control devices are introduced and welding takes its place more frequently in the automatic production line, other definitions will be required.

CHAPTER 7

ELECTRIC RESISTANCE WELDING

7.1 Introduction

Two way exists of utilizing an electric current to produce heat directly in a metal. The current may be used to maintain an arc to the surface of the workpiece, as in arc welding, or heat may be liberated by the passage of the current to the work. In the resistance welding, heat is generated by the resistance to the passage of the current.

Heat in arc welding is generated at the surface and is distributed through the workpieces by conduction. In the resistance method, heat can be liberated throughout the entire cross-section of the joint. The electric current which generates the heat may be introduced to the work through electrodes with which the work makes contact, or it may be induced within the metal by a fluctuating magnetic field which surrounds the work. Although both methods depend on resistance heating, the term resistance welding is often used only for the former. The latter process is known as induction welding.

A variety of resistance-welding methods exist depending on the different ways of creating a locally high resistance so that heating may be concentrated at this point. Actual resistance depends on the resistivity and geometry of the conductor. Since the resistivity is fixed by the workpiece materials, it is usual to create the local high resistance by providing a restricted current path between the parts to be joined, a procedures known as current concentration. All resistance-welding methods require physical contact between the current-carrying electrodes and the parts to be joined. Pressure is also required to place the parts in contact and consolidate the joint and these are features which distinguish the processes from the most of arc welding methods.

7.2 The Electric Resistance Welding Principle

If two pieces of metallic materials to be welded are placed between two low resistance conductors (electrodes), and a low-voltage, high-amperage current is applied, the materials will be heated because of their resistance to the current flow. If some means is provided to clamp the pieces

together, after being thus heated to a plastic temperature, a bond is created at the contacting surfaces between the electrodes. To complete the weld satisfactorily, the current must be interrupted and the pressure must be retained until the weld strengthens after cooling.

The short interval of time of most resistance-welding process, cycle makes possible the welding of thin sections to heavy ones, the welding together of dissimilar metals, and the welding together of metals which have different thickness simultaneously. The metallurgical advantage of this process is that the metal is held at a temperature that is within the grain-growth range for only a short period of time.

Fortunately, temperatures produced by the passage of current through the workpieces to be welded are the highest at the point of contact between the pieces, thus heat does not extend throughout their entire thicknesses. This feature promotes the rapid production of high-quality welds.

The heat is generated by the resistance to the passage of the current according to Joule's law as follows,

$$H=I^2RT \qquad (7.1)$$

where, H=heat induced, I=current in amperes, R=resistance, and T=time.

To realize the greatest heating effect, it is evident that "I" should be large, since H varies as I^2. For this reason, resistance welders utilize low voltages and high amperages.

Electric resistance welding may exist in several forms, such as spot welding, seam welding, projection welding, upset welding, flash welding, and percussion welding.

7.3 Electric Resistance Spot Welding

This process, in which overlapping sheets are joined by local fusion caused by the concentration of current between cylindrical electrodes. Figure 7.1 is a diagrammatic arrangement of the process. The work is clamped between the electrodes by pressure applied through levers, or by pneumatically operated pistons. On small welding machines, springs may be used. Current is generally supplied by a step-down transformer, the work, electrodes and arms of the machine being part of a secondary circuit consisting of

only one or two turns. A spot-welded joint comprises an array of one or more discrete fused areas or spots between the workpieces. Fig.7.2 shows the electric circuit of the resistance spot weld and spot weld.

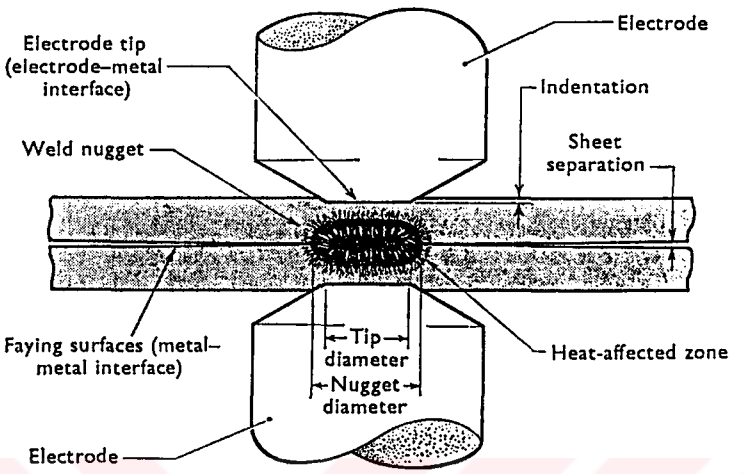

Figure 7.1 Features of the resistance spot weld processes.

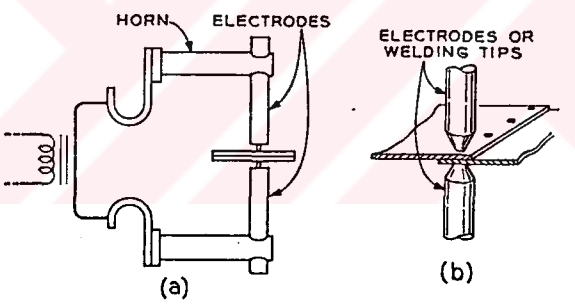

Figure 7.2 (a) Sketch of spot welding circuit. (b) spot weld.

7.3.1 Electrode And Nugget Size

Current concentration is determined by the area of contact between the electrodes and the work, and clearly the size of the weld or nugget or fused metals is closely related to this area. The shear strength of the nugget must usually be sufficient to ensure that when the joint is stressed to failure, and this occurs in the sheet around the nugget. A desirable form of failure is the pulled slug type where fracture occurs in one sheet round the nugget which is left attached to the other sheet.

A method for standardizing the size of the electrode according to the sheet thickness has become accepted which has its origin in the procedure for riveting. Riveted joints are often designed on the basis $d=1.2\sqrt{t}$ where, d is the rivet diameter and t is the sheet thickness. The relationship is probably of this form because of the efficiency of single-row riveted joint, rivet strength/sheet strength, is $(\pi d^2 f_s)/(4ptf_t)$, where p is the pitch of the rivets and f_s and f_t are respectively the shear strength and tensile strength of the rivet and plate. For any given pitch d^2/t is constant. In a riveted joint, the hole for the rivet weakens the plate. With a spot-welded joint, the weld is integral with the plate so that the only weakening occurring is that due to the softening effect of the welding heat. Higher efficiencies can therefore be achieved in welding. Because weld diameter is so closely related to electrode diameter and the electrode diameter d_e is made equal to $\sqrt{t}$. The above discussion should not give the impression that the accepted relationship, although useful, is in essence anything but empirical. Other formulae for relating electrode diameter to sheet thickness such as $d=0.1+2t$ are used which give substantially the same result except for very thin or thick metal where the $\sqrt{t}$ formula is more reasonable.

It is important to recognize when considering the strength of a spot weld that in sheet metal the weld is rarely if ever stressed solely in shear because of distortion which takes place round the weld under load. Under these conditions the ductility of the parent metal at the periphery of the weld can have a dominating influence. A useful indication of weld ductility is obtained by taking the ratio of cross-section strength (f_t) and shear strength (f_s). This ductility ratio $f_t/f_s \rightarrow 1$ for maximum ductility and approaches 0 when extreme brittleness is present. These considerations are particularly important when welding material susceptible to quench hardening because of the high cooling rates in resistance welding.

In practice, the area of contact between electrode and work can not be controlled by using electrodes in the form of rod of the requirement diameter-such electrodes would be mechanically weak and have too high a resistance. Practical electrodes are made of copper or copper alloy bar of substantial diameter machined to a truncated cone with an angle of 30^0. Alternatively, electrodes may be machined with

a domed end, the radius of the dome being used to control the area of contact. Clearly, electrode load and sheet hardness are also significant factors in determining the area of contact with domed electrodes. Contact area is controlled more accurately with truncated cone electrodes and any wear in service can be readily seen. Compared with the domed electrode, however, they result in more obvious surface marking of the workpiece and require more accurate alignment. Although simple symmetrical electrodes are preferred a variety of special shapes is used to obtain access with complicated joints (Fig.7.3).

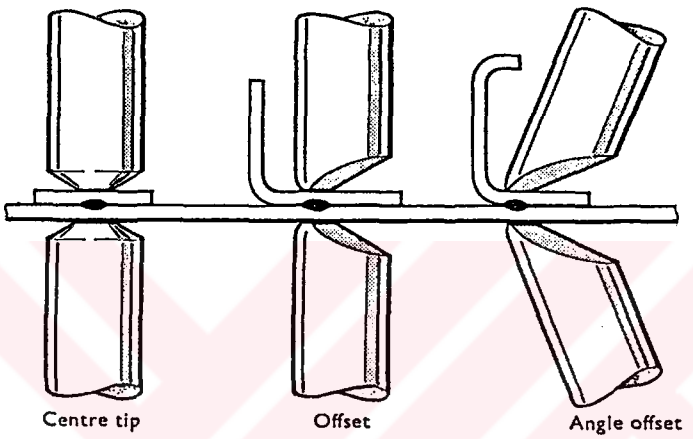

Figure 7.3 Special types of offset electrodes.

7.3.2 Resistance And Force

Having established the relationship between electrode shape and workpiece thickness it is possible to examine the part played by the three important process variables, electrode clamping force, current and time of current flow. When the parts to be welded are clamped between the electrodes the inter-electrode resistance comprises seven separate resistances, as shown in Fig.7.4. These resistances can be written as follows,

1. Resistance of upper electrode.
2. Contact resistance between upper electrode and upper sheet.
3. Resistance of upper sheet.
4. Contact resistance between upper and lower sheets.
5. Resistance of lower sheet.
6. Contact resistance between lower sheet and lower electrode
7. Resistance of lower electrode.

Of these seven resistances where heat can be developed number 4, the interfacial or sheet/sheet contact resistance, is the most important as it is at this position that the nugget and, therefore, the heat is required. Resistance here is important early in the weld period. Consistent weld size depends, among other things, on consistency of surface condition at this interface with low resistivity metals, resistances 2,4, and 6 assume greater importance and the need for their control increased. Aluminium alloys, for example, are subjected to a rigorous pre-weld treatment of de-greasing and pickling a limited time before welding to ensure consistent contact resistance where, such controls are required it is usual to check the contact resistance periodically by measuring the voltage drop when a current is passed across a pair of samples clamped together. An apparatus of the type shown in Fig.7.5 is used and resistance is calculated using Ohm's law. Contact resistance are usually in the range 50-100 μΩ but may be 20μΩ for aluminium.

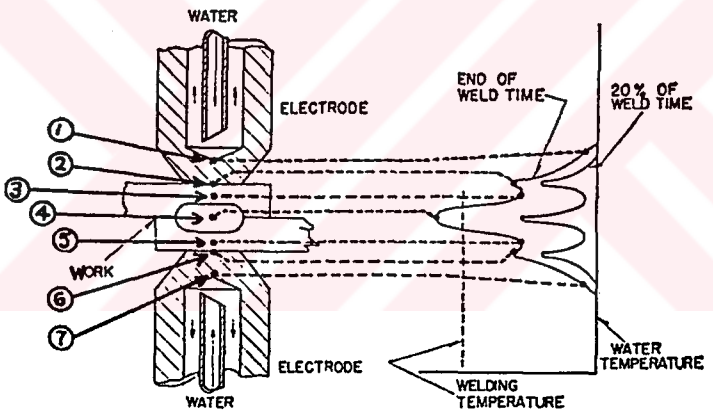

Figure 7.4 Contact resistance and temperature distribution in spot welding.

The body resistances 3, and 5 depend on the resistivity and temperature of the work and can not be altered. Body resistance has a major effect later in the weld period. The body resistance of the electrodes 1, and 7 depend on the resistivity and temperature of the electrodes. Contact resistances 2, and 6, electrode to sheet, are wholly undesirable and kept to a minimum by using high conductivity electrodes and ensuring that there is adequate cleanliness and clamping force. Unfortunately, the requirements of high electrical and thermal conductivity are not compatible with good mechanical strength and wear resistance at elevated temperatures. A variety of copper alloys, for example chro-

mium-copper, cadmium-copper or beryllium-cobalt-copper, are employed which provide a range of properties suitable for different applications. The ill effect of resistance at the work surface, surface pick-up, splashing and electrode wear can be mitigated by water cooling the electrodes internally so that heat is conducted away rapidly. Efficient electrode cooling is essential with high production rates.

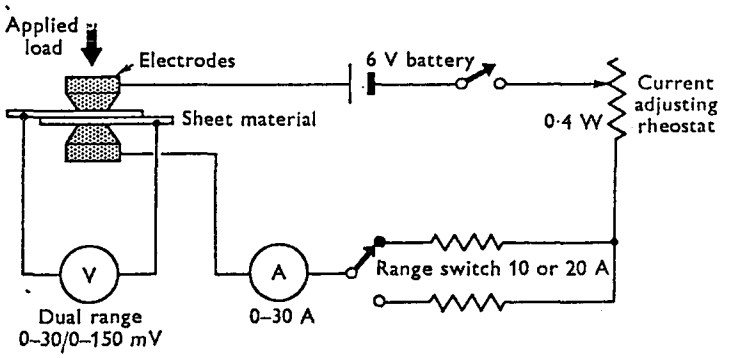

Figure 7.5 Apparatus for measuring surface resistance.

The effect of increasing electrode force is to reduce the contact resistance as shown for a heat-resisting steel in Fig.7.6, but the anomaly is noted that contact resistance is independent of area for any one electrode force. Contact resistance has been defined as comprising two parts; true contact resistance which is influenced by load, surface finish and condition and spreading resistance caused by the restriction of current through local points of contact. Spreading resistance is proportional to the resistivity of the material and the number of points of contact in parallel. These points of contact are possibly associated with the rupturing of surface oxide films where roughness is deformed. Contact resistance, depending on the resistances at the multiple points of contact which are deformed by pressure, does not return to its original value once the load is released.

For consistent operation, high electrode forces would be desirable, but particularly when welding low resistivity metals, resistance can not be reduced too far by raising force as it must be present to develop the welding heat. Excessively high forces are also undesirable because of the increase in surface indentation of the work and wear of the electrodes. Force is maintained for several cycles after the current is cut off to consolidate the nugget.

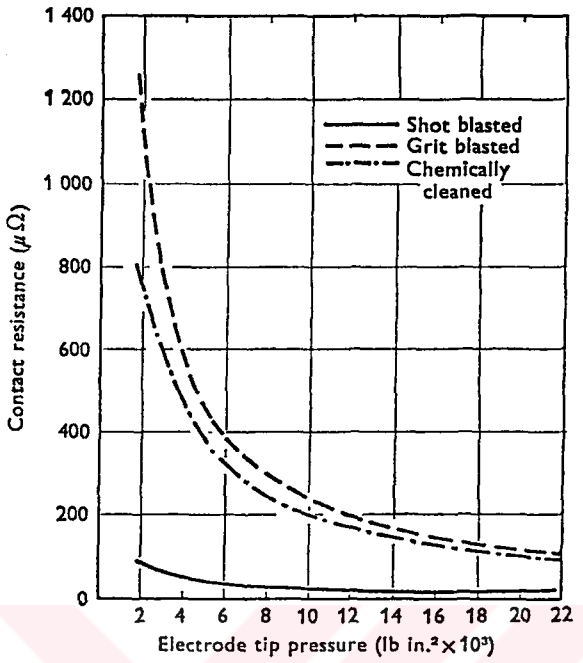

Figure 7.6 Variation of contact resistance with tip pressure[21].

7.3.3 Current And Time

The effects of current and time can be considered together but, while they both affect the quantity of heat developed, it is the current alone which determines the rate of heat development. While the current is passing, some of the heat generated is lost, mainly to the water-cooled electrodes. The size to which a nugget will grow, and indeed whether a nugget will form at all, depends on the heat being generated faster than it is removed by conduction. Current, therefore, is a most critical variable.

When establishing procedures for welding a particular material and thickness, however, the strength/current curve at fixed times is most useful (Fig.7.7). Strength/time curves for fixed currents are similar. Each material has its characteristic curve-steeply rising curves with a sharp cut-off indicating that the setting of current is critical and, therefore, that the metal is difficult to weld.

Because of the selection of electrode sizes in proportion to sheet thickness a certain rationalization in choice of current and time is feasible. From an inspection of experi-

mental and published data Humpage and Burford proposed simple formulae for determining current and time for mild steel. These were of the form:

Current density=120000+ke^{-25t} amp/in.^{2}. (7.2)

where, t is the sheet thickness (in.) and k a constant which for present-day techniques approximates to 300000.

Time=250t cycles (of 50 c/s supply) (7.3)

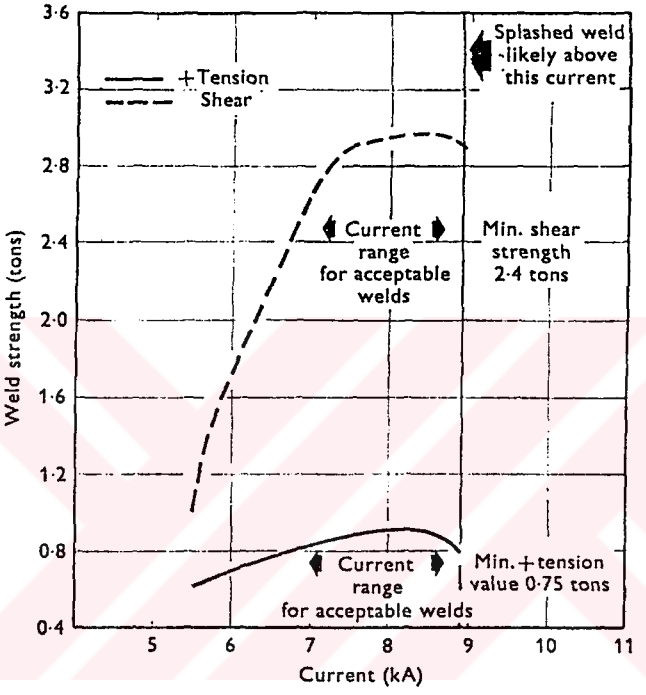

Figure 7.7 Strength/current relationship for spot welds in 0.104 in. thick martensitic stainless steel; weld time 100 cycles [21].

The actual level of current required for any metal tends to be inversely proportional to its electrical and thermal resistivities. Copper is impossible to weld because the total resistance of the joint can not be sufficiently above that of the secondary circuit of which it is a part. The insertion of a shim of high resistance low melting point alloy allows to be generated between the workpieces, but the process is then called resistance brazing. Electrodes having high electrical and thermal resistivities also assists by generating heat and restricting the conduction of heat away from the joint.

The above discussion assumes a constant size of electrode tip because current concentration is of equal importance

with current. In use electrode, tips wear and spread are reduced thereby reducing current density and weld size.

7.3.4 Nugget Formation

Further important aspects of the force, current and time relationship become apparent in tracing the growth of the weld. Resistance welds are characterized by their rapid formation and the steep heating and cooling curves. This is because of their local nature and the proximity of the electrodes.

Having applied the electrode force, the passage of current is initiated and almost immediately, frequently within one cycle, there is a drastic drop in contact resistance. Because of the current concentration and resistances 2,4, and 6, the temperature at the sheet/sheet interface and in two annular regions under the electrodes rises rapidly. Although the contact resistance is lowered quickly, the heated metal in this region provides a locally higher resistance and the temperature at the interface continues to rise. Resistance welding could not be carried out if metals did not have positive temperature coefficients of resistance. Fig.7.8 shows the temperature distribution in a partly finished 2x1/4 in. mild steel spot weld as determined by metallographic means. As the process continues a molten nugget develops, the diameter of which increases rapidly at first and then more slowly as the maximum size is approached which may be up to 10 per cent greater than the electrode diameter. In a spot weld where the parts fit well and there is adequate electrode force, the molten nugget is safely imprisoned between the sheets, although it is subject to hydrostatic pressure from the electrodes. As the heat spreads in the inter stages of the weld cycle, the electrodes begin to sink into the work surface and as a result of plastic deformation the sheets begin to separate at the weld edge. These effects, indentation and sheet separation, set a top limit on current and time. The flow of current through the nuggets causes turbulence in the liquid metal.

The pressure and plastic deformation to which the ring of heated metal sealing the periphery of the nugget is subjected can result in corona bonding, when the workpieces are susceptible to pressure welding as with aluminium. Accidental rupture of this seal results in some of the molten nugget metal being spewed out between the sheets. This

is called expulsion, and the weld is said to be 'splashed'. Expulsion puts a top limit on current and is promoted by low electrode force, bad fit or lack of mechanical support as a result of welding close to an edge. It is also possible for expulsion to occur at the electrode/work interface, because of the too rapid or excessive generation of heat at the interface when scale, for example, has created a locally high resistance. Low resistivity metals are prone to surface splashing because electrode/sheet resistance is a higher proportion of the total resistance.

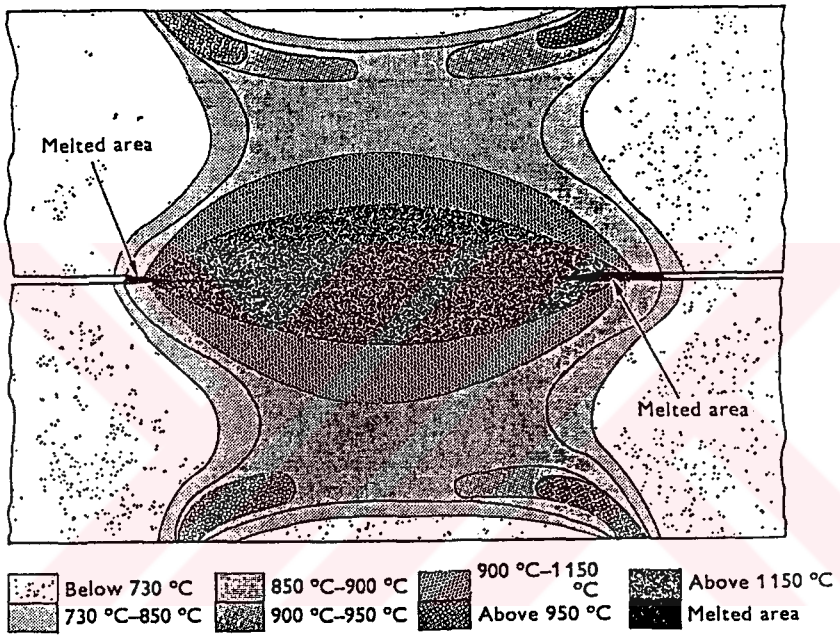

Figure 7.8 Temperature distribution in a mild steel spot weld during the formation of the nugget, as determined by metallographic examination [21].

The process of heating the work and melting a nugget results in thermal expansion which, in spite of the electrode force, tends to separate the electrodes. Since this electrode separation is directly proportional to the heat liberated between the electrodes its measurement may be used as a means of quality control.

7.3.5 Timing In The Resistance Spot Weld

Accurate timing of current flow is the essence of satisfactory spot welding. In addition to producing strong, well-formed spots at a high rate of speed, it is metallurgically important, in most cases, that the heating cycles be

restricted to minimum periods of time. Furthermore, short time periods afford less opportunity for heat dissipation into the parent metal with consequent possibility of distortion.

It is universal practice to reckon times in resistance welding in terms of cycles of the mains supply. Time is not as critical a variable as current when welding mild steel. As welding times are reduced below 10c, however, when thin or high thermal conductivity materials are welded, increased attention to the timing device is required. Greater mechanical precision is also required.

Timers can be mechanical or electronic, synchronous or non-synchronous. Synchronous electronic timers of the digital type can give reproducible times down to 1/4c and are in wide use. Electronic timers based on resistance-capacitor circuits are also in wide use but are less reliable than the digital-type counter which is replacing them.

7.3.6 Series Welding

When it is convenient to approach the work from one side only with the electrodes or where numbers of spots have to be made at the same time a series welding technique is employed, illustrated in Fig.7.9.

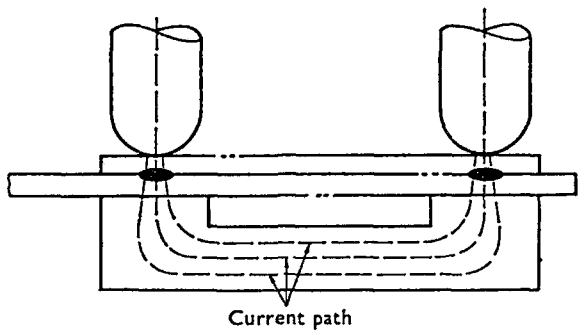

Figure 7.9 Series welding.

Series welding is widely used with multiple-heated machines in the automobile industry. Indirect welding is a special form of series welding in which current may enter through an electrode but leave the work through a contact pad at which point there is no weld because of the large area of contact. The effect of current shunting is of importance in series welding. There are three paths which the current can

take; through the upper sheet, the lower sheet or the backing electrode. The current in the upper sheet is high for the first three cycles because the interfacial resistance which forms part of the circuit with the lower sheet is initially high. At the end of the weld the current is shared almost equally between the sheets.

7.3.7 Heat Balance

There are frequently occasions when metal of two different thicknesses or compositions must be joined. Such differences result in greater heat generation or abstraction on one side than the other and the nugget may grow with its center-line away from the interface resulting in a weak weld. In joints with sheets of equal thickness but unequal resistivity and conductivity, the nugget will grow towards the high resistivity side where, similar materials are welded, but the thicknesses are unequal, the nugget grows towards the thicker side. Equality of fusion into the two different materials may be achieved by increasing the heat generation in the thick or high conductivity metal. This is done by using a smaller diameter electrode (to increase current concentration) or one with a high resistance insert (to reduce heat loss) in contact with the thick or the high conductivity metal if the thick metal is also the one with the higher conductivity the effects of thickness and conductivity can be compensating. With sheet of equal thickness, the nugget would normally move into the low conductivity sheet where most heat is developed. Increasing the thickness of the metal with the higher thermal conductivity moves the nugget in the direction of that metal because the total heat loss along that path is reduced.

7.3.8 Applications

It might be thought that the spot and seam welding processes have a restricted field of application because of the limited variation in joint design which is permissible-that is, lap joints in sheets of the same order of thickness. The processes, however, have extensive application in the joining of sheet metal not only in mild steel but also in stainless steels, heat resisting alloys, aluminium and copper alloys and reactive metals. Dissimilar metal combinations are also welded. Seam welding is not often carried out on metal thicker than 1/8 in. because of the mechanical difficulties in applying pressure and wheel wear, but spot

welding has been used on steel as thick as 3/4 in. Such applications are rare, however, requiring massive machines and long weld times so that the normal upper limit is in the region of 1/4 in. Particularly attractive features of the resistance spot-welding process are the high speed of operation, ease of mechanization, the self-jigging nature of the lap joint and the absence of edge preparation or filler metal.

7.4 Electric Resistance Seam Welding

When a continuous seam is required, as opposed to an array of individual spot welds, two methods are available. Using the equipment described already a series of overlapping spots can be made-a process known as stitch welding. Alternatively, the electrodes may be replaced by wheels or rollers so that work may be moved through the welder continuously without the necessity for raising and lowering the head between welds. The rollers and power driven may or may not be stopped while individual welds are made (Fig.7.10).

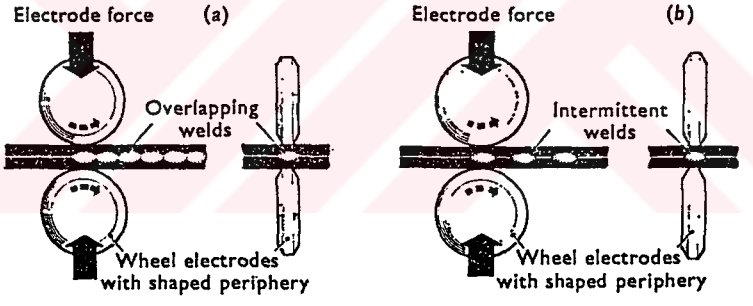

Figure 7.10 Seam-Welding Principle. (a)Overlapping spots; (b)Roller spot.

Current is generally passed intermittently while the electrodes are stationary; partly because trouble with current conduction through moving parts is reduced, but continuous current is also used to a limited extent. A common technique is known as step-by-step seam welding, because while each weld is being made, rotation is stopped and the current is then switched off while the rollers move to the next position.

Adjustment of timing can be made to produce not a continuous seam but a series of individual welds. When this is done, the process is called roller-spot welding. It will be seen, therefore, that spot and seam welding are very

similar and that the terminology refers to the resultant weld. The real distinction is between the use of spot electrodes and roller electrodes.

7.5 Electric Resistance Projection Welding

Current concentration is achieved in this process by shaping the workpiece so that when the two halves are brought together in the welding machine, current flows through limited points of contact. With lap joints in sheet a projection is raised in one sheet through which the current flows to cause local heating and collapse of the projection. Both the projection and the metal on the other side of the joint with which it makes contact are fused so that a localized weld formed. The process is illustrated in Fig.7.11.

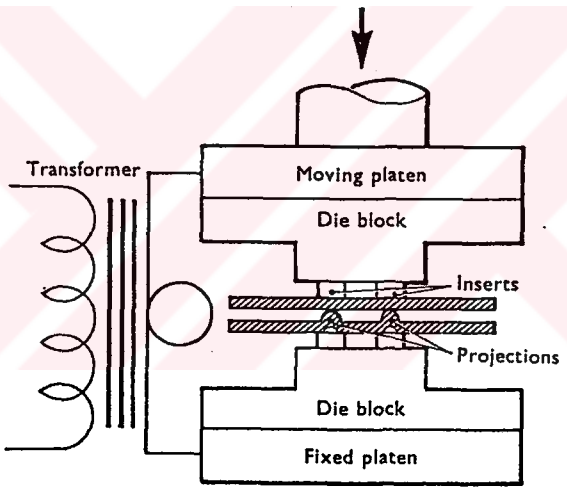

Figure 7.11 Projection welding.

Because current concentration is carried out by the workpiece, the shaped electrodes used in spot welding can be replaced by flat-surfaced platens. These not only conduct to the workpiece they also give support so that there is no deflection except at the projection.

Projection welding is not limited to sheet-sheet joints and any two mild steel surfaces which can be brought together to give line or point contact can be projection welded. Projections can be artificial-produced deliberately by pressing and machining or they can be formed by the natural contours of the parts to be joined. Unlike spot welding there is the possibility of making not only lap welds, but

many other types of joint as well. It is common for three projection welds to be made at the same time. With more than three simultaneous welds, it can not be guaranteed that all the projections will behave identically. Because several welds can be made simultaneously there is no shunting problem, as in spot welding. The method is therefore satisfactory for design where several welds must be made close together.

7.6 Flash Welding

This process is essentially that of placing together, in light contact, two pieces of metal which are to be welded and passing an electric current through them of sufficient voltage and amperage to cause a melting-off and arcing action at the contacting points. This heats them to their fusion temperature and permits the pressure which is then applied to force the fused areas together and form the weld. Fig.7.12 shows this basic application.

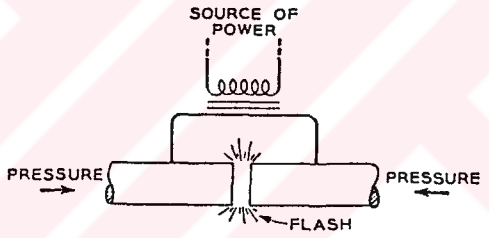

Figure 7.12 The basic flash welder.

The use of this process is usually restricted to welding the end of one piece to that of another, both having the same cross-sectional area. Common among these applications are end welding of strips, bars, rims.

Preparation of surfaces for flash welding is not an important item of cost except when deep pitting and heavy coats of scale, paint, grease, and other foreign materials are present. In good welding practice it is essential that surfaces to which electrodes are clamped be clean to obviate arcing, heating, and general impairment of the free flow of current.

When the welding voltage of up to about 10 is applied at the clamps, current flows through the initial points of contact causing them to melt. These molten bridges are then ruptured and small short-lived arcs are formed. The platen

on which the movable clamp is mounted is moving forward while this takes place and fresh contact are then made elsewhere so that the cycle of events can be repeated. This intermittent process, during which much of the metal contained in the molten bridges is expelled violently in a spectacular manner, is called 'flashing'. Flashing is allowed to continue until the surfaces to be joined are uniformly heated or molten. By this time the moving platen will have advanced, at an increasing rate, to close the gap as metal is expelled, the total distance up to the point of upset being known as the flashing allowance. At this point the rate of movement of the platen is rapidly increased and a high force applied to forge the parts together and expel the molten metal on the surfaces. Ideally, all the molten contaminated metal produced during flashing should be removed in this way to produce a high-quality joint.

7.7 Electric Resistance Upset Welding

Upset welding in its basic form consists of placing two metal workpieces in contact so that their point of contact forms a locality of high electric resistance, passing a sufficiently high amperage and voltage through the juncture to produce heat at the juncture, and applying pressure of sufficient magnitude to force the plastic weld surfaces together to complete the weld.

The upsetting operation follows immediately on flashing, the current not being cut off until upsetting commences. This is required so that the temperature is maintained and adequate plastic deformation can take place without cracking during upsetting. Heating during this period means that lower upset force are required. Upset forces depend in addition upon flashing speed since a high speed gives narrow heating and necessitates higher forces to give plastic flow.

Although the choice between upset and flash welding is usually optional for most joining purposes, the use of the former has generally been abandoned in favor of the latter, the chief reasons being:

1. Greater production speed of flash welding.
2. More favorable power demand.
3. No special preparation of weld surfaces required.
4. Better mechanical properties obtained.

CHAPTER 8

CONTACT RESISTANCE AND METHODS USED TO FIND EXPERIMENTALLY

8.1 Definition Of Contact Types Between Bodies

Contact resistance between bodies contacted to the each other depends on contact types between bodies. Types of contact between bodies changes according to their surface geometry. There are three types of contact depending on surface geometry of bodies. These are plane contact, spot contact, and line contact as shown in Fig.8.1. In the plane contact, the surfaces of bodies are flat and the surface of a body is contacted with the surface of the another body. In the line contact, the surface of a body is contacted with the edge of the another body. In the spot contact, one of the bodies has a spherical surface and this spherical surface is contacted with the surface of the another body.

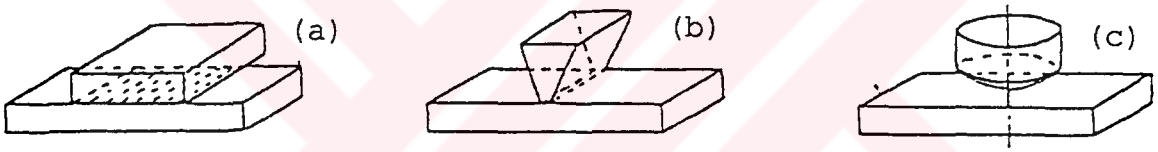

Figure 8.1 Types of contact between bodies. (a) Plane contact. (b) Line contact. (c) Spot contact.

8.2 Material Resistance

This resistance depends on material properties, and the length of current path, and cross-section area of the conductor, and the temperature at the current path. It can be written as,

$$R_m = \rho \frac{l}{s} \quad [\text{Ohm}] \tag{8.1}$$

where, ρ is the electrical resistivity which depends on temperature, l is the length of current path, and s is the cross-section area of the conductor. Table 8.1 shows the values of electrical resistivity for various materials at $20^{\circ}C$ temperature.

Material resistivity can be increased using alloys but this effect decreases at the high temperatures. The electrical resistivity of matrix material is the approximately same

with the resistivity of alloyed material at high temperature.

Material	ρ ($\Omega mm^2/m$)
Aluminium	0.0278
Al-Mg 5	0.059
Pure iron	0.1
Copper	0.0178
Pure nickel	0.069
Pure silver	0.0149
Steel(%0.1C;%0.5Mn)	0.13-0.15
Steel(%0.25C;%0.3Si)	0.18
Tungsten	0.0491
Pure zinc	0.048

Table 8.1 Values of electrical resistivity for various materials at 20°C temperature.

The electrical resistivity increases with hardening, and cold deformation. It also changes with temperature. Fig.8.2.(a) shows the relationship between electrical resistivity and temperature of material. The electrical resistivity of steel changes with value of C. Fig.8.2.(b) shows the relationship between electrical resistivity of steel and value of C within the steel.

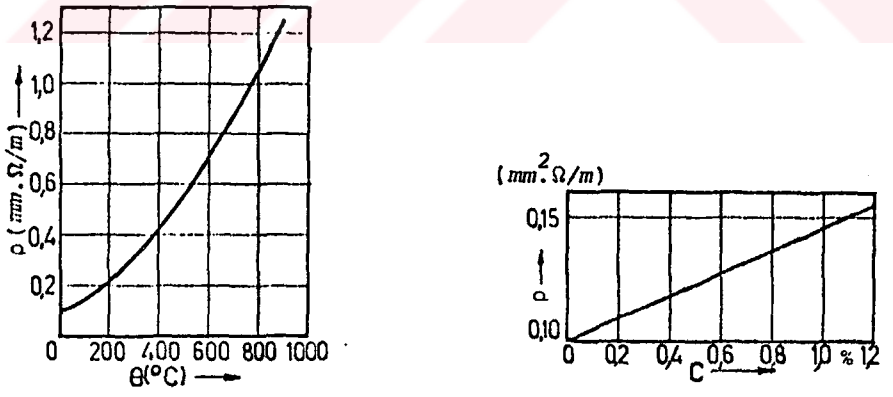

(a) (b)

Figure 8.2 (a)The relationship between electrical resistivity and temperature of materials. (b)The relationship between electrical resistivity of steel and value of C within the steel [8].

The relationship between electrical resistivity and temperature of material for soft steel can be written as follows [53],

$$\rho = 8.56\ 10^{-5}\theta^2 + 4.9\ 10^{-2}\theta + 15.4 \qquad (20 \le \theta \le 800^0C) \qquad (8.2)$$

$$\rho = 2.875\ 10^{-2}(\theta - 800) + 109.4 \qquad (\theta > 800^0C) \qquad (8.3)$$

In the welding of two sheets, current path within the workpieces extends through the outside of the workpiece as shown in Fig.8.3 [17].

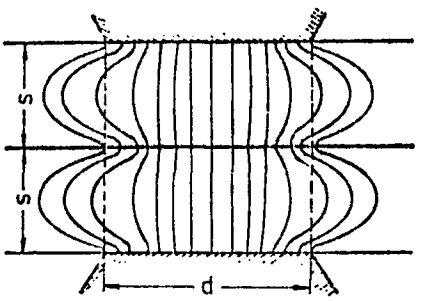

Figure 8.3 Extension of current way in electric resistance spot welding.

The effect of extension is specially important when the rate of "the diameter of electrode tip/the thickness of sheet" decreases. Therefore the material resistance of sheets R_m, is less than material resistance for cylindrical current path. In this case, the material resistance can be written as [30],

$$R_m = \psi R'_m \qquad (8.4)$$

where, R_m is material resistance of a sheet and R'_m is material resistance of a cylindrical workpiece whose diameter is equal to the diameter of the electrode tip, d whose length is equal to the thickness of sheets. ψ depends on d and s, and it can be written as,

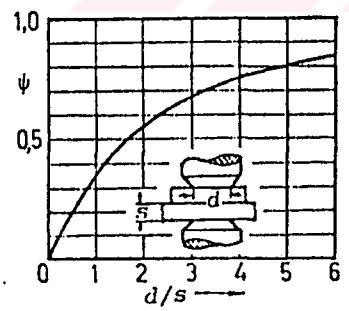

Fig.8.4 The relationship between ψ and d/s.

$$\psi = 1 - \frac{1}{\sqrt{(d/s)^2 + 1}} \qquad (8.5)$$

Fig.8.4 shows relationship between ψ and d/s.

8.3 Contact Resistance

Consider a cylindrical specimen as shown in Fig.8.5.(a) whose diameter is constant and the distance between A and B is equal to "l". If a voltage, U_{AB} is applied between A and B, a current,I passes. In this case, The total resistance between A and B, which is equal to the material resistance, can be written as,

$$R_T = R_M = \frac{U_{AB}}{I} \tag{8.6}$$

where, R_T is total electrical resistance, and R_M is material electric resistance, and U_{AB} is voltage between A and B, and I is current.

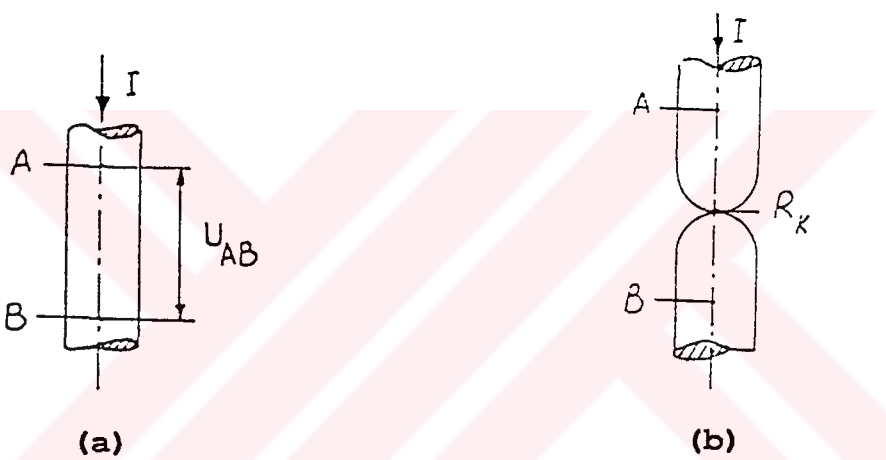

(a) (b)

Figure 8.5 Specimens. (a)One specimen. (b)Two specimens contacted to each other.

If we have two cylindrical specimens which have a spherical tip and spherical tips of cylindrical specimens are contacted to each other as shown in Fig.8.5.(b). In this case, total electrical resistance can be written as,

$$R_T = R_M + R_C \tag{8.7}$$

where, R_C is contact resistance. Here, The total resistance is greater than material resistance. Eq.8.7 can also be written as,

$$R_C = R_T - R_M \tag{8.8}$$

If there are oxide or other contaminants on the contact surface, which are organic films, absorbed gases, and chemical compounds of the base metal, this contact resistance is greater than contact resistance of clean surface. In this case, contact resistance can be written as,

$$R_{KT}=R_B+R_F \qquad (8.9)$$

where, R_F is contact resistance caused by oxide or other contaminants, and R_B is spreading resistance caused by the restriction of current through local points of contact, and R_{KT} is true contact resistance. Fig.8.6 shows restriction of current through local points of contact.

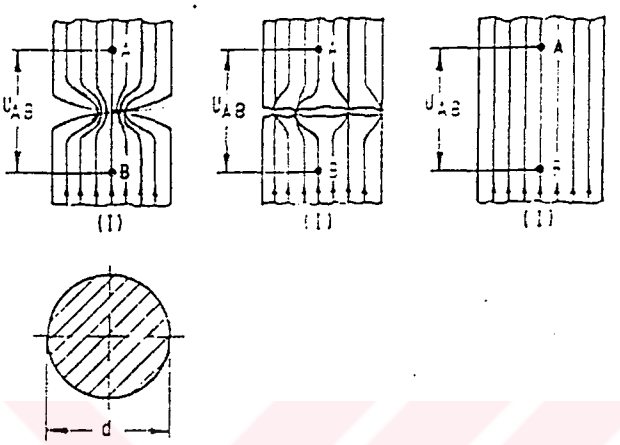

Figure 8.6 Restriction of current through local points of contact.

If there is no oxide or other contaminants on the contact surface, R_F becomes equal to zero, and R_{KT} becomes equal to R_C.

8.4 Contact Surface

It is known that there is surface roughness on all metallic surface in some degree. So that, if two metallic sheets are contacted face to face, there is no contact everywhere on the contact surface of the sheets. Some regions of the contact surface of one sheet do not contact to the contact surface of the another sheet because of the surface roughness. So that electric current does not pass from this area which does not contact and spreading resistance occurs by the restriction of current through local points of contact. Electric current does not also pass from everywhere of the contacted surface because of the oxides, organic films, absorbed gases and chemical compounds of the base metal on the contact surface. We will now investigate this contact surface which can be grouped as follows,

a. Metallic contact points: Contact surfaces contact to each other exactly everywhere on these point and there is

no oxide and contamination. Therefore, there is no electrical contact resistance in these points and electric current pass from these points easily. The contact regions which contain metallic contact points are shown in Fig.8.7 as A_m.

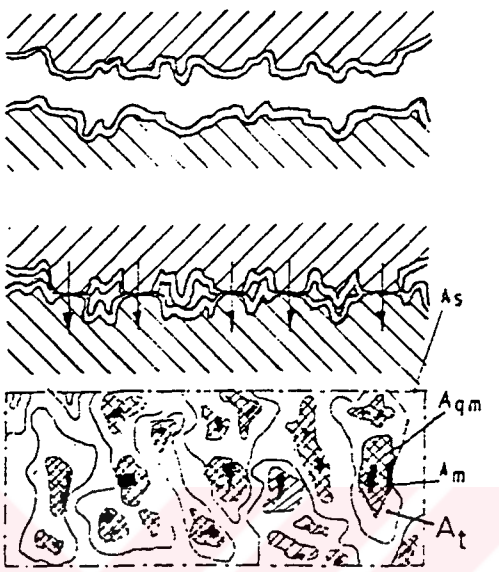

Figure 8.7 Contact surface.

b. Quasi-metallic contact points: There is a thin film on these points. The thickness of the film is equal to 20^0A or less on these points. There is a very little contact resistance on these points, and electric current can also pass from these points easily. This contact resistance can be written as follows,

$$R_f = \frac{\sigma}{A} \quad [\text{Ohm}] \tag{8.10}$$

where, R_f is contact resistance of this thin film, and σ[ohm.m^2] is tunnel resistance, and A(m^2) is the total area for these points. Absorbed oxygen atom can be given as an example for this thin film. The contact regions which contain quasi-metallic contact points are shown in Fig.8.7 as A_{qm}.

c. Contact points covered with foreign film: Contact points are covered with foreign film which can be liquid oil or water film. But these films can be gotten away easily by clamping force so it does not have considerable effect on the contact resistance. Regions which contain these types of contact points are shown in Fig.8.7 as A_t.

d. Contact points covered with a thick film: This film contains oxides, absorbed gases and chemical compounds of the base metal on the contact surface. It is not conductor. So, it must be ruptured by clamping force. This type of contact points is also shown in Fig.8.7 as A_t.

The condition of the contact surface affects the dimension of the weld nugget and the tensile strength of the workpieces after welding. Fig.8.8 shows the relationship between increase in the weld nugget and tensile strength of the workpiece after welding for various conditions of the contact surface[22].

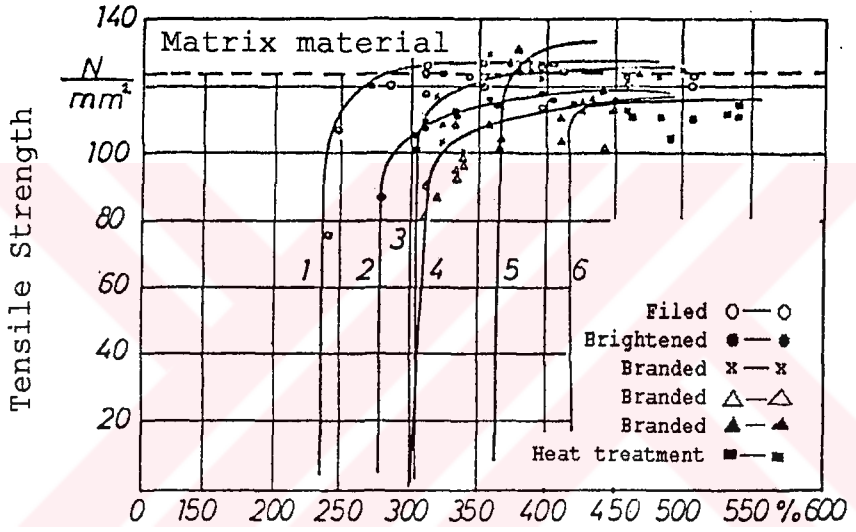

Figure 8.8 The relationship between increase in the weld nugget and tensile strength of the workpiece after welding for various conditions of the contact surface[22].

When clamping force becomes bigger than a certain value, plastic deformation occurs in the micro contact points and the film is ruptured by plastic deformation. Electric current can pass from these points if the film is ruptured. If surface roughness is lower than a certain value, the stress in the micro contact becomes lower than yield-stress of the material so that the film can not be ruptured by the clamping force. Because There is no plastic deformation in these micro contact points. In this case, we can say that clamping force must be bigger than a certain value to be able to rupture this film which is not conductor.

8.5 Sphere Model To Find Contact Resistance

In this method, it is assumed that contact surface is spherical. The radius of the contacted circular area for load, F_s is b_μ as shown in Fig.8.9. The radius of the contacted circular area for any load is shown as r, and it changes by changing load. dr is unit change in the radius of the contacted circular area corresponding unit change of load. Assume that two spherical electrode are clamped by clamping force and there is no workpiece between electrodes. In this case, the unit change of electrical resistance, dR corresponding unit change in the radius of contacted circular area can be written as,

$$dR = \rho \frac{dr}{s} \tag{8.11}$$

where, s is cross-section area of the contact surface and it is equal to $2\pi r^2$. In this case, Eq.8.11 can be written as,

$$dR = \rho \frac{dr}{2\pi r^2} \tag{8.12}$$

The electrical resistance for one circular electrode can be found by integrating Eq.8.12 from b_μ to r_a as follows,

$$R_{1KS} = \frac{\rho}{2\pi} \int_{b_\mu}^{r_a} \frac{dr}{r^2} = \frac{\rho}{2\pi} \left(\frac{1}{b_\mu} - \frac{1}{r_a} \right) \tag{8.13}$$

where, R_{1KS} is the electrical resistance for one circular electrode, and r_a is the radius of the electrode.

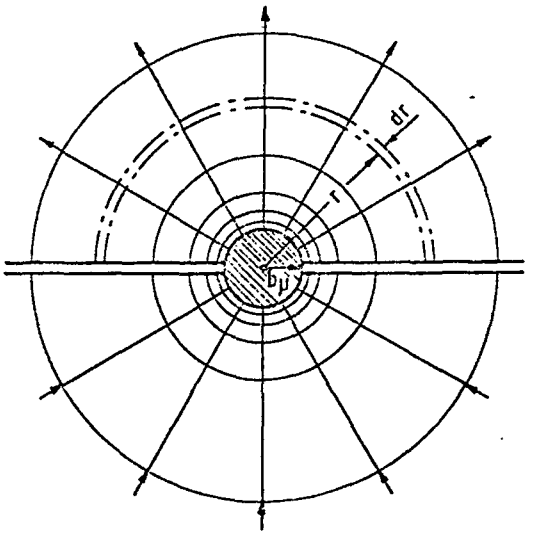

Figure 8.9 Contact surface for sphere model.

In the case of contacted two spherical electrodes, electrical resistance can be found as,

$$R_{e2KS} = 2R_{1KS} = \frac{\rho}{\pi}\left(\frac{1}{b_\mu} - \frac{1}{r_a}\right) \qquad (8.14)$$

where, R_{e2KS} is the electrical resistance for contacted two spherical electrodes. The radius of electrode, r_a is much greater than b_μ for electrode-sheet contact. So it can be assumed that $r_a \to \infty$. In this case, Eq.8.14 can be written as,

$$R_{e2KS} = \frac{\rho}{\pi b_\mu} \qquad (8.15)$$

The value, R_{e2KS} found above is total electrical resistance. Contact resistance can be found using Eq.8.8 as follows,

$$R_C = R_{e2KS} - R_M \qquad (8.16)$$

But, R_M is much less than R_{e2KS}. So, it can be neglected. In this case, R_C becomes equal to R_{e2KS}. The relation in Eq.8.14 can be written for one micro contact point as follows,

$$R_{\mu C} = \frac{\rho}{\pi}\left(\frac{1}{a_\mu} - \frac{1}{r_\mu}\right) \qquad (8.17)$$

where, $R_{\mu C}$ is electrical resistance for one micro contact point where it is in contact surface between sheets, a_μ is the radius of the contacted circular area for a micro contact point, and r_μ is the radius of the micro contact point.

Assume that there are n micro contacts between sheets. They are parallel resistances and the total resistance between sheets can be found by using relation as,

$$\frac{1}{R_T} = \frac{1}{R_1} + \frac{1}{R_2} + \cdots + \frac{1}{R_n} \qquad (8.18)$$

where, R_T is total resistance for parallel resistances and $R_1, R_2, \ldots . R_n$ are parallel resistances. If parallel resistances are equal to each other, the total resistance can be found as,

$$R_T = \frac{R}{n} \qquad (8.19)$$

where, $R_1 = R_2 = \ldots . = R_n = R$

Using relations Eq.8.17 and Eq.8.19, the total electrical resistance between sheets for all micro contact points can be written as,

$$R_{T\mu C} = \frac{1}{n}\frac{\rho}{\pi}\left(\frac{1}{a_\mu} - \frac{1}{r_\mu}\right) \tag{8.20}$$

To find total contact resistance, the contact resistance between electrode and sheet has to be taken account and material resistance has to be subtracted from total resistance. In this case, the total contact resistance can be written as,

$$R_C = \frac{1}{n}\frac{\rho}{\pi}\left(\frac{1}{a_\mu} - \frac{1}{r_\mu}\right) - R_m + \frac{\rho}{\pi b_\mu} \tag{8.21}$$

To find only contact resistance between sheets, Eq.8.20 can be used if material resistance is neglected.

8.6 Elliptical Model To Find Contact Resistance

In this method, it is assumed that contact surface is elliptical as shown in Fig.8.10. Electrical resistance in the case of contacted two elliptical electrodes can be found using the similar way with the sphere model as follows,

$$R_{2KS} = \frac{\rho}{\pi a_\mu}\arctan\sqrt{\frac{r_a^{\,2} - a_\mu^{\,2}}{a_\mu^{\,2}}} \tag{8.22}$$

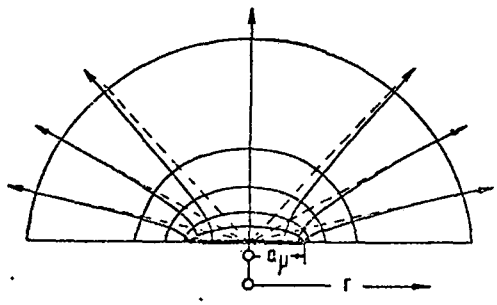

Figure 8.10 Contact surface for elliptical model.

If it is assumed that $r_a \to \infty$,

$$\arctan\infty = \frac{\pi}{2} \tag{8.23}$$

In this case, Eq.8.22 can be written as follows,

$$R_{e2KS} = \frac{\rho}{2a_\mu} \tag{8.24}$$

The contact resistance of contacted two elliptical electrodes can be written by using Eq.8.8 as follows,

$$R_C = \frac{\rho}{\pi a_\mu} \arctan \sqrt{\frac{r_a^2 - a_\mu^2}{a_\mu^2}} - g\frac{\rho}{\pi r_a^2} 2\sqrt{r_a^2 - a_\mu^2} \tag{8.25}$$

where, g is a factor and it can be found by using relation as follows,

$$g = \sqrt{\left(1.12 - \frac{a_\mu}{r_a}\right)\frac{a_\mu}{r_a}} \tag{8.26}$$

When material resistance is calculated, it is assumed that workpiece is cylindrical. In fact, it is elliptical. So that factor,g is used to improve the value found for cylindrical workpiece. g is approximately equal to 0.6. The contact resistance between sheets can be calculated using the way in the sphere model.

8.7 Finding Average Radius Of Contacted Circular Area For Micro Contact Points

When the clamping force,F_k is applied to the electrodes, plastic deformation occurs in the micro contact points between sheets. In this case, total area which is found by summing contacted circular areas of the micro contact points has to be equal to a certain minimum value,A_t to be able to carry the clamping force. If it is assumed that the radii of the contacted circular areas of the micro contacts are equal to each other, the total area can be written as follows,

$$A_T = n\pi\bar{r}_\mu^2 \tag{8.27}$$

where, n is the number of micro contacts, $\bar{r}_\mu$ is the average radius of the contacted circular areas of the micro contacts. The relation between total area and contact hardness of the micro contact point can be written as follows[24],

$$A_T = \frac{F_k}{H_t} \tag{8.28}$$

where, F_k is clamping force, and H_t is contact hardness. Contact hardness can be found approximately as follows[24],

$$H_t = 0.5\text{-}0.7H_v \tag{8.29}$$

where, H_v is Vickers hardness of the material. In this case, Eq.8.27 can be written as follows,

$$A_T = n\pi\bar{a}_\mu^2 = \frac{F_k}{0.5H_v} \tag{8.30}$$

Using Eq.8.30, the average radius of the contacted circular area for micro contact points can be calculated as follows,

$$\bar{a}_\mu = \left[\frac{F_k}{0.6H_v\pi n}\right]^{0.5} \tag{8.31}$$

where, F_k and H_v are known. "n" must be found using experimental methods to be able to calculate average radius of the contacted circular area for micro contact points.

CHAPTER 9

DEFINITION OF THE PROBLEM

9.1 Introduction

To find the relationship between contact resistance and clamping force, two different methods have been used in this study. In addition, contact resistance has been measured for various clamping forces, and the relationship between contact resistance and clamping force has been found experimentally.

In the first method, finite element method has been used to find the relationship between contact resistance and clamping force. In the second method, special workpieces have been prepared and plastically deformed micro contact points have been occurred on the contact surface between sheets by clamping force, and this plastically deformed micro points have been numbered to be able to calculate the relationship between contact resistance and clamping force by using a microscope.

9.2 Solving The Problem By Using Finite Element Method

It is too difficult to solve this problem by using only one special computer program. So that the problem has been divided into pieces, and various computer programs in Fortran Language have been developed to solve this problem. Finite element analysis used to solve this problem involves the following steps:

1. Mesh generation of the workpieces.
2. Finding the stress distribution on the workpieces.
3. Transforming the stresses on the nodes to the force.
4. Finding the load applied to one micro contact for every micro contact points.
5. Mesh generation of the micro contact point.
6. Finding the radius of contacted circular area of a micro contact point for various load.
7. Calculating the contact resistance for various clamping forces.

It is known that there is surface roughness on every two surfaces of the sheets. But, it is assumed that there is

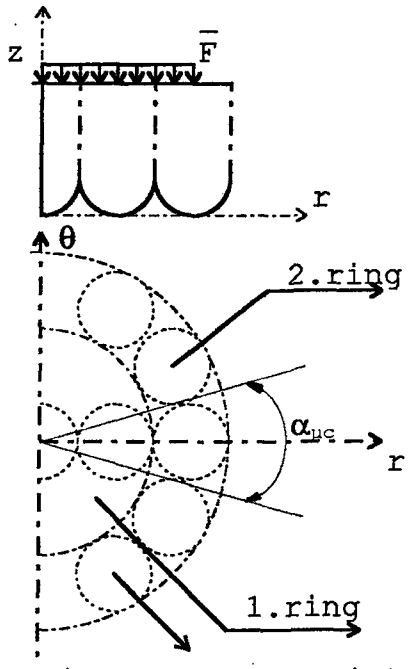

Figure 9.1 The model which is assumed to solve the problem.

only surface roughness on the contact surface between sheets. Because, only contact resistance between sheets has been investigated in this study, and it is also known that the greatest contact resistance is in the contact region between sheets which is the most important region in the electrical resistance spot welding Fig.9.1 shows the model which is assumed to solve this problem.

9.2.1 Mesh Generation Of The Workpieces

It has been assumed that there is no roughness on the surfaces of the workpieces in this step of the investigation. Cylindrical workpieces have been used to be able to solve the problem axi-symmetrically. It is also known that the load is symmetric with respect to z axis. So that this is a kind of axi-symmetric problem. A quarter shape is taken as the finite element model. Because, model is also symmetric with respect to contact surface. The elements which are used to solve the problem by using finite element method are the four-node quadrilateral elements. The model consists of 4698 elements. Total number of the nodes is 4978. The degree of freedom of the nodes is two (u,v). Mesh generation of the shape has been made by using a special computer program developed in Fortran language. The division numbers, the thickness of the workpiece, and the length of an element are given as program input values. In this case, full mesh is obtained automatically. Fig.9.2 shows the mesh generation of the workpiece.

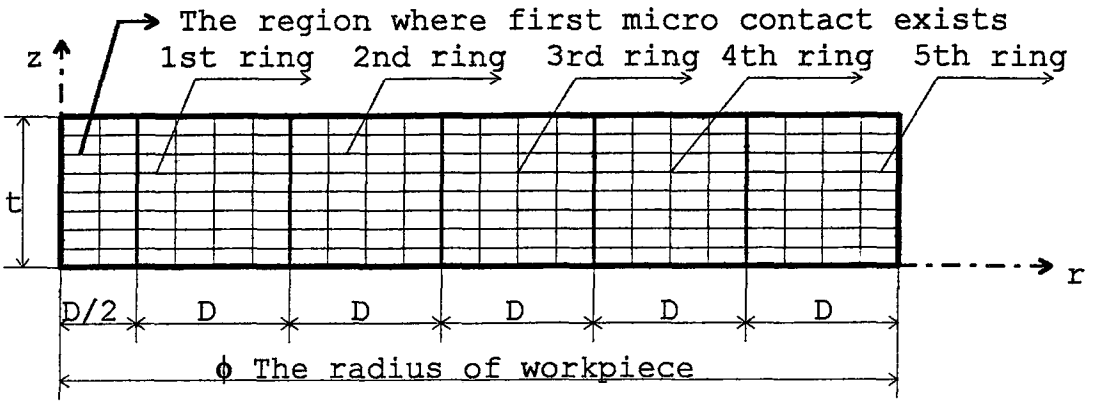

Fig.9.2 Mesh generation of the workpiece where, t is the thickness of the workpieces, and D is the diameter of a micro contact point.

9.2.2 Finding The Stress Distribution In The Workpieces

Stress components on the nodal points have been found for every nodal points by using a special computer program developed in Fortran language. Boundary conditions, external forces and material properties used in this special computer program have been found as follows:

9.2.2.1 Boundary Conditions

The shape and load are symmetric with respect to z axis as shown in Fig.9.3. So that, the displacements, u_{ij} of the nodes are equal to zero on axis along z-direction. The shape is also symmetric with respect to r-θ plane which is contact surface. So that, the displacements, v_{ij} of the nodes are equal to zero on axis along r-direction. It can be seen that the displacements u_{ij} and v_{ij} of the node which is in the origin are equal to zero.

9.2.2.2 External Forces

A nodal force distribution is induced by the total force imposed to the system on the outer surface as shown in Fig.9.3. The force vector corresponding unit area can be found as follows,

$$\bar{F} = \frac{F_K}{\pi r_{et}^2} \qquad (9.1)$$

where, F_K is the clamping force, and r_{et} is the radius of the electrode tip.

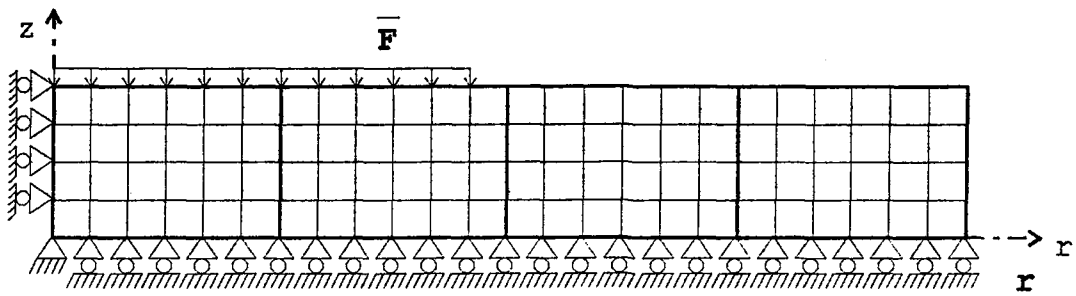

Figure 9.3 Boundary conditions and external forces.

9.2.2.3 Obtaining Mechanical Properties Of The Materials

The materials used to solve problem in this study have been selected as Ç 1020 and Ç 1040 steel. The mechanical properties of materials are measured by using Instron machine in Mechanical Engineering Department Of Dokuz Eylül University as shown in Table 9.1.

Material	Yielding stress σ_y (daN/mm^2)	σ_0 (daN/mm^2)	K(daN/mm^2)	n
Ç 1020	24.7	19.3	112.6	0.65
Ç 1040	42.7	27	169.2	0.531

Table 9.1 The mechanical properties of Ç 1020, and Ç 1040 at 20^{0}C temperature.

9.2.3 Transforming The Stresses On The Nodes To The Force

The stress components on the nodes have been transformed to the force components by using a special computer program which is prepared in Fortran language. The method explained in Chapter 5 has been used to transform the stresses to the force in this computer program.

9.2.4 Finding Load Corresponding One Micro Contact Point For Every Micro Contact Points

A special computer program has been prepared to find the loads corresponding the micro contact points. They have been found and written to the files in computer. Let's discuss the way used in this program to find out the load

corresponding one micro contact point. First, nodal forces on the contact surface are selected. Total value of nodal forces on the contact surface is equal to the clamping force applied to the system. These nodal forces have been used to find out the load corresponding one micro contact point.

In this step of investigation, it has been assumed that there is surface roughness whose shape is spherical on the contact surface. It has also been assumed that the work-piece occurs from the regions as a ring (Fig.9.2). First, the force carried by a ring must be found to be able to find out the force carried by a micro contact point on this ring. Nodal forces on a ring are carried by micro contact points on the same ring. But, nodal force between rings must be divided by 2. Because, this nodal force affects both adjacent rings.

In the model, it has been assumed that there is a micro spherical contact point in the origin, and there are regions as a ring around this micro contact point as shown in Fig.9.1, and they contain micro contact points. First micro contact in the origin carries force which is found by adding nodal forces on the area where this micro contact point exists.

There are more than one micro contact points in the rings as shown in Fig.9.1. It can be seen that the loads carried by micro contact points which are in the same ring are equal to each other because of the symmetry.

The total force carried by a ring has been found by adding the nodal forces on this region. Angle, $\alpha_{\mu C}$ has to be found to be able to calculate the number of micro contact point on a ring, and it can be found as follows,

$$\alpha_{\mu C} = 2\arcsin\frac{r_\mu}{n_r 2r_\mu} = 2\arcsin\frac{1}{2n_r} \qquad \text{[Radian]} \qquad (9.2)$$

where, n_r is the number of ring, and r_μ is the radius of micro contact point which is constant for all micro contact points. The number of micro contact points on a ring can be found as follows,

$$n_{\mu C} = \frac{2\pi}{\alpha_{\mu C}} \qquad (9.3)$$

Now, the force carried by one micro contact point in a ring

can be found as follows,

$$F_{\mu c} = \frac{F_r}{n_{\mu c}} \tag{9.4}$$

where, F_r is the force carried by a ring, and $F_{\mu c}$ is the force corresponding one micro contact point in this ring.

9.2.5 Mesh Generation Of The Micro Contact Point

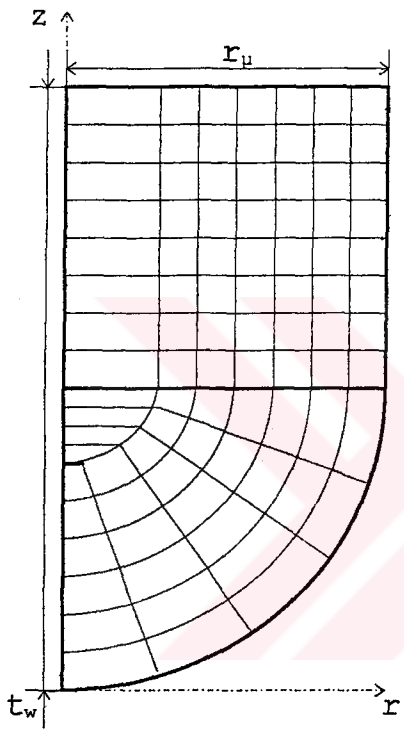

Figure 9.4 Mesh Generation of the micro contact point where t_w, is the thickness of the workpieces, and r_μ is the radius of the micro contact point.

Let's consider a body as shown in Fig.9.4 where, the length of the body is equal to the thickness of the workpiece, and the radius of the body is equal to the radius of the micro contact point, and one of the body's tip is spherical whose radius is also equal to the radius of the micro contact point.

Let's consider two bodies as discussed above are contacted to each other on spherical tips and clamped by micro contact force.

The bodies and load are symmetric with respect to z axis and there is a symmetry with respect to contact surface. So, This is a kind of axisymmetric problem and a quarter shape is taken as the finite element model (Fig.9.4).

The elements used to solve problem by using finite element method are the four-node quadrilateral elements. The model consists of 1169 elements. Total node number is 1272. The degree of freedom of the nodes is two (u,v). Mesh generation of the shape has been made by using a special computer program developed in Fortran language. The division numbers, the length and the radius of the body are given as program input values. In this case, full mesh is obtained automatically. Fig.9.4 shows mesh generation of the micro contact point.

9.2.6 Finding The Radius Of Contacted Circular Area Of A Micro Contact Point For Various Loads

In the beginning of the calculation, there is only one contacted nodal point on the contact surface. Namely, there is only one nodal point on the r axis. Because, the shape of the tip of the micro contact point is spherical. It is the main problem that how much force has to be applied to the micro contact point to contact second adjacent nodal point. To be able to find this contact force, first the displacements on the nodes have been found for any external force by using a special computer program in Fortran language where elasto-plastic finite element solution has been used. These displacements have been added to the coordinates of the nodes. When this summation is done, if second adjacent node contacts, the external force used to find these displacements are true, and it is called as contact force. If second node does not contact, external force used to find these displacements have to be changed and it has to be continued to solve this problem until true contact force is found. Then, the problem has been solved again to find how much force has to be applied to the micro contact point to contact third nodal point.

It has been continued to solve the problem using this way until a certain number of node,n. After this number of node, it is not possible to solve the problem using this way. Infinitesimally small elements must be used to be able to solve the problem from beginning to the end using this way. But, it is not possible to be used infinitesimally small elements because of the excessive computer times for iterative solution processes. After this critical node, maximum force which can be carried for a certain radius of contacted circular area has been found. The radius of contacted circular area has to be greater to be able to carry a greater force and then, next adjacent node is contacted. In this case, the radius of contacted circular area becomes greater, and the maximum force for this radius of contacted circular area has been found. It has been continued to the calculation until the radius of contacted circular area becomes equal to the radius of micro contact point.

Material properties shown in Table 9.1 have been used in this step of calculation. The force vector corresponding unit area can be found by using Eq.9.1 where, r_{et} is equal to the radius of micro contact point. Boundary conditions used in this special computer program have been found as follows,

9.2.6.1 Boundary Conditions

The shape and the load are symmetric with respect to z axis as shown in Fig.9.5. So that the displacements, u_{ij} of the

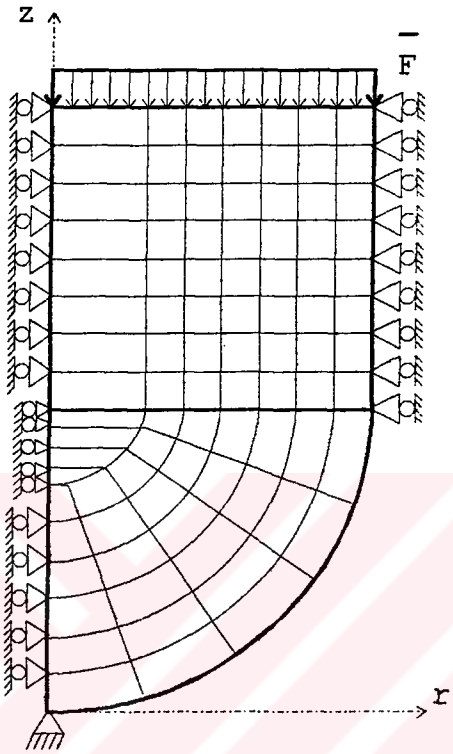

Figure 9.5 Boundary conditions and external forces for a micro contact point.

nodes are equal to zero on the axis along z-direction. The shape is also symmetric with respect to contact surface. So that the displacements, v_{ij} of the nodes which are on the contact surface are equal to zero on axis along r-direction. It can be seen that the displacements, u_{ij} and v_{ij} of the node which is in the origin are equal to zero. It can be assumed that the displacements, u_{ij} of the nodes on the edge where coordinate, r is equal to the radius of the micro contact point are equal to zero. Because, there is a very small plastic deformation in the nodes along this edge.

9.2.7 Calculating Contact Resistances For Various Loads

Contact resistances for various loads have been calculated by using a special computer program in Fortran language. The radii of contacted circular area for various loads are given as program input values in this program.

In the calculation of contact resistance, first, the contact resistance for a micro contact point is found. In this calculation, Eq.8.14 has been used to find only contact resistance of a micro contact point by assuming that there is no oxides or contaminants on the contact surface and neglecting material resistance. It is known that micro contact points are parallel to each other. So that the total contact resistance between sheets can be found by using relations discussed in Chapter 8 in detail.

9.3 Calculating The Contact Resistance By Using Experimental Results

Sphere model discussed in Chapter 8 in detail has been used in this investigation. Special workpieces have been prepared to be able to find out the number of the plastically deformed micro contact points which are occurred on the contact surface between sheets by clamping force.

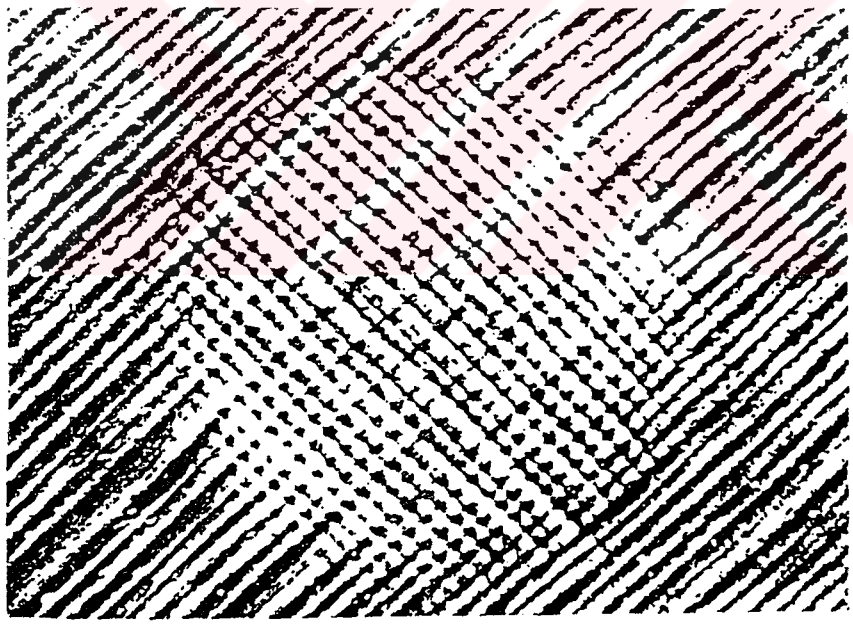

Figure 9.6 The surface of workpiece clamped by clamping force.

One of the surfaces of the workpiece has been cut to provide lines as shown in Fig.9.6 on their surface by using milling machine. The surfaces prepared by cutting have been contacted to each other where, the lines on the contact surface of the workpieces are perpendicular to each other as shown in Fig.9.7. Plastically deformed micro contact

points occur where the lines are intersected when the clamping force is applied to the workpieces.

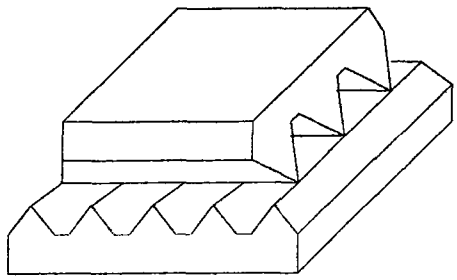

Figure 9.7 Placing the workpieces.

When clamping force has been applied to the workpieces, plastically deformed micro contact points occur on the contact surface. Experiment has been repeated for various clamping forces, and the plastically deformed micro contact points have been numbered using a microscope to be able to calculate the contact resistance for various clamping force using the way discussed in Chapter 8 in detail. Fig.9.6 shows the surface of the workpiece clamped by clamping force.

In the calculation of contact resistance, Eq.8.31 has been used to find the average radius of the contacted circular area, and Eq.8.20 has been used to find electrical contact resistance between sheets.

In the special workpieces, The distance between lines is equal to 0.35mm. It is also equal to the diameter of the micro contact point. So that, the radius of the micro contact point, r_μ is equal to 0.175mm.

9.3.1 Experiment Device

An experiment device has been produced in Mechanical Engineering Department of Dokuz Eylül University as shown in Fig.9.8, and Fig.9.9. There are a Weighing Cells and Force Transducers in this experiment device. So the clamping force can be measured. Contact resistance for various clamping forces can also be measured using a LCR Databridge. Clamping force is increased by reducing of the electrode speed by using a reducer in this experiment device, and the clamping force which is equal to 600daN can be applied to the workpiece by hand.

9.3.2 Obtaining Mechanical Properties

The material used to solve the problem in this step of the investigation has been selected as Ç 1020. The electrical resistivity of this material is equal to 0.171ohm.mm^2/m. The Vickers hardness of this material has been measured in Mechanical Engineering Department of Dokuz Eylül University, and it is equal to 180daN/mm^2.

Figure 9.8 The experiment device.

9.4 Measuring The Contact Resistance

A LCR Databridge and the experiment device discussed above have been used to measure the contact resistance for various clamping force. Fig.9.10 shows how the contact resistance is measured. First, two workpieces have been clamped between electrodes, and total resistance, R_{T1} has been measured for various clamping force. R_{T1} can be written as,

$$R_{T1} = R_{UW} + R_{UE} + R_{UC} + R_{UM} + R_{CBS} + R_{LM} + R_{LC} + R_{LE} + R_{LW} \qquad (9.5)$$

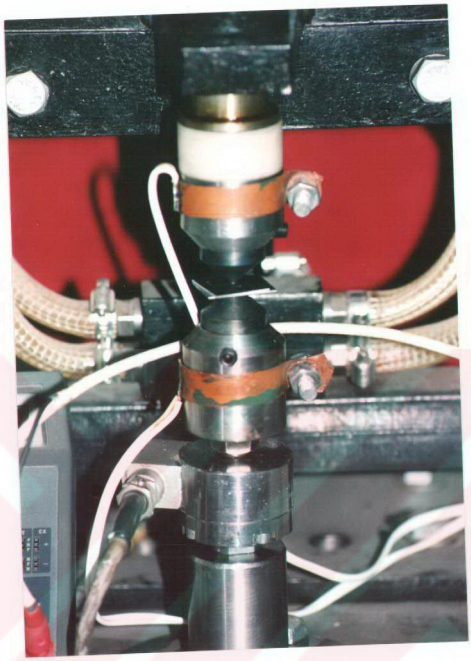

Figure 9.9 The experiment device.

where, R_{UW} is the electrical resistance of upper wire, and R_{UE} is the material resistance of upper electrode, and R_{UC} is the contact resistance between upper electrode and sheet, and R_{UM} is the material resistance of upper sheet, and R_{CBS} is the contact resistance between sheets, and R_{LM} is the material resistance of lower sheet, and R_{LC} is the contact resistance between lower electrode and sheet, and R_{LE} is the material resistance of lower electrode, and R_{LW} is the electrical resistance of lower wire.

Secondly, one workpiece has been clamped between electrodes and total resistance, R_{T2} has been measured for various clamping force. R_{T2} can be written as follows,

$$R_{T1} = R_{UW} + R_{UE} + R_{UC} + R_M + R_{LC} + R_{LE} + R_{LW} \tag{9.6}$$

where, R_M is the material resistance of a sheet, and the difference between R_{T1} and R_{T2} can be found as follows,

$$R_{T1}-R_{T2}=R_{UM}+R_{CBS}+R_{LM}-R_M \quad (9.7)$$

where, $R_{UM}=R_{LM}=R_M$. Because, the thicknesses of sheets are equal to each other for all measurements. So, Eq.9.7 can be written as,

$$R_{T1}-R_{T2}=R_{CBS}+R_M \quad (9.8)$$

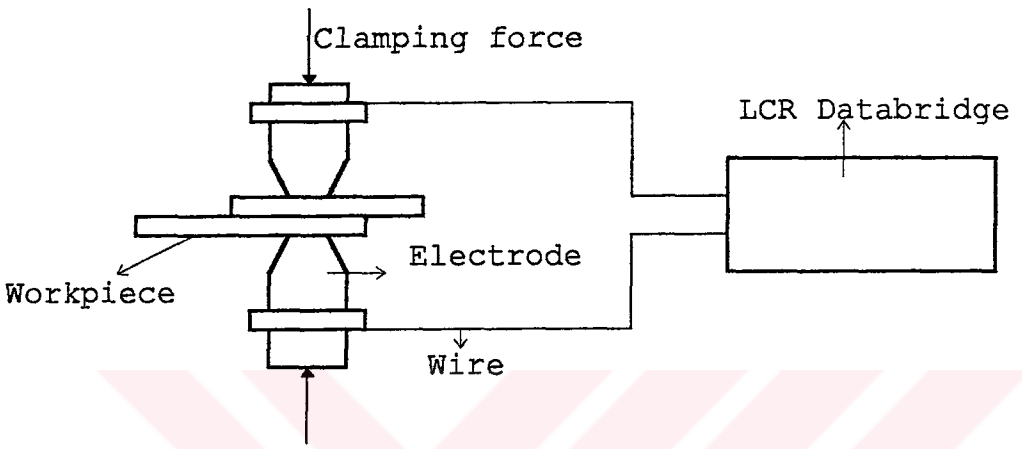

Figure 9.10 Measuring the contact resistances for various clamping force.

The material resistance is much less than contact resistance between sheets. So that, the material resistance can be neglected. In this case, the contact resistances for various clamping forces can be found as follows,

$$R_C=R_{T1}-R_{T2} \quad (9.9)$$

In this investigation, R_{T1}, and R_{T2} have been measured for various clamping forces, and contact resistances have been calculated using Eq.9.9.

CHAPTER 10

RESULTS AND DISCUSSION

10.1 Stress Distribution In The Workpiece

A special computer software program developed in Fortran language has been used to find out stress distribution in the workpiece. In this program, clamping force, the thickness of the workpiece, and the radius of electrode tip have been given as program input values. Namely, these values have been taken as variables.

In the first step of the calculation, the radius of the electrode tip and the thickness of the workpiece have been kept as constant values where, the radius of the electrode tip is equal to 1500μm, and the thickness of the workpiece is equal to 750μm. Stress distributions in the workpiece for various clamping forces from 25daN to 400daN by increasing 25daN in every step have been found and written to the files in computer. Then, the stresses on the nodes which are on the contact surface have been selected. Thus, the stress distributions on the contact surface for various clamping forces have been found. Some results found by using this way are shown in Figures from Fig.10.1 to Fig.10.4.

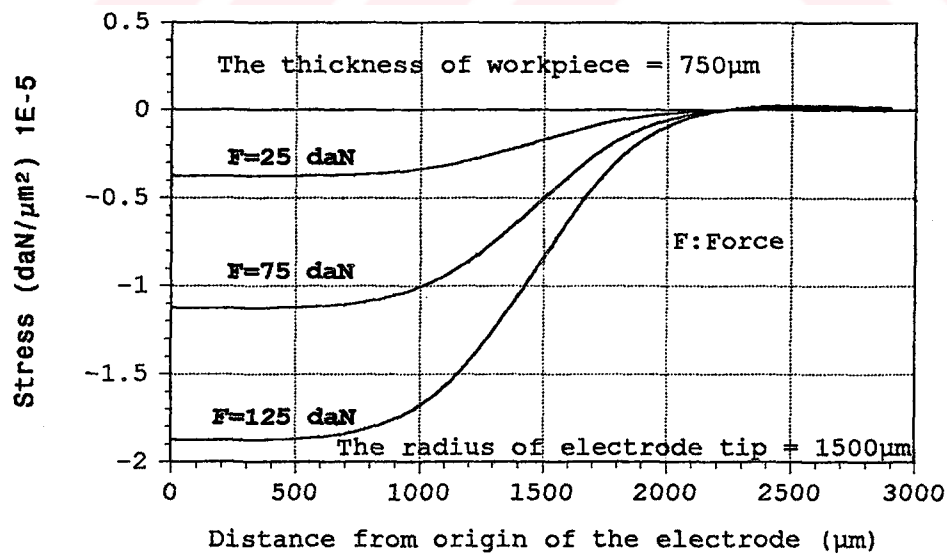

Figure 10.1 Stress distribution [σ_z] along contact surface between workpieces loaded with the forces above in the electric resistance spot welding.

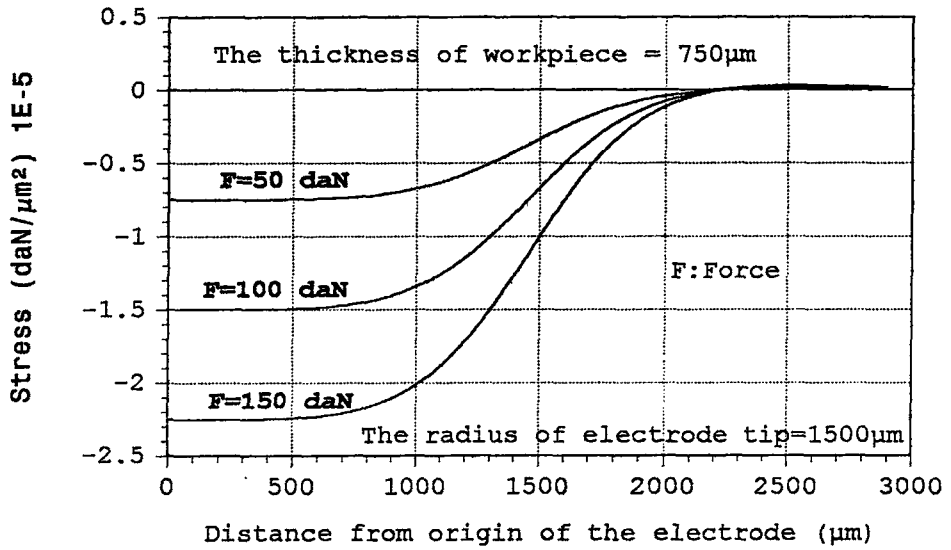

Figure 10.2 Stress distribution [σ_z] along contact surface between workpieces loaded with the forces above in the electric resistance spot welding.

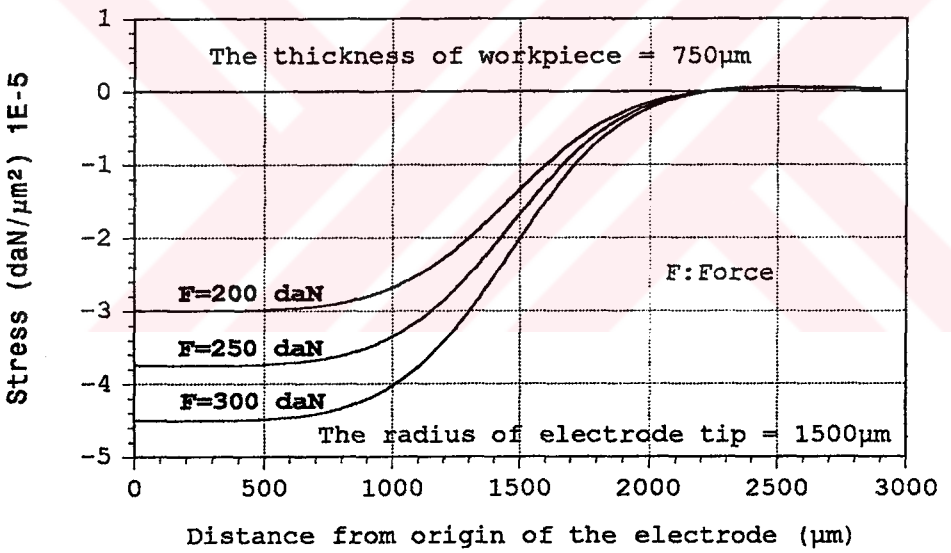

Figure 10.3 Stress distribution [σ_z] along contact surface between workpieces loaded some force in the electric resistance spot welding.

Fig.10.4 shows the relationship between stresses on the contact surface and distance from the origin of the electrode for various clamping forces which are 200daN, 250daN, and 300daN. If we compare the diagrams in this figure, the stresses increase gradually with increasing distance from origin of the electrode until a certain point, but this increment is too small to see in these graphics.It can be seen more easily in Fig.10.5 where the radius of the electrode tip is equal to 2000µm. After this point, it can

be seen that stresses decrease gradually until a certain point which is equal to approximately 600μm for all graphics. The stresses decrease rapidly after this point and then stresses become equal to zero at a certain point which is equal to approximately 2200μm. This point is the same for all graphics in this figure. Small stresses in the opposite direction to the clamping force exist beyond this point. These stresses are one of the causes of the sheet separation. It can also be seen that stresses increase with increasing clamping force, but the area where stresses exist does not change with increasing clamping force. So, the dimension of the weld nugget does not change with changing clamping force very much. Namely, the change of the clamping force does not affect the dimension of the weld nugget very much for truncated cone electrodes.

It is also known that excessively high forces are undesirable because of the increase in surface indentation of the work and wear of the electrodes. So that, it can be said that it is necessary to find an optimum clamping force.

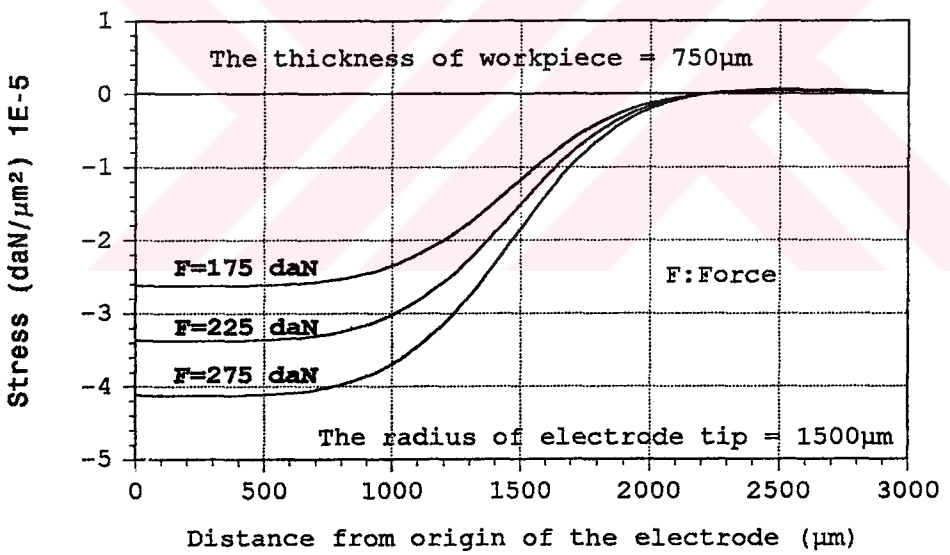

Figure 10.4 Stress distribution [σ_z] along contact surface between workpieces loaded some force in the electric resistance spot welding.

Let's consider a point near the weld nugget, and assume that clamping force is not enough to weld in this point. But, clamping force can be enough to weld for a greater clamping force in the same point. So that, the dimension of the weld nugget can change although the area where stresses exist does not change with changing clamping force. But

this change in the dimension of the weld nugget is very small and it can be neglected.

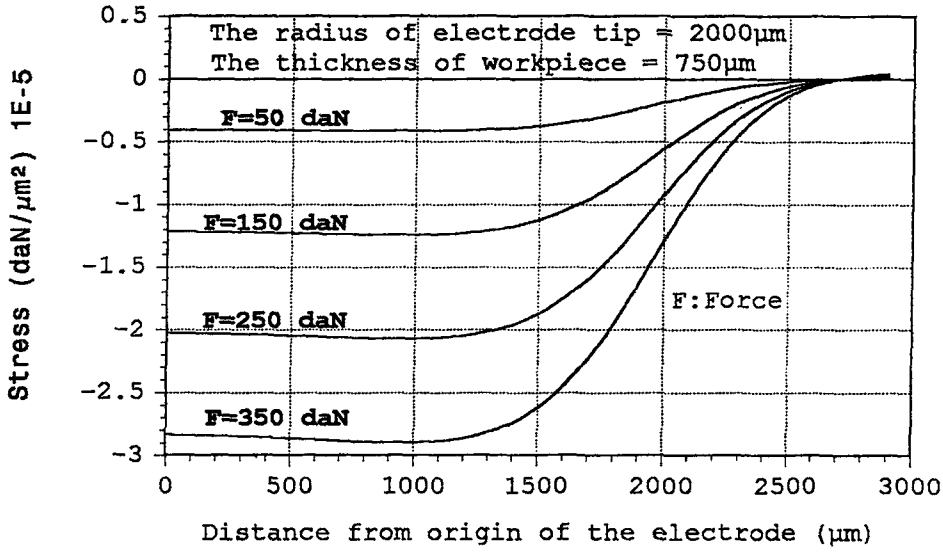

Figure 10.5 Stress distribution [σ_z] along contact surface between workpieces loaded some force in the electric resistance spot welding.

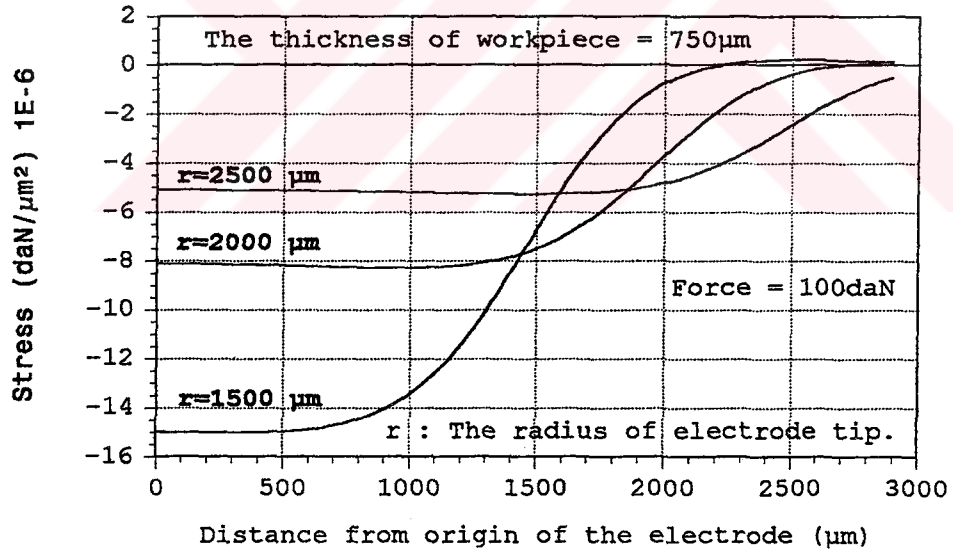

Figure 10.6 Stress distribution [σ_z] along contact surface between workpieces loaded with 100daN force for various electrode tips in the electric resistance spot welding.

In the second step of the calculation, the thickness of the workpiece, and clamping force have been kept as constant values where, the thickness of the workpiece is equal to 750μm. Fig.10.6 and Fig.10.7 show the relationships between stresses on the contact surface and distance from the

origin of the electrode for various radii of the electrode tips where, clamping force is equal to 100daN in Fig.10.6 and it is equal to 200daN in Fig.10.7. If we compare the graphics in Fig.10.7, the stresses increase gradually with increasing distance from the origin of the electrode until a certain point.

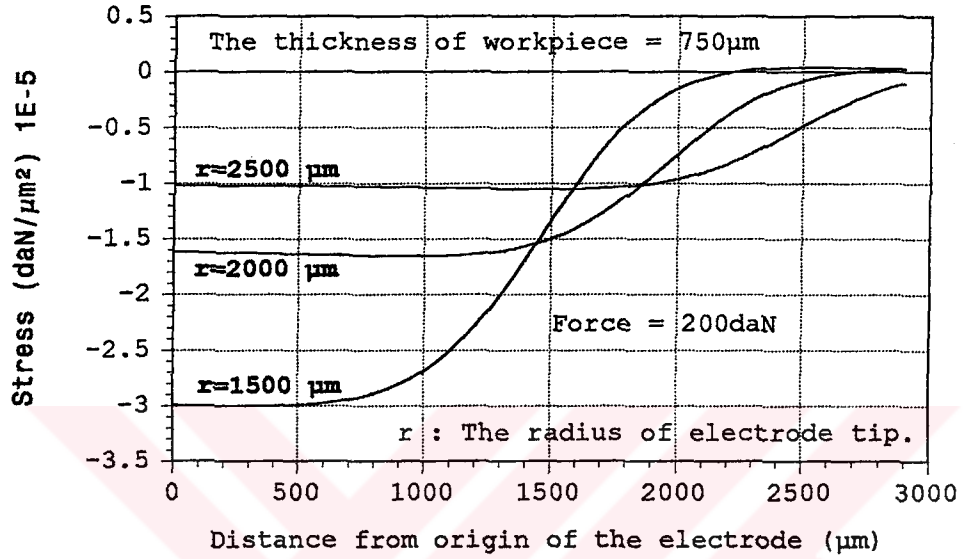

Figure 10.7 Stress distribution [σ_z] along contact surface between workpieces loaded with 200daN force for various electrode tips in the electric resistance spot welding.

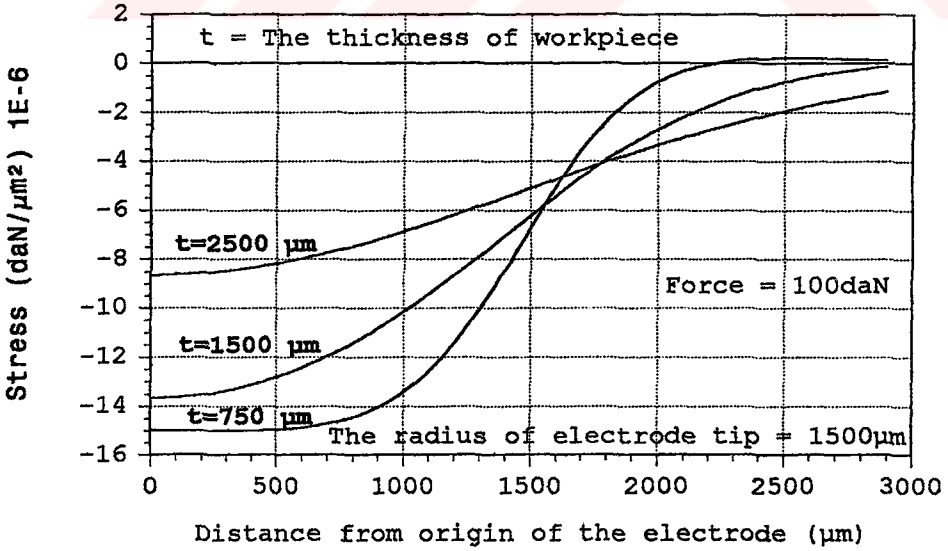

Figure 10.8 Stress distribution [σ_z] along contact surface between workpieces loaded with 100daN force for various thicknesses of the workpiece in the electric resistance spot welding.

This increment is also too small to see in the graphics. After this point, it can be seen that stresses decrease gradually until a point which is different for every graphic. The stresses decrease rapidly after these points and then stresses become equal to zero at the points which are also different for every graphic.

So that, it can be said that the dimension of the weld nugget increases with increasing radius of the electrode tip. It can also be seen that the stresses on the contact surface decrease with increasing radius of the electrode tip. So that, we need more heat or contact resistance for welding.

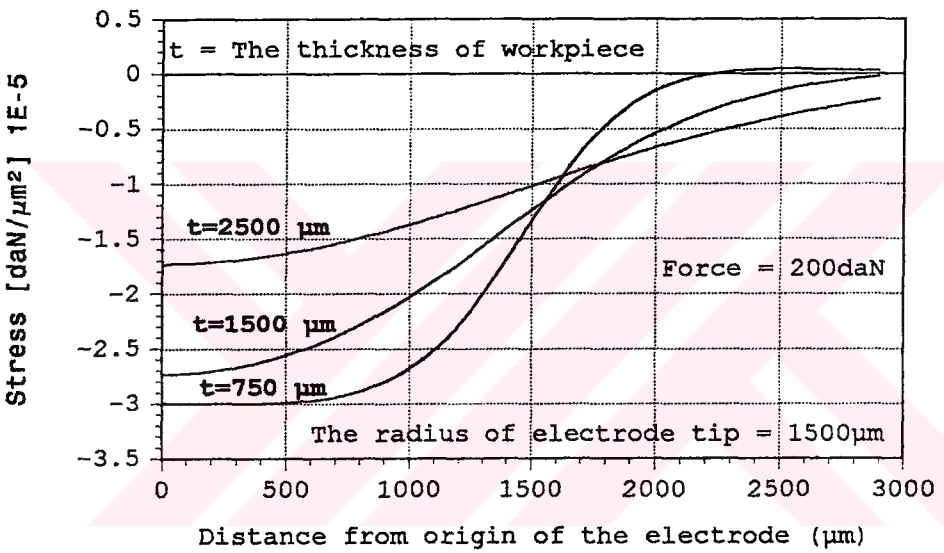

Figure 10.9 Stress distribution [σ_z] along contact surface between workpieces loaded with 200daN force for various thicknesses of the workpiece in the electric resistance spot welding.

In the third step of the calculation, the radius of the electrode tip, and clamping force have been kept as constant values where, the radius of the electrode is equal to 1500µm. Fig.10.8, Fig.10.9, and Fig.10.10 show the relationships between stress on the contact surface and distance from the origin of the electrode for various thicknesses of the workpieces where, clamping force is equal to 100daN, 200daN, and 300daN in Fig.10.8, Fig.10.9, and, Fig.10.10 respectively. If we compare the graphics in Fig.10.10, the stresses decrease with increasing thickness of the workpiece so we need much heat or contact resistance to weld. The area where stresses exist increase with increasing thickness of the workpiece. So that, the dimension

of the weld nugget increases with increasing thickness of the workpiece.

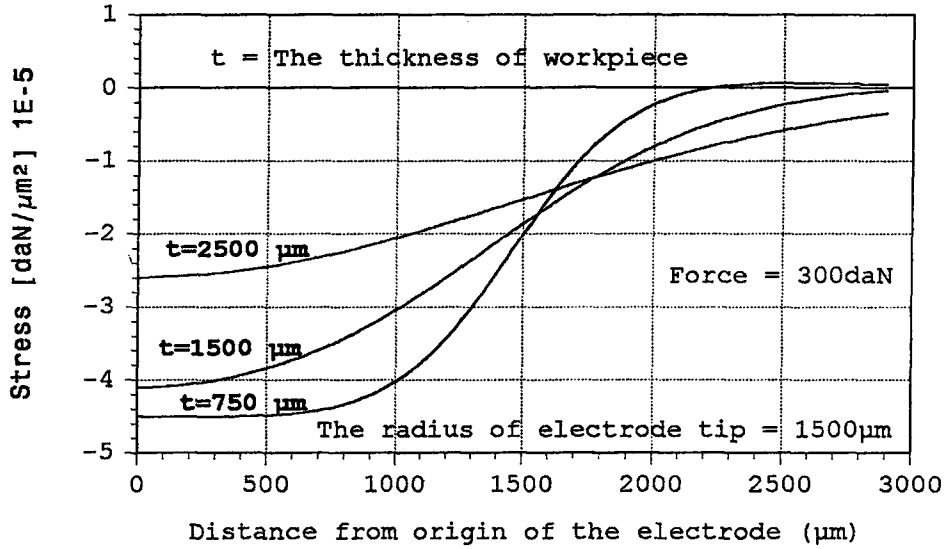

Figure 10.10 Stress distribution [σ_z] along contact surface between workpieces loaded with 300daN force for various thicknesses of the workpiece in the electric resistance spot welding.

10.2 Force Distribution On The Contact Surface

Forces corresponding micro contact points have been found by using a special software computer program developed in Fortran language. Fig.10.11, and Fig.10.12 show the forces corresponding micro contact points for various clamping forces where, the thickness of the workpiece is equal to 750µm, and the radius of the electrode tip is equal to 1500µm. They have been kept as constant values.

If we compare the graphics in Fig.10.12, the second micro contact force is greater than the first micro contact force. There is only one micro contact point in the origin of the workpiece. A ring around first micro contact point contains more than one micro contact points. Some regions among micro contact points do not carry any load. Namely, the areas carrying load are restricted because of this regions. The areas carrying load are also restricted in practice because of the surface roughness. So that, the second micro contact force is greater than the first micro contact force. After the second micro contact force, forces decrease with increasing number of micro contact point. It

can also be seen that micro contact forces increase with increasing clamping force.

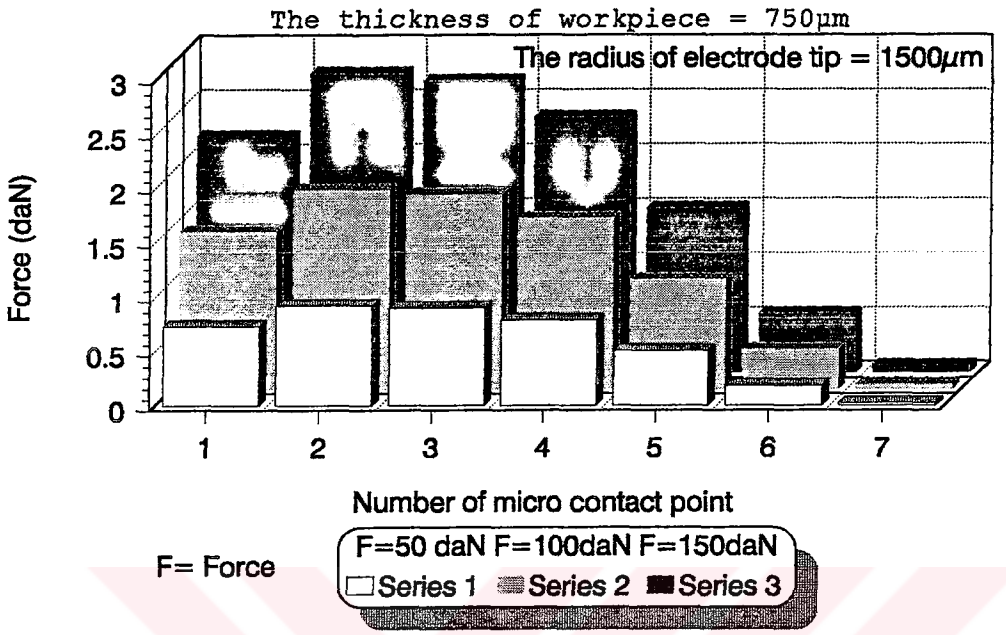

Figure 10.11 Force distribution on micro contact points between workpieces for various clamping forces.

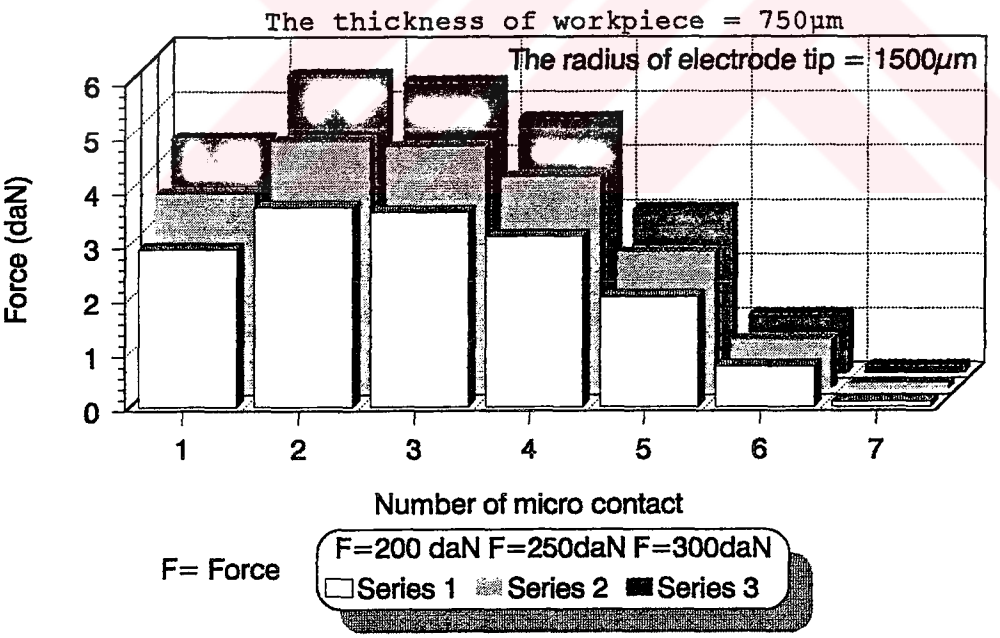

Figure 10.12 Force distribution on micro contact points between workpieces for various clamping forces.

10.3 Stress Distribution On The Micro Contact Point

Stress distribution on the micro contact point has been

found for various loads to find out how stress distribution is on micro contact surface, and to find out where the highest stress is on the micro contact surface by using a special software computer program developed in Fortran language.

Figures from 10.13 to 10.16 show the stress distribution on the micro contact surface for various loads.

Let's investigate the graphics in Fig.10.15, This figure shows the relationship between stress components and number of nodal point on the micro contact surface where, micro contact force is equal to 1.5daN, the thickness of the workpiece is equal to 750μm, and the number of last contacted nodal point is equal to 19.

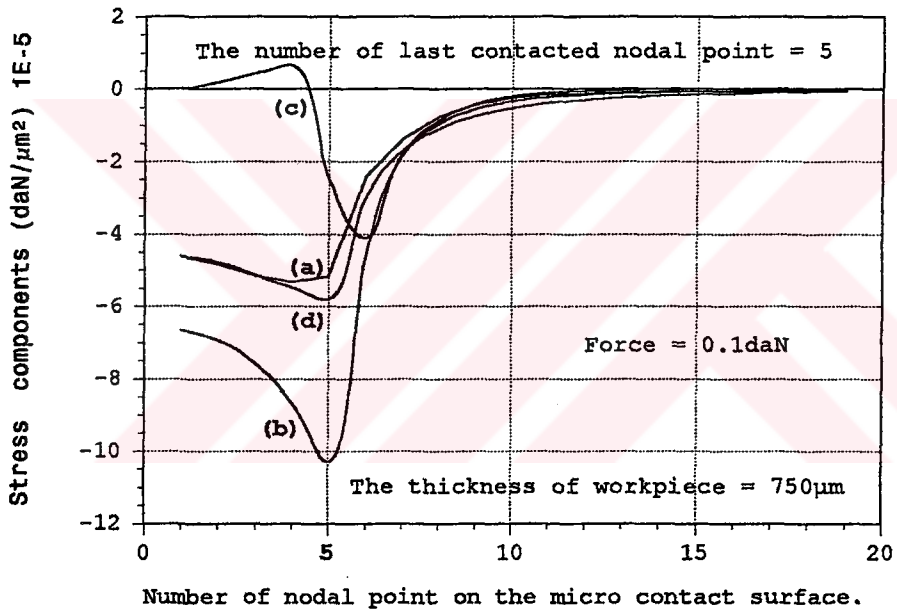

Figure 10.13 Stress distribution along contact surface on a micro contact point loaded with 0.1daN. (a)σ_r. (b)σ_z. (c)τ_{rz}. (d)σ_θ.

It can be seen that the stress components,σ_z which is in the direction of clamping force is greater than other stress components. It can also be seen that the highest stress is in the last contacted nodal point on the contact surface. This stress which is equal to 211daN/mm^2 is more greater than yield stress of the material where the yield stress of the material is equal to 24.7daN/mm^2. So that, plastic deformation occurs in the micro contact points.

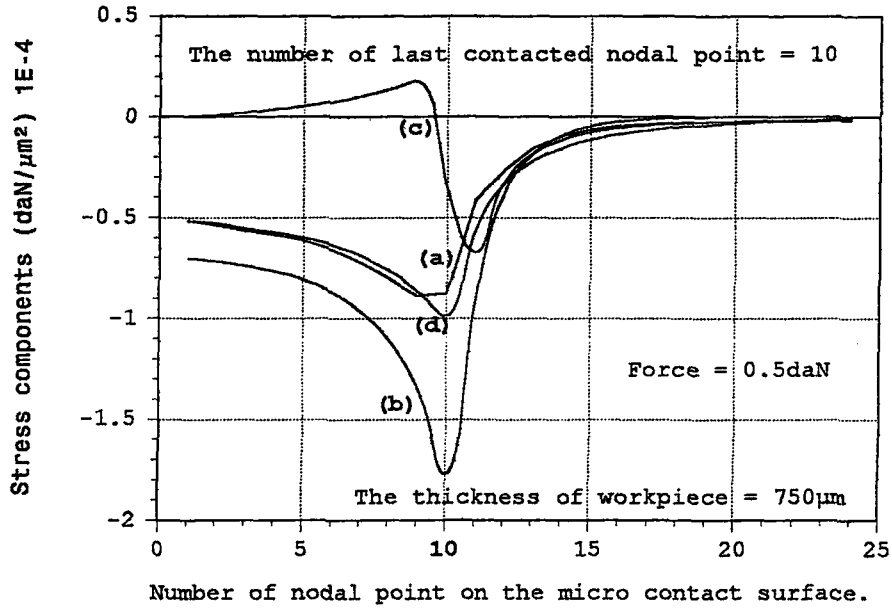

Figure 10.14 Stress distribution along contact surface on a micro contact point loaded with 0.5daN. (a)σ_r. (b)σ_z. (c)τ_{rz}. (d)σ_θ.

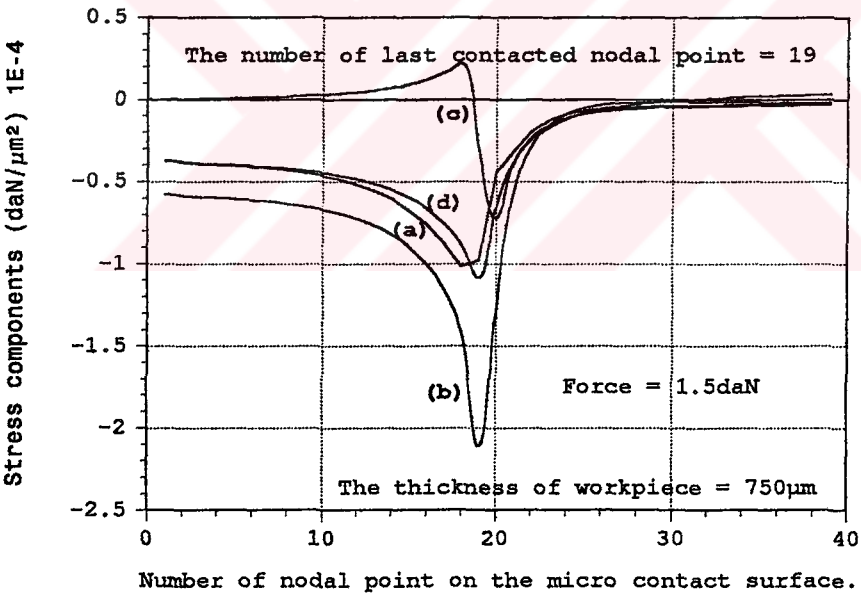

Figure 10.15 Stress distribution along contact surface on a micro contact point loaded with 1.5daN. (a)σ_r. (b)σ_z. (c)τ_{rz}. (d)σ_θ.

Contact force which is 1.5daN occurs on the contact surface for 100daN clamping force as shown in Fig.10.11. The highest stress on the contact surface of the workpiece is equal to 15daN/mm^2 for this clamping force (Fig.10.2). Now, it can be seen that stresses which are much more greater than yield stress occur on the contact surface of the micro

contact point although the stresses on the contact surface of the workpiece is lower than yield stress for a clamping force. Namely, although the stresses on the contact surface of the workpiece without surface roughness is lower than yield stress, stresses higher than yield stress occur on the surface of the micro contact point because of the restriction of the area carrying load.

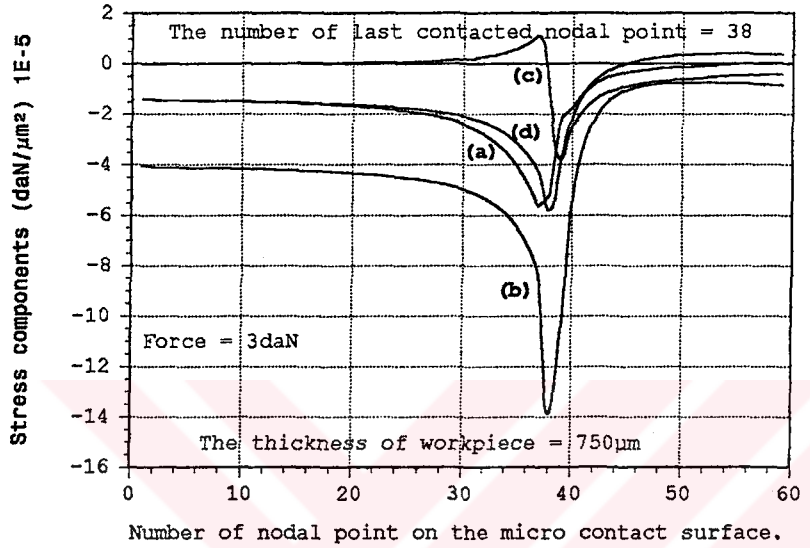

Figure 10.16 Stress distribution along contact surface on a micro contact point loaded with 3daN. (a)σ_r. (b)σ_z. (c)τ_{rz}. (d)σ_θ.

10.4 The Relationship Between Contact Resistance And Clamping Force Found By Using Finite Element Method

In this step of investigation, first, the relationship between contact force and radius of contacted circular area of the micro contact point has been found to be able to find out the relationship between contact resistance (sheet/sheet) and clamping force. Fig.10.17 shows the relationship between contact force and radius of contacted circular area of the micro contact point which is found by using a special software computer program developed in Fortran language. In this program, the material of the workpiece, and the radius of micro contact point have been given as program inputs. The relations have been found for various materials of workpiece, and radii of micro contact point.

Fig.10.18 shows the relationship between contact resistance and clamping force for various radii of electrode tip found

by using finite element method, and Fig.10.19 also shows the relationship between contact resistance and clamping force for various radii of spherical electrode found by using experimental method. When the graphics in figures have been investigated, it can be seen that contact resistance decreases with increasing clamping force.

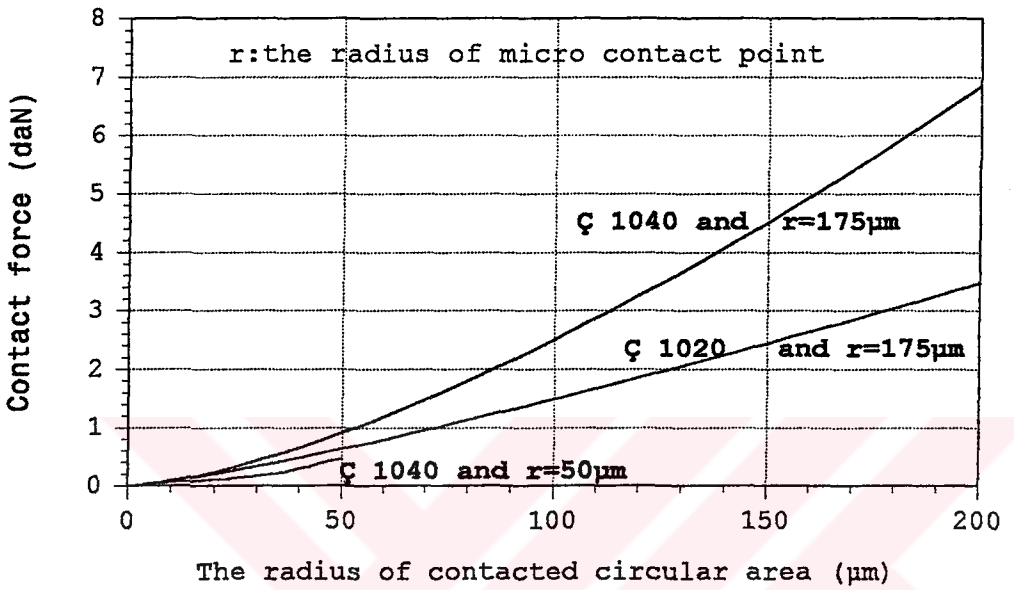

Figure 10.17 The relationship between radius of contacted circular area and contact force for various materials and radii of micro contact point

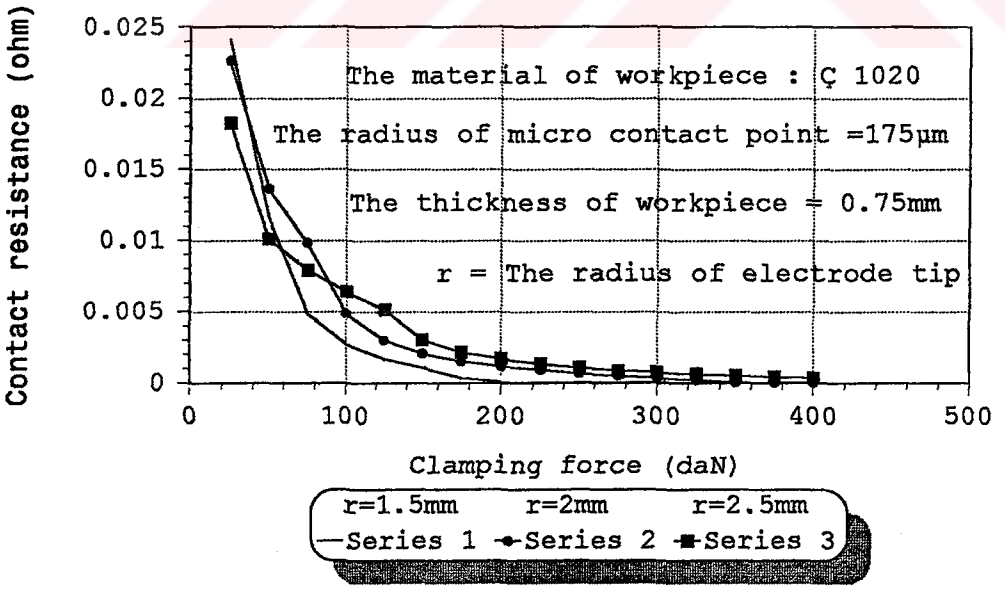

Figure 10.18 The relationship between contact resistance and clamping force for various radii of electrode tip found by using finite element method.

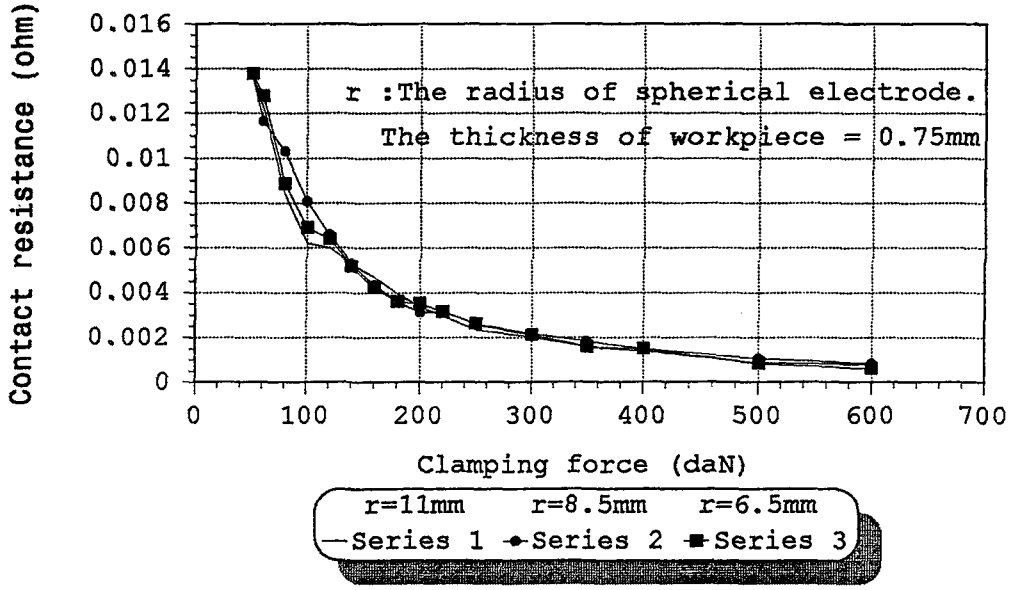

Figure 10.19 The relationship between contact resistance and clamping force for various radii of spherical electrodes found by using experimental method.

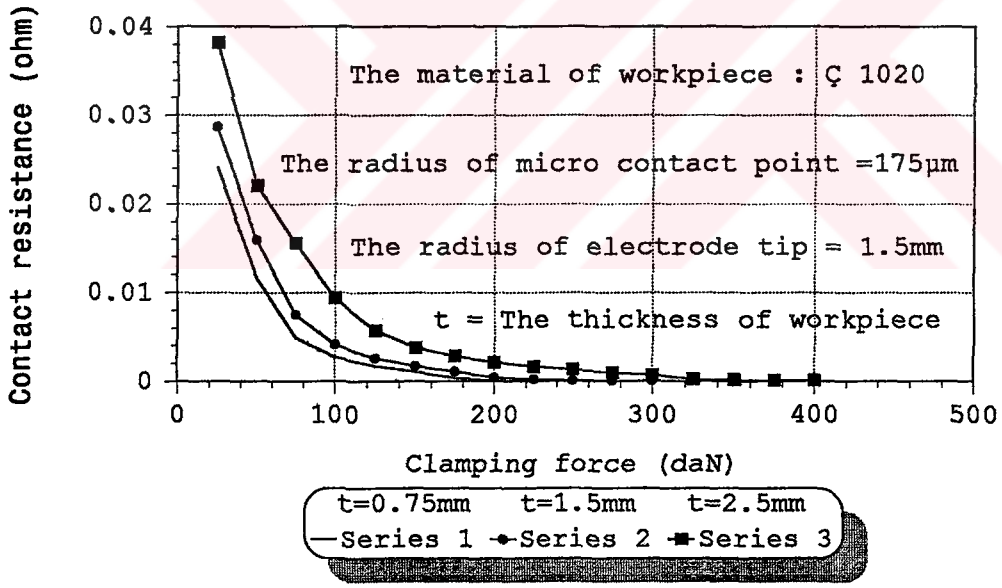

Figure 10.20 The relationship between contact resistance and clamping force for various thicknesses of workpieces found by using finite element method.

It can also be seen that contact resistance does not change very much with changing radius of electrode tip. So that it can be said that the radius of electrode tip has no considerable effect on contact resistance.

Fig.10.20 shows the relationship between contact resistance and clamping force for various thicknesses of workpieces found by using finite element method. If we investigate the graphics in figure, It can be seen that contact resistance increases with increasing the thickness of workpiece. So that it can be said that the thickness of workpiece affects the contact resistance.

Fig.10.21 shows the relationship between contact resistance and clamping force for various materials of workpieces. These relations have been found by using finite element method. When the graphics in figure have been investigated, it can be seen that the material of workpiece affects the contact resistance. Namely, contact resistance changes with changing materials of workpieces for a constant clamping force.

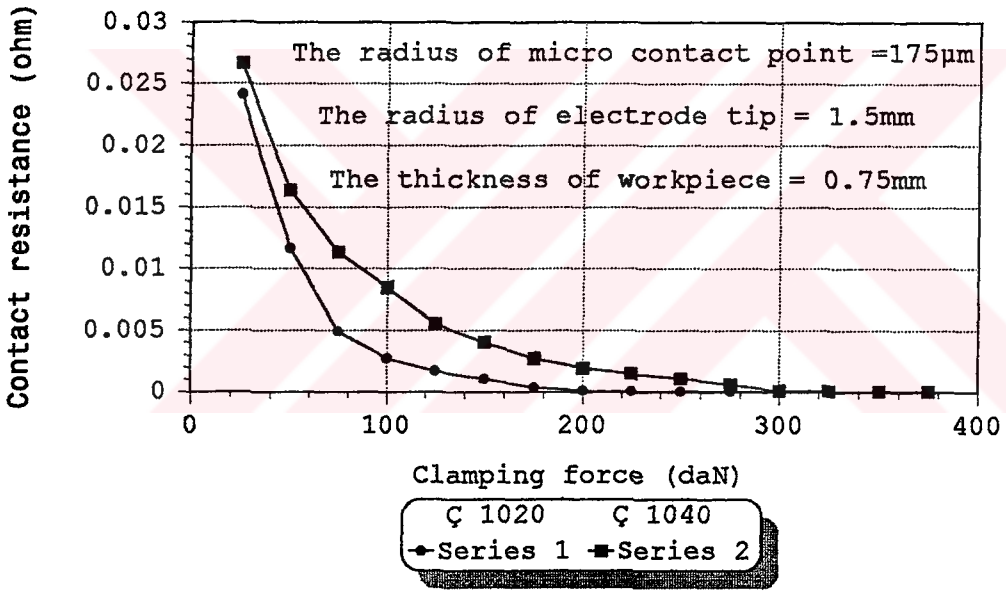

Figure 10.21 The relationship between contact resistance and clamping force for various materials of workpieces found by using finite element method.

Fig.10.22 shows the relationship between contact resistance and clamping force for various radii of micro contact points. There is more surface roughness on the surface of the workpiece where the radius of micro contact point,r is 0.175mm than another workpiece where r=0.05mm. Contact resistance of the first workpiece is greater than contact resistance of the another workpiece for a constant clamping force. Namely, the contact resistance between sheets increases with increasing the radius of micro contact point.

Therefore, it can be said that the contact resistance between sheets increases with increasing surface roughness for a constant clamping force.

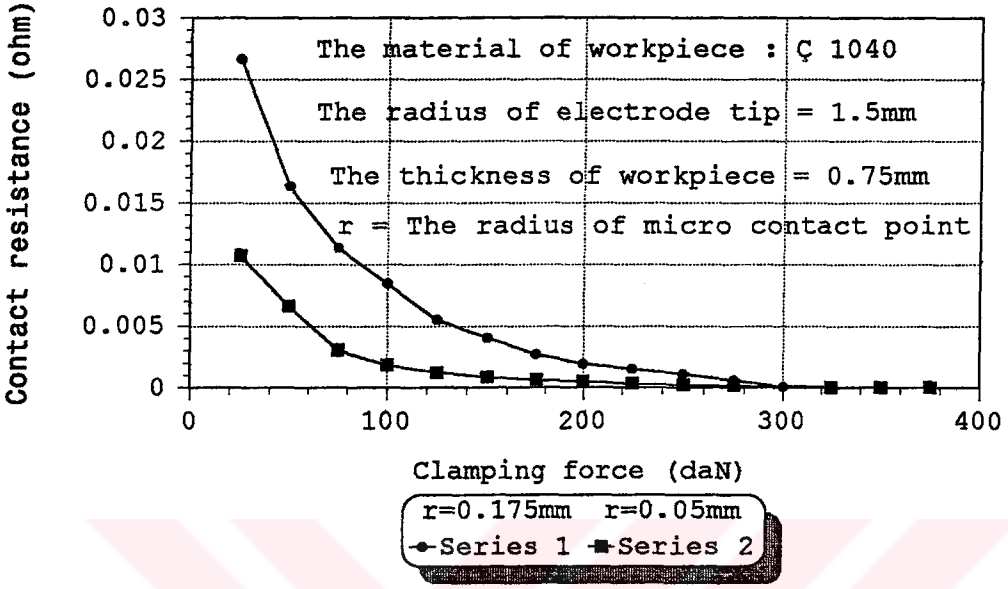

Figure 10.22 The relationship between contact resistance and clamping force for various radii of micro contact points found by using finite element method.

10.5 Comparing The Results

The results found by using finite element method where, the radius of micro contact point is equal to 175μm, and the results found by experimental measurements for truncated cone electrode have been shown in Fig.10.23 where, the thickness of the workpiece is equal to 0.75mm, and the radius of electrode tip is equal to 1.5mm. If we investigate the graphics in figure, there is a difference between graphics for small clamping forces. Because, it is assumed that the tips of micro contact points are spherical so, there are nodal contacts in the tips of micro contact points on the contact surface for small clamping forces but, nodal contact is usually not seen in practice. After a certain clamping force (75daN), there is a very close agreement between graphics. So that, the results found by using the developed software computer program are realistic.

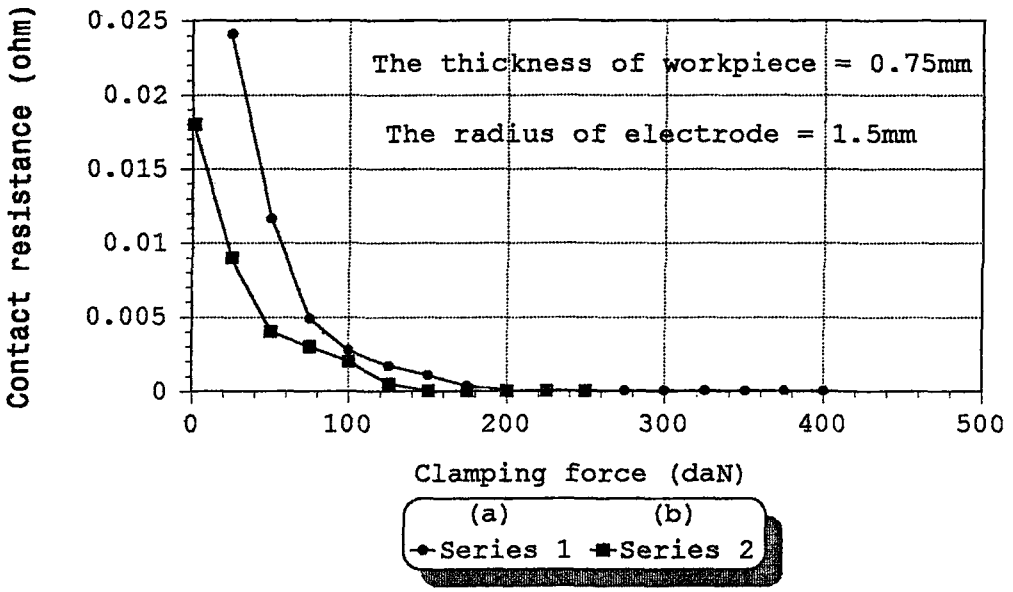

Figure 10.23 The relationship between contact resistance and clamping force. (a) The results found using finite element method. (b) The results found by experimental measurements

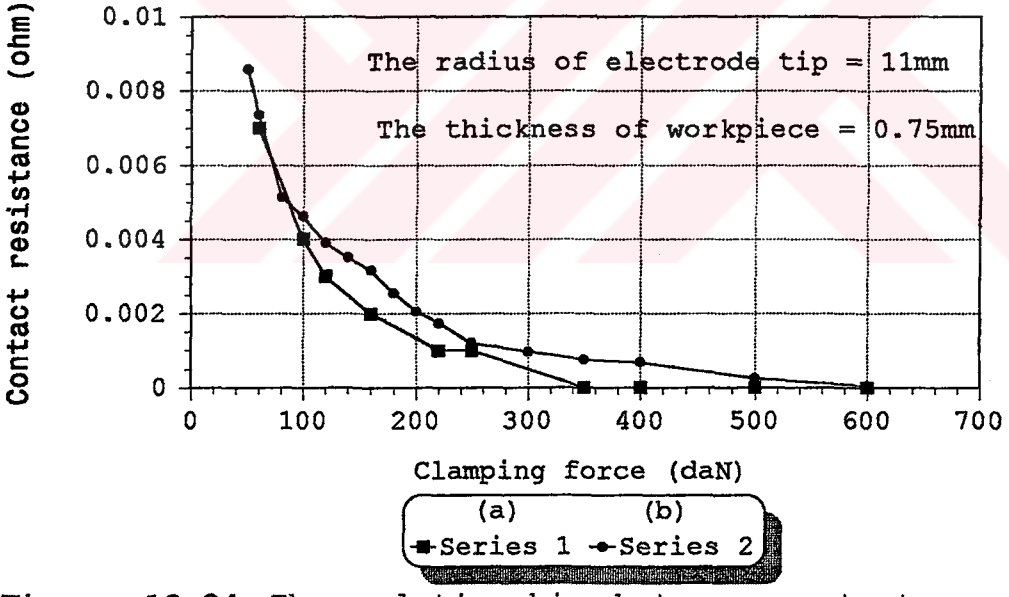

Figure 10.24 The relationship between contact resistance and clamping force. (a) The results found by experimental measurements. (b) The results found using sphere method.

The results found by using experimental method, which is sphere model, and the results found by using experimental measurement for spherical electrode have been shown in Fig.10.24 where, the thickness of the workpiece is equal to 0.75mm, and the radius of electrode tip is equal to 11mm. When the graphics in this figure have been investigated, it can be seen that there is a very close agreement between graphics. So that, the results found by using experimental method are also realistic.

CHAPTER 11

CONCLUSIONS

In this investigation, finite element method and an experimental method have been used to find relationship between contact resistance and clamping force. Some experimental measurements have also been carried out to show the validity of the solution. In addition, stress distributions in the workpiece, and on the spherical surface of the micro contact point, the forces applied to the micro contact points, and effects of the thickness of the workpiece, and the electrode tip, and the material of the workpiece to the contact resistance have been investigated. When the problem has been solved by using finite element method, the effects of temperature have been neglected because of the fact that the contact resistance disappears at much less than 1 cycle after the start of welding.

The followings can be concluded from the results of this study:

1- A special computer software program has been developed to find out the relationship between contact resistance and clamping force.

2- Small stresses in the opposite direction to the clamping force on the contact surface exist beyond a certain point, and these stresses are one of the causes of the sheet separation.

3- The area where stresses exist on the contact surface between sheets does not change with changing clamping force. So that, the change of the clamping force does not affect the dimension of the weld nugget very much for truncated cone electrodes. It is also known that excessively high forces are undesirable because of the increase in surface indentation of the work and wear of the electrodes. So that, it can be said that it is necessary to find an optimum clamping force.

4- The area where stresses exist on the contact surface between sheets and stresses on the contact surface change with changing the radius of electrode tip. So that, the dimension of the weld nugget and heat or contact resistance needed to weld also change with changing radius of the electrode tip.

5- The area where stresses exist on the contact surface between sheets increases with increasing the thickness of the workpiece for a constant radius of electrode tip. So that, the thickness of the workpiece also affects the dimension of the weld nugget.

6- Although the stresses on the contact surface of the workpiece without surface roughness is lower than yield stress for a clamping force, stresses higher than yield stress occur on the surface of the micro contact point because of the restriction of the area carrying load

7- The radius of electrode tip has no considerable effect on contact resistance between sheets.

8- The thickness of the workpiece affects the contact resistance between sheets.

9- The material of the workpiece affects the contact resistance between sheets. Namely, contact resistance changes with changing materials of workpieces for a constant clamping force.

10- The contact resistance between sheets increases with increasing surface roughness for a constant clamping force.

11- The results found by using finite element method indicate a reasonable agreement with results found by experimental measurement for truncated cone electrodes. The results found by using experimental method which is sphere model also show a reasonable agreement with the results found using experimental measurement for spherical electrode.

As a result of this, developed computer programs and experimental method give realistic results.

32. Lheureux,G.E.,Blotte,E.J.,"Le Soudage Par Resistance." ,Dunod,1965.
33. Lo,S.H.,"A New Mesh Generation Scheme For Arbitrary Planar Domains.",Int.J.For Num.Met.In Eng.Vol 21,pp 1403-1426,1985.
34. Lobasov,I.M.,"A Method Of Calculating Welding Current In Spot Welding Using A Computer.",Weld Prod.,Vol 30, n9,Sep,pp 46-47,1983.
35. Marcal,P.Y.,King,O.P.,"Elasto-plastic Analysis Of Two-dimensional Stress System By The Finite Element Method. ",Int.J.Mech.Sci.,Vol 9,pp 143-155,1967.
36. Mendelson,A.,"Plasticity:Theory And Application.",The Macmillan Company,New York,1968.
37. Moore,A.J.,"Deformation Of Metals In Static And Sliding Contact.",Proc.Roy.Soc.,pp 195-231,1948.
38. Morris,J.L.,"Welding Processes And Procedures.", Prentice-Hall,Inc.,1954.
39. Nath,B.,"Fundamentals Of Finite Elements For Engineers.",The Athlone Press Of the University Of London, 1974.
40. Nayak,G.C., Zienkiewicz, O. C., "Elasto-plastic Stress Analysis. Generalization For Various Constitutive Relations Including Strain Softening.",Int.J.Num.Meth. Eng.,Vol.5,pp 113-135,1972.
41. Owen,D.R.J., Salonen,E.M., "Three-Dimensional Elasto-Plastic Finite Element Analysis.",Int.J.For Num.Met.In Eng.,Vol 9,pp 209-218,1975.
42. Özel,A.,Belevi,M.,"Increasing The Strength Of Silent Chain By Residual Stresses.",Ph.D.Thesis,Dokuz Eylül University,Graduate School Of Natural And Applied Sciences,İzmir,1993.
43. Radaj,D.,"Finite Element Analysis Of Temperature Field ,Residual Stresses And Distortion In Welding.", Schweissen Schneiden,Vol 40,n6,Jun,pp 84-87,1988.
44. Rawicz,A.,"Relationship Between Tearing Strength and Electrical Resistance in Welded Microjoints.",IEEE Trans.Reliab.,Vol 34,n2,Jun,pp 98-101,1985.
45. Satoh,T.,Katayama,J.,Abe,H.,"Temperature Distribution And Breakdown Oxide Layer During Resistance Spot Welding Using Two-Dimensional Model.",International Institute of Welding, (IIW-III-371-69),1969.

46. Schwab,R.,"A Computing Program For The Numerical Temperature Field Calculation In Resistance Welding, Having Particular Regard To The Transformer Characteristic, Current Flow Distribution And Thermoelectric Effects.", Schweissen Schneiden, V38 n1, Jan, pE11-E13, 1986.
47. Schwab,R.,"Numerical Calculation Of Temperatures In Resistance Welding As Illustrated By Commutator Welding.", Schweissen Schneiden V.38,n8,Aug, pp 120-122, 1986
48. Studer,F.J.,"Contact Resistance In Spot Welding.", American Welding Journal,Vol.18,n10,pp 374-380,1939.
49. Şen,S.,Önel,K.,"Study Of Extrusion And Upsetting By Using Finite Element Method.",Ph.D.Thesis,Dokuz Eylül University,Graduate School Of Natural And Applied Sciences,İzmir,1992.
50. Timoshenko,S.,"Theory Of Elasticity.",McGraw-Hill Company,1951.
51. Ugural,A.C.,Fenster,S.K.,"Advanced Strength And Applied Elasticity.",Edward Arnold,London,1981.
52. Yamada,Y., Yoshimura,N., Sakurai,T., "Plastic Stress-Strain Matrix And Its Application For The Solution Of Elastic-Plastic Problems By The Finite Element Method.",Int.J. Mech.Sci.,Vol 10,pp 343-354,1968.
53. Yamamoto,T.,Okuda,T.,"A Study Of Spot Welding Of Heavy Gage Mild Steel.",International Institute Of Welding, (IIW-III-389-70),1970.
54. Zienkiewicz,O.C.,"The Finite Element Method.",McGraw-Hill Book Company Limited,1979.
55. Zienkiewicz,O.C.,Phillips,D.V.,"An Automatic Mesh Generation Scheme For Plane And Curved Element Domains.",Int.J.Num.Meth.Eng.,n3,519-28,1971.
56. Zienkiewicz,O.C.,Valliapan,S.,and King,I.P.,"Elasto-plastic Solutions Of Engineering Problems 'Initial Stress',Finite Element Approach.",International Journal For Numerical Methods In Engineering,Vol.1,pp 75-100,1969.
57. Zlamal,M.,"Curved Elements In The Finite Element Method.",SIAM J.Num.Anal.,n11,pp 347-62,1974.